Politecnico di Torino
I Facoltá di Ingegneria

Doctoral Thesis
in Mathematics for Engineering Sciences

ANOMALOUS TRANSPORT: FROM THEORIES ABOUT OSMOTIC PRESSURE TO A NEW APPROACH IN THE FRAMEWORK OF DYNAMICAL SYSTEMS

(Settore Disciplinare MAT/07)

Author:
Lucia Salari

Supervisor:
Prof. Lamberto
Rondoni

About five in the afternoon he went out
and found still others standing around.
He asked them, Why have you been standing here
all day long doing nothing?
Because no one has hired us, they answered.
He said to them, You also go and work in my vineyard.
(Matthew 20:6-7)

Preface

This Doctoral Thesis contains only part of the achievements brought about by my PhD-Programme. I mean only a part, not because I neglected to write them down in this thesis, but because there are some kind of results which cannot be expressed in writing. I learned a lot. First of all I learned the great importance of learning. Then, in learning what it means to do research, I understood the importance of not doing everything by myself but of listening in order to collaborate. I learned what means humbleness. I learned that sharing and mutual aid in scientific work is fundamental even if it is not easy. I learned that a result is not complete neither interesting until you are able to share it.

Moreover, this thesis work would not have been possible without inspirng and fruitful collaboration with a large number of people. First of all my natural family which between earth and heaven supported me throughout these three years. Then my present Family which supported me with a patient and caring love. Then my greatest gratitude goes to my supervisor who taught me all I learned in this field and supported me by any means. I also want to thank wholeheartedly Francesca and Rachele for giving me the right motivation to support the hard final work. Finally a special thank to Chiara Lubich and the Mathzero international group that gives me inspiration, strength, courage and thrust to deal with this PhD adventure, and many more.

Abstract

Osmosis is a fundamental physical process involved in many biological phenomena and is exploited in many thecnological applications. In the last decade, the interest for osmosis problems has grown with the ever-incresing development of nano-thecnologies and the classical theories, like the Van't Hoff or Morse equations for osmotic pressure, have been observed to fail in many circumstances and this has prompted the development of a quantity of models trying to describe osmotic processes in non-classical regimes. Recently some authors tried to modify the classical laws introducing some parameters of the problem neglected before such as the solute-solvent interaction and the finite volume of solute molecules, or the mechanism of transport of molecules inside the pores of the membrane. This last issue concerning is of particular interest and deserves further investigation. In a current article that focuses on a new kind of phenomenon called "transient osmosis" we find, first of all, a clarification of the phenomenon of interest, because osmosis is an equilibrium phenomenon and does not depend on the process which leads to it. Moreover the proposed model presents the features of a process similar to osmosis, but influenced by the anomalous beahvior of transport inside the pores.

In accordance with these ideas, the aim of our work is to build a mathematical model to describe the behavior of molecules inside the pores of membranes at the nanometric scale, where a wide variety of anomalous transport phenomena occurs. We take our inspiration observing the features of a tipical tool used to simulate transport of matter in nanopores: the polygonal billiards. An idealization of them has been given in terms of chains of deterministic maps, and this is the way we undertake in this work. Therefore we introduce a class of chains of deterministic maps, which we call slicer maps, which enjoy some features of the dynamics of polygonal billiards, trying to reproduce the same wide range of anomalous behaviors. We manage to do this

by furnishing our map of infinitely many scales and we study the transport behaviors trhough the analysis of the mean square displacement produced by the dynamics of these maps. We also compare the behavior of our maps with a sthocastic model often used to study anomalous transport problems: the Lévy walk. We evince that a trivial deterministic map, like our slicer map, seems to behave indistinguishably from a Lévy walk.
Nevertheless these chain of slicer maps have an infinite range of scales introduced by hand, hence they are rather different fro polygonal billiards, from this point of view. Therefore, we try to overcame this difficulty different kind of modifications, both in the dynamics and in the process of producing infinitely many scales. These variations of the model raise some new questions that remain open to further investigations.

Contents

Chapter 1

Introduction

Osmosis is a fundamental physical process concerning the passage of solvent molecules across a membrane separating two liquid solutions [1]. Osmosis is involved in many biological phenomena as fluids exchange in animal cells and water transport in plants [2]. It also is involved in many technological applications such as controlled drug delivery and water purification [3],[4]. In the last decade, the interest for osmosis problems has grown with the ever-incresing development of nano-technologies and in particular of their application to the modern challenges of biomedicine and pharmacology [5]. As a result, the classical theories have been observed to fail in many circumstances and this has prompted the development of a quantity of models trying to describe osmotic processes in non-classical regimes, i.e. in non-ideal diluted mixtures.

1.1 The Osmotic Problem

The best known model for osmotic pressure, applicable to ideal dilute mixtures, was proposed by Van't Hoff in 1885 [6] and is expressed by the celebrated equation:

$$\pi = RTC \tag{1.1}$$

where π is the osmotic pressure, R is the universal gas constant, T is the absolute temperature and C is the molar concentration of the solute. A similar equation was proposed also by Morse [7]:

$$\pi = RTm \tag{1.2}$$

where m is the volume molal concentration of the solute.
These classical theories are predictive, in the sense that they don't require adjustable parameters, but they are applicable only in the limited regime of ideal solutions with dilute solute concentration.
To go beyond these limits the classical relations have been generalized in the years in several forms.
For example for non-ideal dilute solutions, the virial series [8],[9],[10] has been proposed:

$$\pi_1 = RT\left(\frac{c}{M} + A_2c^2 + A_3c^3 + \dots\right) \tag{1.3}$$

where M is the molecular weight of the solute, A_2, A_3,... are the second, third, etc. virial coefficients and c is the mass concentration of solute.
For non-ideal and non-dilute solutions the following logarithmic equation has been considered [11],[12],[13],[14]:

$$\pi_2 = \left|\frac{RT}{V^\circ}\right| \ln\left(\frac{p^\circ}{p}\right) \tag{1.4}$$

where V° is the molar volume of pure solute, p° and p are the vapor pressures of the pure solvent and of the solvent in the solution, respectively. Both pressures p° and p are measured at the same T and P and are assumed to obey Boyle's law.

1.2 Recent Models

We find a further generalization of such theories also in more recent works. Granik et al. [15] develope a model based on a system of Fick diffusion

equations obtaining the following expression for the osmotic pressure:

$$\pi = RT\Psi \tag{1.5}$$

with

$$\Psi = \frac{C_{1,A}\lambda_A\tau_{2,A}C_{2,A} - (C_{1,B} + \lambda_B\tau_{2,B}C_{2,B})(C_{1,A} + \lambda_A C_{2,A})}{C_{1,B} + \lambda_B C_{2,B}} \tag{1.6}$$

where $C_{n,i},\ i = A, B$ are the molar concentrations of solvent, solute and solutions in the regions A and B separated by a membrane, λ_i are parameters describing the relative sizes of solute and solvent and $\tau_{2,A}$ e $\tau_{2,B}$ represents the solute fractions which pass through the membrane.

In the literature we can find validation of the theory of Granik et al., by means of some experiments and of a certain analysis of already known data [16]. These authors surely introduce some innovation with respect to the classical models of osmosis and they claim that their model holds more generally than classical theories. Nevertheless successive experiments of Pizzi et al. showed that the theory by Granik et al. in general substantially diverge from experimental data [17]. Moreover they introduced a new expression of the osmotic pressure, at low pressures and low concentrations, taking into account the specific interaction of solvent and solute and the finite volume of the solute molecules:

$$\pi = \frac{KT}{v}\left[1 + \frac{k_p y_H^\delta}{v}\,C + \left(\frac{k_p y_H^\delta}{v}\,C\right)^2\right] \tag{1.7}$$

Here C is the solute concentration, T the absolute temperature, v the volume of solvent molecules, y_H a parameter which is meant to express the interaction between solvent and solute molecules, δ, K and k_p are constants related to the model characteristics.

Another interesting approach to osmosis problem is the work of Cosentino et al. [18]. In it a modification of the diffusion coefficient [19] is used to obtaine a non-linear diffusion equation describing the behavior of brownian particles that interacts with each other with Van der Walls forces.

We want to stress that all these recent theories and in many others (cf. e.g.

[20], [21]), differently from the classical ones, based on a thermodynamic derivation of osmotic pressure and, in particular, on the chemical potential equation, need to consider new elements in studying osmosis, as for example the solute molecules size and their interactions.
Moreover in these theories the problem of osmosis is referred to the transport of the molecules of solution inside the pores of the 'semipermeable membrane'.
This fact, on one side suggest that to fully understand the osmotic problem beyond the classical regime one has to consider the transport of mass of solvent and solute through the pores of the membrane.
However, this formulation of the problem is not correct because if the solute molecules can pass through the pores of the membrane dividing the solutions, stricltly speaking, there can be no osmotic pressure.
Osmosis, indeed, is tipically an equilibrium phenomenon and does not depend on the process which leads to it and then we cannot relate it to the passage of solute particles in the membrane. At the same time at the nanoscale we observe a wide variety of phenomena that require new analysis and interpretation as they do not follow the classical thermodynamic and hydrodinamic laws.

1.3 Transient Osmosis

The recent work of Igarashi, Rondoni, Botrugno and Pizzi [22] calls our attention precisely to the problem mentioned above, analyzing the dynamics of concentrations of a solution inside a system consisting of two containers connected by narrow and short channels. When the size of solute molecules becomes smaller but still comparable with pore size, their flow across the pore itself tipically becomes anomalous in fact they violated the basic tenets of kinetic theory which requires the mean free paths of molecules to be much smaller then the size of their containers [23], [24], [25], [26], [27], [28]. The

authors of the work [22] shows how this fact may lead to a sequence of quasi-stationary states in which the amount of solute from both sides of the membrane remains practically constant for very long periods of time. In this situation, pressure gradients develop, similarly to those due to the osmotic process.

One thus has the occurrence of transient phenomena apparently similar to osmosis, but completely different from that, since they are nonequilibrium phenomena which sooner or later will result in a state of equilibrium at zero pressure. In any case the relaxation to equilibrium in this context must take into account a multitude of different parameters, including the size of membrane pores, as well as those of solute and solvent particles, etc. These phenomena different from osmosis, differ also from the free flux of fluids as described by hydrodinamics. We can imagine a new class of intermediate phenomena that vary depending on the relative size of solute, solvent and the cross section of membrane's pore. For example in a case in which both the solvent and the solute molecules pass through the membrane at different velocities, it develops a transitional imbalance of pressure, this new phenomenon has been called 'transient osmosis'. Unlike the case of standard osmosis, in transient osmosis it becomes obviously relevant the rate of transport of matter through the membrane.

Therefore, the connection between the problem of osmotic pressure and the problem of anomalous transport of matter becomes of interest and leads us to wonder about the possibility of building new models, describing the transport of matter through the channel of microporous and mostly nanoporous membranes.

1.4 Polygonal Billiards

Among the models of transport of matter in membranes with pore of size of the same order of the molecules, at low densities we find the polygonal

billiards [23], [24].
A polygonal billiard is a dynamical system generated by the motion of a point particle with constant unit speed inside a bounded domain. Its dynamics are not chaotic, in the sense that they have vanishing Lyapunov exponents, and present a very rich range of transport properties, but their mathematical complexity prevents an analytical detailed study. An idealization of billiards has been given in terms of chains of deterministic maps [29], [30], [31] and this is the way we undertake in this work. We will infact build a simple deterministic map able to mimic the fundamental characteristics of polygonal billiards, such as non-chaoticity and preservation of volumes.

1.5 Normal and Anomalous Diffusion

Commonly mass transport processes generated by gradients in chemical potential are described by in terms of Fickian diffusion relating the mass flux to gradients in local density. Fick's first law is expressed by [32]:

$$J(x) = -D\frac{\partial c}{\partial x} \tag{1.8}$$

where J is the mass flow, D is the diffusion coefficient, c is the mass concentration and x is the position in space. This law, which can be justified in kinetic theory [33], provides the phenomenological basis for the mathematics of diffusion in molecular systems, leading to the second-order partial differential equation:

$$\frac{\partial c}{\partial t} = D\frac{\partial^2 c}{\partial x^2} \tag{1.9}$$

known as Fick's second law, where t is the time variable. The well-known Gaussian evolution

$$c(x,t) = (4\pi Dt)^{-1/2} e^{-x^2/4Dt} \tag{1.10}$$

resultS from an initial δ-function distribution, and the linearity of (1.9) ensures that the diffusion of a system of molecules can be considered as the evolution of a superposition of Gaussian. In particular, we can recover from

(1.10) the linear growth in the mean square displacement for macroscopic diffusion process:

$$\langle x^2(t)\rangle = \int_{-\infty}^{\infty} x^2 c(x,t)dx = 2Dt \tag{1.11}$$

We note that it has become customary to call diffusive any phenomenon displaying a linear relation between the mean square displacement and time as in (1.11), namely

$$\langle \Delta x^2(t)\rangle_\mu \sim t \tag{1.12}$$

asymptotically in time, with $\langle \cdot \rangle_\mu$ being the average with respect to the relevant probability measure. In this work we do the same. Accordingly to this in general the diffusion coefficient is given by [34], [35]:

$$D = \lim_{t\to\infty} \langle \frac{1}{2t} \Delta x^2(t)\rangle_\mu \tag{1.13}$$

In analogy to this, we consider the following definition to characterize the transport law, in non diffusive regime [36], [37]:

Definition 1.1. *Let $\langle \Delta x^2(t)\rangle$ be the mean square displacement of the particles system, i.e. the variance of the probability distribution of the particles, and assume that the generalized diffusion coefficient is finite, i.e.*

$$\lim_{t\to\infty} \frac{\langle \Delta x^2(t)\rangle}{t^\gamma} = T \in (0,\infty), \tag{1.14}$$

then

(i) If $\gamma < 1$ the transport is called sub-diffusive

(ii) If $\gamma = 1$ the transport is called diffusive

(iii) If $\gamma > 1$ the transport is called super-diffusive (in particular is called ballistic in the case $\gamma = 2$)

γ is called transport exponent.

1.6 Outline of the Thesis

The present work is organized as follow: in the first chapter we gave an overview of the problem of osmosis from the classical models and their modifications, till the most recent studies, and we illustrated the connection of osmosis with the problem of anomalous transport. Moreover we mentioned the structure of polygonal billiards that we aim to reproduce and the main notation and definitions we will refer in our work.
In chapter 2 we outline the mathematical background to the modeling of transport, introducing the basis of the classical dynamical systems theories and giving some examples relevant for our aim, as baker and multi-baker transformations. Moreover we outline an example of weakly chaotic systems.
In chapter 3 we briefly introduce the billiards systems, focusing on polygonal billiards and on a particular study of polygonal channels.
In the central chapters 4 and 5 we introduce and study our slicer model. In chapter 4 we provide the definition of the model and we go through its mathematical details presenting asymptotic results for mean square displacement and for successive moments, both analitically and numerically. In chapter 5 we present the comparison with a Lévy walk model underlying the indistinguishability between the two dynamics.
Finally, in chapter 6 we propose some variations of our model, that brings to some open questions mentioned in the conclusions.

Chapter 2

Dynamical Systems

In this chapter we give the mathematical background on which we have built the models proposed in this work.
We start from an introduction of classical continuous and discrete dynamical systems [38], then we introduce some statistical properties of dynamical systems [38], [39] and we conclude presenting some relevant examples, as baker [29], [39] and multi-baker [29], [31], [40] transformations, with related properties.
Moreover in the same framework we outline an approach to reach anomaluos behavior starting with deterministic chaos and then reducing the degree of chaos of the system [41].

2.1 Continuous Dynamical Systems

Let us consider a system of differential equations:

$$\frac{dx}{dt} := \dot{x} = f(x) \tag{2.1}$$

where $x = x(t) \in \mathbb{R}^n$ is a vector valued function of an independent variable and $f : U \to \mathbb{R}^n$ is a smooth function defined on some subset $U \subseteq \mathbb{R}^n$. We say that the vector field f generates a flow $\phi_t : U \to \mathbb{R}^n$, where $\phi_t(x) = \phi(x, t)$ is a smooth function defined for all x in U and t in some interval $I = (a, b) \subseteq \mathbb{R}$,

and ϕ satisfies (2.1) in the sense that

$$\frac{d}{dt}\,\phi(x,t)|_{t=\tau} = f\left(\phi(x,\tau)\right) \tag{2.2}$$

for all $x \in \mathbb{R}$ and $\tau \in I$. We note that, in its domain of definition, ϕ_t satisfies the group properties

(i) $\phi_0 = \mathrm{Id}$

(ii) $\phi_{t+s} = \phi_t \circ \phi_s$

Systems in which the vector field does not contain time explicitly, are called autonomous.
We refer to the space underlying the autonomous systems as the phase space. Often initial conditions

$$x(0) = x_0 \in U \tag{2.3}$$

are given, in which case we seek a solution $\phi_t(x_0)$ such that

$$\phi_0(x_0) = x_0. \tag{2.4}$$

In this case $\phi_t(x_0) : I \to \mathbb{R}^n$ defines a trajectory, or orbit of differential equation (2.1) based at x_0.

Definition 2.1. *The pair (U, ϕ_t) of the phase space U, with the flow ϕ_t generated by the vector field f is called dynamical system.*

An important class of solutions of (2.1) are fixed points. Fixed points $\bar{x} \in U$ are defined by the vanishing of the vector field f : $f(\bar{x}) = 0$.

Definition 2.2. *A fixed point $\bar{x}$ is said to be stable if for every neighborhood V of $\bar{x}$ in U there is a neighborhood $V_1 \subset V$ such that every solution $x(x_0, t)$ with $x_0 \in V_1$ is defined and lies in V for all $t > 0$. A fixed point is called unstable if it is not stable. If, in addition, V_1 can be chosen so that $x(t) \to \bar{x}$ as $t \to \infty$ then $\bar{x}$ is said to be asymptotically stable.*

Definition 2.3. *A fixed point $\bar{x}$ is called an hyperbolic fixed point when the Jacobian matrix of first partial derivative of f, Df, evaluated in $\bar{x}$, has no eigenvalues with zero real part.*

In the case of linear systems, i.e. $\dot{x} = Ax$, where A is an $n \times n$ matrix with constant coefficients, we can classify the subspaces spanned by the eigenvectors of A in the following way:
the stable subspace, spanned by the eigenvectors whose eigenvalues have negative real parts;
the unstable subspace, spanned by the eigenvectors whose eigenvalues have positive real parts;
the center subspace, spanned by those eigenvectors whose eigenvalues have zero real parts.
In the nonlinear case we define local stable and unstable manifolds, $W^s_{loc}(\bar{x})$ and $W^u_{loc}(\bar{x})$ respectively, of $\bar{x}$ as follows

$$\begin{aligned} W^s_{loc}(\bar{x}) &= \{x \in V : \phi_t(x) \to \bar{x} \text{ as } t \to \infty, \text{ and } \phi_t(x) \in V \text{ for all } t \geq 0\} \\ W^u_{loc}(\bar{x}) &= \{x \in V : \phi_t(x) \to \bar{x} \text{ as } t \to -\infty, \text{ and } \phi_t(x) \in V \text{ for all } t \leq 0\} \end{aligned} \tag{2.5}$$

where $V \subset \mathbb{R}^n$ is a neighborhood of the fixed point $\bar{x}$. Linear and nonlinear systems posses limit sets other than fixed points; for example, closed or periodic orbits frequently occur.

Definition 2.4. *An orbit located at x_0 is called periodic if there exists $0 < T < \infty$ such that $\phi_t(x_0) = \phi_{t+T}(x_0)$ for all t.*

2.2 Discrete Dynamical Systems

The flow of the system (2.1) gives rise to a discrete time dynamical system, e.g. by taking $G(x) = \Phi_1(x)$, and writing:

$$x_{n+1} = G(x_n) \tag{2.6}$$

Given an initial condition x_0, an orbit of the map (2.6) is a sequence of points $\{x_0, x_1, x_2, \ldots, x_n\}$. In the linear case, i.e. for $x_{n+1} = Bx_n$, where B is a constant coefficient matrix, we can define stable, unstable and center subspaces

in a analogous manner to that for linear vector fields:
the stable subspace, spanned by the eigenvectors of matrix B whose eigenvalues have modulus < 1;
the unstable subspace, spanned by the eigenvectors of matrix B whose eigenvalues have modulus > 1;
the center subspace, spanned by those eigenvectors of matrix B whose eigenvalues have modulus $= 1$.
The orbits in the stable and unstable subspaces are characterized by contraction and expansion, respectively. If B has no eigenvalues of unit modulus, the eigenvalues alone serve to determine stability. In this case $x = 0$ is called a hyperbolic fixed point. And in general:

Definition 2.5. *A fixed point $\bar{x}$ for the map G is called a hyperbolic fixed point if $DG(\bar{x})$ has no eigenvalues of unit modulus.*

Stable and unstable manifolds are defined analogously to the case of flows

$$\begin{aligned} W^s_{loc}(\bar{x}) &= \{x \in V : G^n(x) \to \bar{x} \text{ as } n \to \infty, \text{ and } G^n(x) \in V \text{ for all } n \geq 0\} \\ W^u_{loc}(\bar{x}) &= \left\{x \in V : G^{-n} \to \bar{x} \text{ as } n \to -\infty, \text{ and } G^{-n}(x) \in V \text{ for all } n \geq 0\right\} \end{aligned} \tag{2.7}$$

and the corresponding global manifolds are defined by taking the unions of backwards and forward iterates of the local manifolds.

Definition 2.6. *The map ϕ_t is said to be topologically transitive on U if there exists a point $x \in U$ such that its orbit is dense in U.*

2.3 Statistical Properties

Let $G : X \to X$, be a mapping of the metric space X. An invariant measure μ for G is a measure with the property that $\mu(G^{-1}(A)) = \mu(A)$ for all measurable sets A. A probability measure μ is a measure for which $\mu(X) = 1$. The triple (X, μ, G) is called classical dynamical system.

Definition 2.7. *Let $G : \mathbb{R}^n \to \mathbb{R}^n$ define a discrete dynamical system and let $g : \mathbb{R}^n \to \mathbb{R}$ be a real valued function. The quantity*

$$\bar{g}(x) = \lim_{N\to\infty} \frac{1}{N} \sum_{k=0}^{N-1} g\left(G^k(x)\right), \tag{2.8}$$

is called, if it exists, time average of g on the trajectory of x.
For a continuous flow $\phi_t : \mathbb{R}^n \to \mathbb{R}^n$ the time average of g on the trajectory of x is

$$\bar{g}(x) = \lim_{T\to\infty} \frac{1}{T} \int_0^T g\left(\phi_t(x)\right) dt. \tag{2.9}$$

Definition 2.8. *Let $U \subset \mathbb{R}^n$ and $g : U \to \mathbb{R}^n$ such that $g \in L_1(U, \mu)$. The quantity*

$$\langle g \rangle := \int_U g d\mu \tag{2.10}$$

is called ensamble average of g.

The existence of the time averages (2.8) or (2.9) is guaranteed, under quite general conditions, by Birkhoff theorem:

Theorem 2.3.1. *Le (X, μ, G) be a classical discrete dynamical system and let g be a function in $L_1(x, \mu)$. Then the limit*

$$\bar{g}(x) = \lim_{N\to\infty} \frac{1}{N} \sum_{k=0}^{N-1} g\left(G^k(x)\right) \tag{2.11}$$

exists μ-almost everywhere, and moreover

$$\bar{g}\left(G(x)\right) = \bar{g}(x), \quad \langle \bar{g} \rangle = \langle g \rangle.$$

Definition 2.9. *A property is said to hold μ-almost everywhere if the set of elements for which the property does not hold is of measure zero with respect to the given measure μ. In this case one also says that the property holds for a typical element.*

Definition 2.10. *A dynamical system is called ergodic if*

$$\bar{g}(x) = \langle g \rangle \tag{2.12}$$

μ-almost everywhere.

Definition 2.11. *A dynamical system (X, μ, G), is said to be mixing if for each pair of measurable sets A and B in X the following holds*

$$\lim_{n\to\infty} \mu(G^{-n}(A) \cap B) = \mu(A)\mu(B). \tag{2.13}$$

Definition 2.12. *Let $G : \mathbb{R}^n \to \mathbb{R}^n$ define a discrete dynamical system and select a point $x \in \mathbb{R}^n$. Suppose that there are subspaces $V_i^{(1)} \supset V_i^{(2)} \supset \ldots \supset V_i^{(n)}$ in the tangent space at $G^i(x)$ and numbers $\mu_1 \geq \mu_2 \geq \ldots \geq \mu_n$ with the properties that*

1. *$DG(x)(V_i^{(j)}) = V_{i+1}^{(j)}$*
2. *$dim\ V_i^{(j)} = n + 1 - j$*
3. *$\lim_{N\to\infty} \frac{1}{N} \log \left\| DG^N(x)(v) \right\| = \mu_j$ for all $v \in V_0^{(j)} \backslash V_0^{(j+1)}$.*

The quantities μ_j are called the Lyapunov exponents of G.

If $x = \bar{x}$ is a fixed point for G, then the subspaces $V_i^{(j)} = V^{(j)}$ do not depend upon i and are simply the eigenspaces associated with eigenvalues of $DG(\bar{x})$. The Lyapunov exponents are the logarithms of the moduli of these eigenvalues.

Definition 2.13. *The map G is said to be chaotic in the sens of Ljapunov on X if it is topologically transitive and it has a positive Ljapunov exponent for a typical x_0.*

With 'typical' we mean that this statement applies to any point that we randomly pick up on X with non-zero probability.

Definition 2.14. *The dynamics G on a phase space U is called time reversal invariant if there exists an involution $i : U \to U$ such that $iG(x) = G^{-1}i(x)$ $\forall x \in U$.*

An involution i is a map such that $i^2 = Id$, hence $iG^n = G^{-n}i$ $\forall n$ if G is time reversal invariant.

Definition 2.15. *Two dynamical systems (X, μ, G) and (Y, ν, F) are isomorphic if there exists a μ-almost everywhere invertible map $h : X \to Y$ which preserves the measure, i.e.*

$$\nu\left(h\left(A\right)\right) = \mu(A) \quad \textit{and} \quad \mu\left(h^{-1}\left(B\right)\right) = \nu(B) \tag{2.14}$$

for all measurable sets $A \subset X$ and $B \subset Y$. And such that for all t

$$F^t \circ h = h \circ G^t \tag{2.15}$$

We proceed now to address some relevant examples of deterministic map defyining some dynamical systems.

2.4 Relevant Examples

2.4.1 The Baker Transformation

Let the phase space be the 2-dimensional torus $M = [0, 1] \times [0, 1]$, where the sides at 0 and 1 are identified.

Definition 2.16. *The map $B : M \to M$ such that:*

$$B(x, y) = \begin{cases} \left(2x, \dfrac{y}{2}\right) & \textit{for } 0 \leq x < \frac{1}{2} \\ \left(2x - 1, \dfrac{y+1}{2}\right) & \textit{for } \frac{1}{2} \leq x < 1 \end{cases} \tag{2.16}$$

B is called baker map.

This map is a transformation of the square into itself which expands distances in the x-direction (the unstable manifold) and contracts them in the y-direction (the stable manifold). As we can see in the Fig. 2.1 the map consists of two steps: in the first step the unit square becomes a rectangle occupying the region $0 \leq x \leq 2$; $0 \leq y \leq 1/2$. This operation does not change the area of the original region. Next, the rectangle is cut in the middle and the right half is put on top of the left half, to recover a square. This doesn't change the area either. This transformation is reversible except

on the lines where the area was cut in two and glued back. The inverse defined on the same phase space M, is given by:

$$B^{-1} : (x,p) \longmapsto \begin{cases} \left(\frac{x}{2}, 2y\right) & \text{for } 0 \leq y < \frac{1}{2} \\ \left(\frac{x+1}{2}, 2y-1\right) & \text{for } \frac{1}{2} \leq y < 1 \end{cases} . \tag{2.17}$$

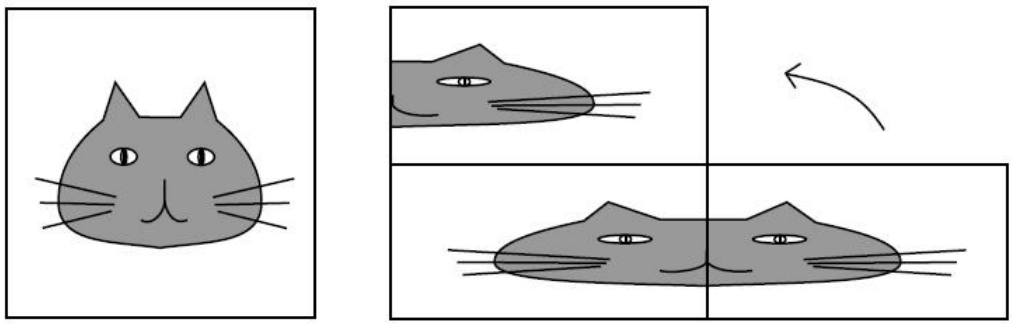

Figure 2.1: Baker map

The baker map is ergodic and mixing [29]. This map is one of the simplest illustrations of how a stretching can work togheter with compression and folding to produce deterministic chaos. Indeed, so much chaos that baker dynamics posses the random properties of a sequence of tosses of a balanced coin with equal probabilities for heads and tails. This is possible by means of an isomorphism beetween the baker map and a Bernoulli shift.

Definition 2.17. *Let I be a finite set of symbols (alphabet), $I = \{0, 1, \ldots, n-1\}$ and let $N = I^{\mathbb{Z}}$ the space of the bi-infinite sequences of symbols of the alphabet,*

$$N = \{(\ldots, x_{-1}, x_0, x_1, \ldots) : \ x_i \in I\} \tag{2.18}$$

Let Ψ be a trasformation that acts on N as the translation of a position to the left, namely it associates to the sequence $x = (\ldots, x_{-1}, x_0, x_1, \ldots)$ the vector $\Psi(x) = x' = (\ldots, x'_{-1}, x'_0, x'_1, \ldots)$ such that

$$x'_k = x_{k+1}.$$

Finally we give to N the Borel-space structure, i.e. we built on N a σ-algebra of measurable sets, taking as generators the cylinders:

$$C_k^l := \{x \in N \ : \ x_k = l, \quad k \in \mathbb{Z}, \ l \in I\}$$

and to build the measure ν, we take n positive, real numbers $p_0, \ldots, p_{n-1}$ such that $\sum_{l \in I} p_l = 1$, and we set

$$\nu(C_k^l) = p_l.$$

The dynamical system (N, Ψ, ν) so built is called Bernoulli shift and we denote it by $B_{p_0,\ldots,p_{n-1}}$.

The Bernoulli shift is a model that describes a sequence of independent events, each one with an assigned pobability. The simplest one, $B_{\frac{1}{2},\frac{1}{2}}$, corresponds to the coin tossing game.

Proposition 2.4.1. *The baker map and the Bernoulli shift $B_{\frac{1}{2},\frac{1}{2}}$ are isomorphic.*

Proof. Let (M, μ, Φ) and (N, ν, Ψ) be the two dynamical system and let $x = (a, b)$ be points of M and y the sequences of N. If we consider the binary expression of a and b

$$a = 0.a_0a_1a_2 \ldots \ , \ b = 0.b_0b_1b_2 \ldots \ , \quad a_i, b_i \in I = 0, 1$$

then we can define h associating to $x \in M$ the point $y = h(x) \in \mathbb{N}$, given by

$$\begin{aligned} y &= (\ldots, y_{-2}, y_{-1}, y_0, y_1, y_2, \ldots) \\ &= (\ldots, b_1, b_0, a_0, a_1, a_2, \ldots), \end{aligned}$$

namely

$$y_i = a_i \quad \text{for } i \geq 0, \quad y_i = b_{-i-1} \text{ for } i < 0.$$

The corrispondence is defined and bijective almost everywhere; and it is equally easily possible to verify that h commutes with the dynamics and preserves the measure [39]. □

2.4.2 Multibaker Map

Moving from the definition of baker map, we can now introduce the so-called multibaker map [29]. We take as phase-space a chain of squares of side $a = 1$, where the baker map acts in the same fashion already described in the previous section, streching and cutting each one of the squares but redistributing the cut pieces on several neighbouring squares. The definition of the map is the following (cf. Fig.2.2)

Definition 2.18. *Let* $\hat{M} = [0,1)^2 \times \mathbb{Z}$. *The map* $\hat{B} : \hat{M} \to \hat{M}$ *such that*

$$\hat{B}(x,y;m) = \begin{cases} \left(2x, \frac{y}{2}; m-1\right) & \textit{for } 0 \le x \le \frac{1}{2} \\ \left(2x-1, \frac{y+1}{2}; m+1\right) & \textit{for } \frac{1}{2} \le x \le 1 \end{cases} \tag{2.19}$$

is called multibaker map.

Here we can recognize the action of the baker map on the coordinates (x,y). This action is combined with displacement $m \to m \pm 1$ along the chain.

The multibaker map is invertible with the following inverse

$$\hat{B}^{-1} : (x,y;m) \longmapsto \begin{cases} \left(\frac{x}{2}, 2y; m+1\right) & \text{for } 0 \le y < \frac{1}{2} \\ \left(\frac{x+1}{2}, 2y-1; m-1\right) & \text{for } \frac{1}{2} \le y < 1 \end{cases} \tag{2.20}$$

The multibaker dynamics is not only invertible but also time reversal invariant, i.e. there exists an involution i satysfying

$$iB = B^{-1}i$$

which is given by:

$$i(x,y,m) := (1-y, 1-x, m) \tag{2.21}$$

The multibaker map is uniformly hyperbolic with stretching factor 2 and thus posses a positive Lyapunov exponent equal to $\log 2$ [40].
This system is a model of deterministic diffusion, indeed the redistribution

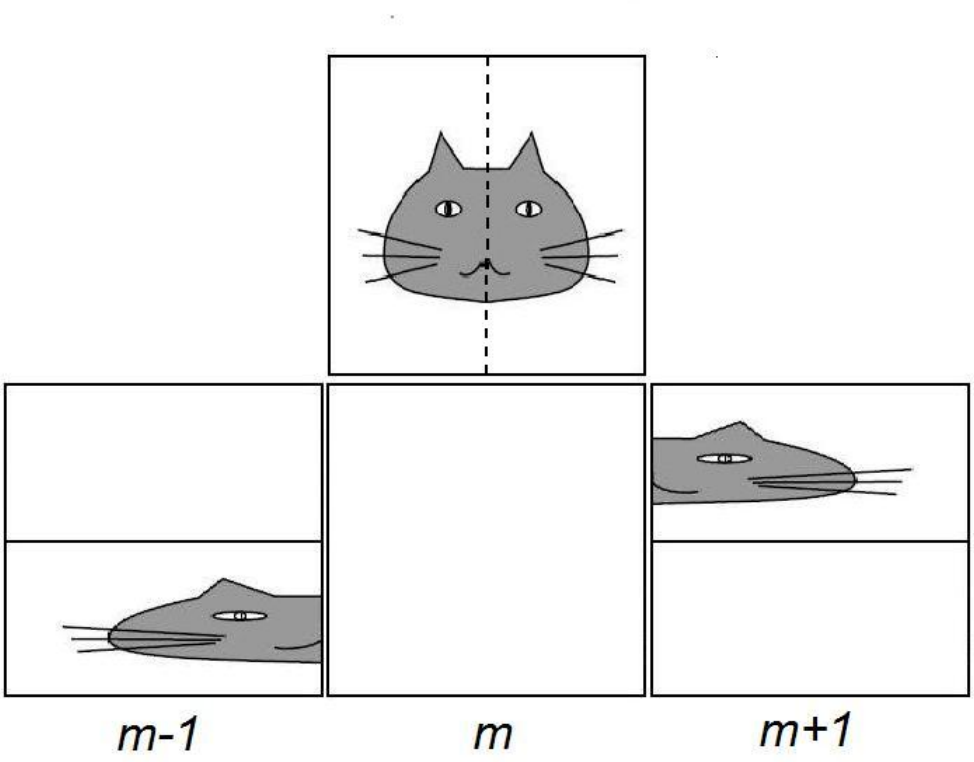

Figure 2.2: Action of multibaker map on initial conditions in a generic cell m.

of the cut pieces to neighbouring squares along the chain induces a diffusive transport law. In other words, (1.12) holds with respect to the Lebesgue measure on the 0-th square, for the observable $x(t)$ representing the position of $(x, y, 0)$ after t steps. Moreover since the multibaker map is area-preserving the Lebesgue measure $dm = dxdy$ is invariant and this fact gives equal probability $1/2$ to the displacement to the right and to the left. Accordingly, this chaotic model is isomorphic to the standard symmetric random walk, hence we can say that it describes normal diffusion with diffusion coefficient equal to $D = \frac{1}{2}$ (cf. Eq. 1.13).

2.5 Deterministic Standard and Anomalous Diffusion

As we have said, multibaker maps reproduce diffusion by means of very simple deterministic dynamics. In general if the resulting dynamics of an ensamble of particles for given equations of motion has the property that a diffusion coefficient $D > 0$ (1.13) exists, we speak of deterministic diffusion [29], [30], [42]. In this section we will outline another simple model of standard deterministic diffusion before moving to a model of deterministic anomalous diffusion. We will follow R.Klages' notes, Ref. [41].
Let's consider a point particle. The orbit of such a particle starting at initial condition x_0 may be generated by a chaotic dynamical system $(M, \mu, \hat{B}_a)$ with equations of motion $x_{n+1} = \hat{B}_a(x_n)$. To define $\hat{B}_a : M \to M$ we begin with a generalization of the Bernoulli shift, starting from $B_a : [0, 1) \to [1-a/2, a/2)$ that acts as follow:

$$B_a(x) := \begin{cases} ax & \text{if } 0 \leq x < 1/2 \\ ax + 1 - a & \text{if } 1/2 \leq x < 1 \end{cases} \tag{2.22}$$

with $a \geq 2$ a control parameter. Notice that for $a > 2$ the map defines an open system. Indeed, when points are mapped into the interval $(1/a, a-1/a)$ they left the interval of definition. We can call this interval escape region and this map the box map. We then consider a chain of $L \in \mathbb{N}$ boxes and we extend B_a in a periodic way along the chain, i.e. on the whole real line, by the following lift

$$\hat{B}_a(x + 1) = B_a(x) + 1 \tag{2.23}$$

The phase space M is then given by the whole real line. In Fig.2.3 there is an illustration of the map B_a. By means of the escape-rate formalism [29], [30], it is possible to calculate in a rigorous way the diffusion coefficient for each value of the parameter a, for example for $a = 4$ it results:

$$D(4) = \frac{1}{4}\frac{L^2}{(L+1)^2} + O(L^{-4}) \to \frac{1}{4} \ (L \to \infty). \tag{2.24}$$

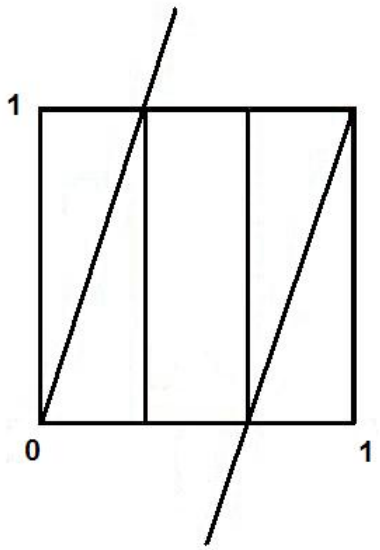

Figure 2.3: Open Bernoulli Shift B_a

Since this coefficient exists and is finite, we can speak of deterministic diffusion.

Now we want to move towards anomalous diffusion considering a variant of the previous piecewise linear model. To this end let's introduce the Pomeau-Manneville map [43], $P_{a,z} : [0,1] \to [0,1]$, which acts as follow

$$P_{a,z}(x) = x + ax^z \text{ mod1} \tag{2.25}$$

where the dynamics is defined by $x_{n+1} = P_{a,z}(x_n)$. This map has two control parameters, $a \geq 1$ and the exponent of nonlinearity $z \geq 1$. For $a = 1$ and $z = 1$ this map just reduces to a map isomorphic to our familiar Bernoulli shift, however, for $z > 1$ it provides a nontrivial generalization of it. Since the map is smooth around $x = 0$, the dynamics resulting from the left branch of the map is determined by the stability of this fixed point, whereas the right branch is just of Bernoulli shift-type of map yielding ordinary chaotic dynamics. There is thus a competition in the dynamics between these two different

branches, indeed, one can observe that long, almost periodic phases, determined by the marginal fixed point around $x = 0$ are interrupted by chaotic bursts reflecting the Bernoulli shift-like part of the map with slope $a > 1$ around $x = 1$ [44], [45].

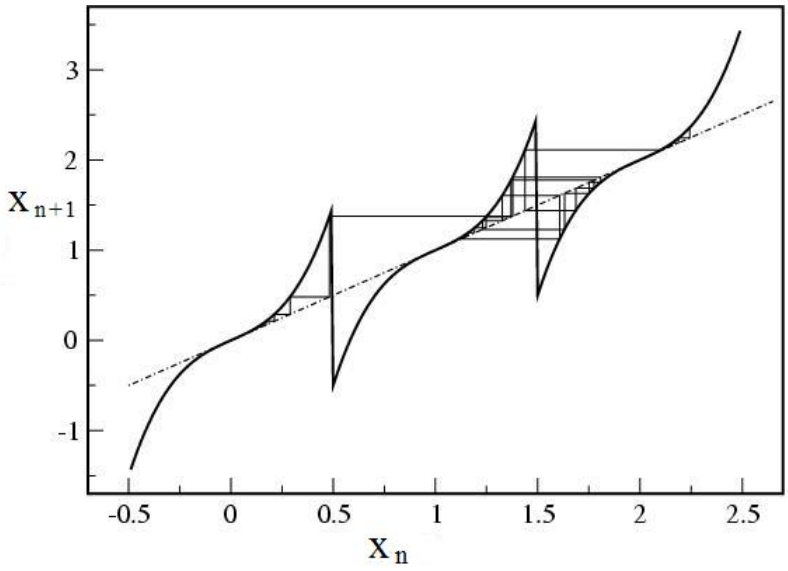

Figure 2.4: The extended Pomeau-Manneville map

As done before for the map B_a, we define a spatially extended version of the Pomeau-manneville map: for this purpose we just continue $P_{a,z}(x) = x + ax^z$, with $0 \leq x < 1/2$ onto the real line by the translation $P_{a,z}(x+1) = P_{a,z}(x) + 1$, under reflection symmetry $P_{a,z}(-x) = -P_{a,z}(x)$. The resulting model is displayed in Fig.2.4. Now if we proceed calculating the mean square displacement (1.12) either analytically or from computer simulations one finds that for $z > 2$

$$\langle x^2(n) \rangle \sim \ n^\alpha \ , \ \alpha < 1 \tag{2.26}$$

in the large n limit, cf. (1.12). This implies that the diffusion coefficient (1.13)

$$D = \lim_{n \to \infty} \frac{\langle x^2(n) \rangle}{2n} \tag{2.27}$$

vanishes, despite the fact that particles can go anywhere on the real line. So we encounter a type of diffusive beahviour that is anomalous, and precisely subdiffusive (cf. Def. 1.1).
The generalized diffusion coefficient T (1.14), given by

$$T = \lim_{n\to\infty} \frac{\langle \Delta x^2(n) \rangle}{n^\gamma} \tag{2.28}$$

behaves as a function of a and in an approximation, by means of continuous time random walk theory, can be calculated analititcally. The result is:

$$T_i = p l_i^2 \begin{cases} \dfrac{a^\gamma \sin(\pi\gamma)}{\pi\gamma^{1+\gamma}}, & 0 < \gamma < 1 \\ a\left(1 - \frac{1}{\gamma}\right), & 1 \leq \gamma < \infty \end{cases} \tag{2.29}$$

where p is the escape region, l_i, $i \in \{1, 2\}$, is a typical jump lenght and $\gamma := 1/(z-1)$. From our perspective it is important to note that this model of anomalous diffusion is obtained perturbing a chaotic model, so that it is not uniformly hyperbolic anymore. However, the dynamics remains chaotic, in the sense of having a positive Lyapunov exponent.

Chapter 3

Billiards

Billiards form an important class among dynamical system with singularities, both in the general theory and in applications. By billiards we mean a dynamical system generated by the motion by inertia of a point mass within a domain with smooth, or piecewise smooth boundary with specular reflections at the boundary.
In this chapter we outline first some general definitions about billiards [46], [47], [48]. Then we focus on the sub-class of polygonal billiards [49], [50] and among these we choose to report some results from [23], [24] about transport behavior of non-interacting particles in simple polygonal channels.

3.1 General Definitions

Definition 3.1. *Let Q be a compact closed connected domain in $\mathbb{R}^d$ or on a d-torus $\mathbb{T}^d = \mathbb{R}^d/\mathbb{Z}^d$. Let the boundary ∂Q be a finite union of smooth compact manifolds of codimension one, $\partial Q = \Gamma = \Gamma_1 \cup \ldots \cup \Gamma_r$, $r \geq 1$. We call Q a billiard table and ∂Q its wall.*

Definition 3.2. *Let the set $\Gamma^* = \bigcup_{i \neq j} (\Gamma_i \cap \Gamma_j)$ be a finite union of smooth compact submanifolds of codimension ≥ 2. Γ^* is called the singular part of ∂Q. This set includes all the corner points of the wall ∂Q. Let $\tilde{\Gamma} = \Gamma \backslash \Gamma^*$. A point $q \in \tilde{\Gamma}$ is called regular point.*

Let M be a unit tangent bundle of Q, i.e.

$$M = \left\{x = (q, v); q \in Q, v \in S^{d-1}\right\} \tag{3.1}$$

where $S^{d-1} \subset \mathbb{R}^{d-1}$ is a unit sphere. A point $x = (q, v) \in M$ is called a line element with a footpoint q. We denote with π_q and π_v the natural projections of M onto Q and S^{d-1} respectively, so that $\pi_q(q, v) = q$ and $\pi_v(q, v) = v$. We consider on M the normalized Liuville measure $d\mu = c_\mu dqdv$, where dq and dv are the Lebesgue measure on Q and S^{d-1} respectively, and $c_\mu = \left(|Q| \cdot \left|S^{d-1}\right|\right)^{-1}$ is the normalizing factor. Here $|Q|$ is the volume of the domain Q and $\left|S^{d-1}\right|$ is the $(d-1)$-dimensional volume of the unit sphere in $\mathbb{R}^d$. M will be the phase space for the billiard systems.

3.2 Billiard Flows

Here we construct the dynamics on billiard table. Let $q \in Q$ denote the position of the moving particle and $v \in S^{d-1}$ its velocity vector. Of course $q = q(t)$ and $v = v(t)$ are functions of time $t \in \mathbb{R}$. When the particle moves inside the table, so that $q \in \text{int}Q$, it mantains a constant velocity:

$$\dot{q} = v \quad \text{and} \quad \dot{v} = 0 \tag{3.2}$$

(here the dot denotes the time derivative). When the particles collides with the regular part of the boundary, i.e. $q \in \tilde{\Gamma}$, its velocity vector istantaneously get reflected across the tangent line to Γ at the point q. This is specified by the classical rule 'the angle of incidence equals the angle of reflection' and it can be expressed by:

$$v_+ = v_- - 2(n(q) \cdot v_-)n(q) \tag{3.3}$$

where v_+ and v_- are the incoming and outgoing velocity vectors, and $n(q)$ is the inward unit normal vector to the wall Γ at the point of reflection q. The vector $n(q)$ is well defined at all regular points of ∂Q. If the particle hits the singular set Γ^* in general has not a unique continuation and thus it normally

stops there and its further trajectory is not defined.
Let $\tilde{M} \subset M$ denotes the set of states (q, v) on which this dynamics of the moving particle is defined at all times $-\infty < t < +\infty$. Thus we obtain a one-parameter group of transformations (flow):

$$\Phi_t : \tilde{M} \to \tilde{M} \tag{3.4}$$

Definition 3.3. *The group of transformations $\{\Phi_t\}$ is called a billiard in Q.*

A billiard flow Φ_t has a natural cross-section Ω associated to the wall of the billiard table defined by Birkhoff coordinates (q_n, v_n). q_n is the arclenght position of the n-th bounce measured along the billiard boundary and $v_n = |v|\, sen\theta_n$ is the velocity component parallel to the boundary, where θ_n is the angle between the outgoing trajectory and the normal to the boundary. In this framework the dynamics is given by the first return map $T : \Omega \to \Omega$, s.t. $T(q_n, v_n) = (q_{n+1}, v_{n+1})$, which goes from the n-th collision to the (n+1)-st collision [51].

3.3 Polygonal Billiards

A class of interest for our work, among billiards, are the polygonal billiards.

Definition 3.4. *Let P be a bounded domain in $\mathbb{R}^2$ or on the standard torus $\mathbb{T}^2$, whose boundary ∂P consists of a finite number of (straight) line segments. A polygonal billiard is a dynamical system generated by the motion of a point particle with constant unit speed inside P and with elastic reflection at the boundary.*

Definition 3.5. *A polygon P is called rational if the angles between its sides are of the form $\pi m/n$, where m, n are integer. It is called irrational otherwise.*

There are various numerical and mathematical works on the ergodic, mixing and transport properties of rational and irrational polygons [50], [52], [53], [54], [55]. It is known, for instance, that rational polygons are not ergodic

and that they posses periodic orbits. But it is not known wheter generic irrational polygons have any periodic orbit. On the other hand , it is known that irrational polygons whose angles admit a certain superexponentially fast rational approximation are ergodic [52]. However, the models are limited in number, the triangular billiards being the most studied models, and many questions concerning them remain open. Despite the vanishing topological entropy of polygonal channels, pairs of orbits almost always separate [56]. Consequentely, these systems present a certain sensitive dependence on the initial conditions, and their dynamics may appear highly disordered, indistinguishable to the eye from chaotic motions.
In [23] are considered a special kind of polygons which consist of channels that are periodic in the x direction, but bounded by walls in the y direction. The wall consists of straight edges and are arranged in a saw-tooth configuration such that the top and bottom walls are 'in phase', i.e. the peaks of the upper and lower walls have the same horizontal coordinate. The channel can therefore be represented as an elementary cell, as depicted in Fig. 3.1, replicated along the x-axis. The height of this cell is denoted by h and his length is setted to $2\Delta x = 1$. The height of the isosceles triangles comprising the "teeth" along the top and bottom cell walls are denoted by Δy_t and Δy_b respectively.

The particles dynamics in this kind of polygonal channels gives a good approximation of the transport behavior in a pore of a microporous membrane at low densities [23], [24]. The evolution of momenta and positions of the particles in this system are determined by solving the free-flight equations of motion.
Despite being the simplest particle system that could be conceived this system presents a surprising array of transport behaviors. It can be observed to be, sub-diffusive, super-diffusive and apparently diffusive, strongly depending on the boundary geometry as we can observe in Fig. 3.2 and in Fig. 3.3. In Fig. 3.2 the evolution of mean square displacement, as a function of time, is reported for a series of parallel saw-tooth system (with $\Delta y_t = \Delta y_b = \Delta y$)

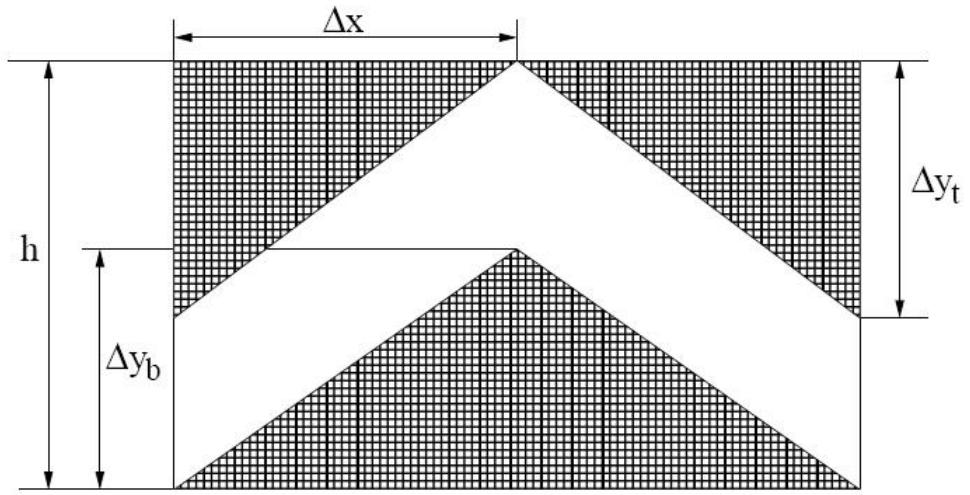

Figure 3.1: Minimal element of polygonal channel

for two different choices of the ratio $\Delta y/\Delta x$. Whereas in Fig. 3.3 are shown in the table different results for the transport exponent γ (cf. 1.14) for the same system and for four different assigned values of height-width ratio.

The authors of [23] claim that this dependence of the transport law on the geometry of the system characterizes such transport as 'complex'. Notion of complexity of billiards dynamics, based on symbolic dynamics, are commonly considered [57], [58] but in the context of [23],[24] the focus is on the complexity of the mass transport as a function of the parameters of the system, rather then the complexity of the dynamics for one given set of parameters. Accordingly to these considerations the authors of [23] introduce the notion of transport complexity, that we report here for completeness.

Definition 3.6. *Consider a transport model, whose geometry is determined by the parameter y, which ranges in the interval $[0, h]$, and such that its transport law is given by*

$$\lim_{t\to\infty} \frac{\langle \Delta x^2(t)\rangle}{t^\gamma} = T \in (0, \infty) \tag{3.5}$$

with γ function of y varying in $[0, 2]$ and $\langle \Delta x^2(t)\rangle$ the mean square displacement, when y spans in $[0, h]$. Let $\Delta\gamma(y_m, y_M) \in (0, \infty]$ be the differ-

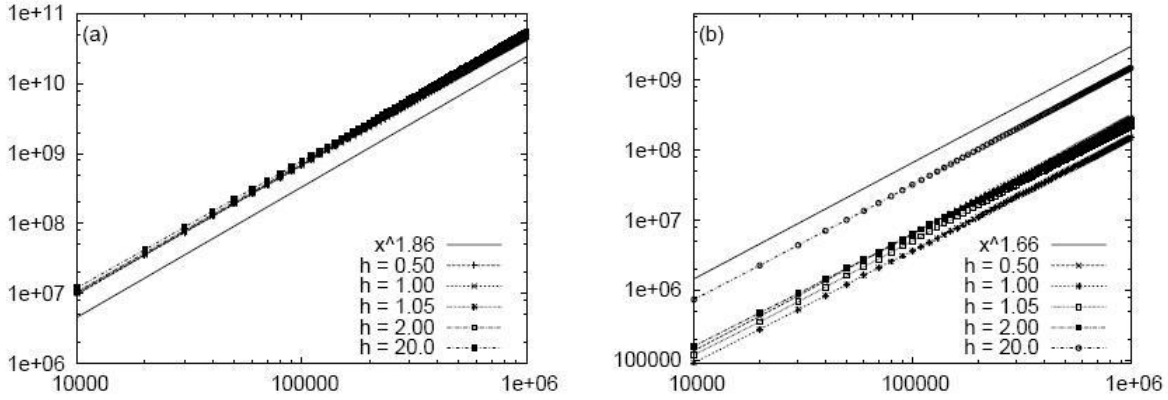

Figure 3.2: Evolution of mean square displacement for parallel saw-tooth systems as function of time. Both in figure (a) and (b) we can evince a super-diffusive behaviour characterized by the transport exponents respectively $\gamma = 1.86$ and $\gamma = 1.66$. These two figures correspond to two different choice of a parameter which characterize the geometry of the system, left panel is related to $\Delta y/\Delta x = 0.25$ and right panel is related to $\Delta y/\Delta x = 1$.

ence between the largest and the smallest value of γ, for y in the subinterval $(y_m, y_M) \subset [0, h]$, where $\Delta\gamma(y_m, y_M) = \infty$ if in (y_m, y_M) there are points for which (3.5) is not satisfied by any $y \geq 0$.

(i) The transport complexity of first kind of the transport model in (y_m, y_M) is the number

$$C_1(y_m, y_M) = \frac{h\ \Delta\gamma(y_m, y_M)}{2\ (y_M - y_m)} \in [0, \infty) \tag{3.6}$$

if it exists.

(ii) The transport complexity of second kind of the transport model for $y = \hat{y}$ is the exponent $C_2 = C_2(\hat{y})$, if it exists, for which the limit

$$\lim_{\epsilon \to 0} \frac{C_1(\hat{y} - \epsilon, \hat{y} + \epsilon)}{\epsilon^{C_2(\hat{y})}} \tag{3.7}$$

is finite.

$\Delta y/\Delta x$	saw-tooth systems				
	$0.5\Delta y$	$1.0\Delta y$	$1.05\Delta y$	$2.0\Delta y$	$20\Delta y$
0.25	1.85	1.83	1.82	1.85	1.85
1	1.66	1.64	1.62	1.67	1.68
2	1.83	1.85	1.82	1.80	1.79
3	1.86	1.87	1.84	1.80	1.70

Figure 3.3: Transport exponents for saw-tooth boundary base triangles with different values of height-width ratio $\Delta y/\Delta x$. For each pore height tested the observed exponent out to 10^6 time units is given.

(iii) The transport complexity of third kind of the transport model for $y = \hat{y}$ is the limit

$$C_3(\hat{y}) = \lim_{\epsilon \to 0} \Delta\gamma(\hat{y} - \epsilon, \hat{y} + \epsilon) \tag{3.8}$$

Billiards thus provide a significant model for the study of the transport of matter in non standard conditions, but at the same time they are too complex to be studied analitically in details. An idealization of billiards with convex obstacles has been given in terms of chains of deterministic maps [29], [30], [31] which, even not expressing the emergent phenomena in their totality, allow a rigourous approach. Therefore similarly we want to build a deterministic map, that can be studied analitically, which resembles the dynamics of polygonal billiards. In particular we want to obtain non diffusive behavior from dynamics which preserve phase space volumes and are not chaotic, like polygonal billiards.

Chapter 4

The Slicer Dynamics

In Chapter 2 we have seen how, reducing the degree of chaos of a deterministic map, we can obtain anomalous behavior. Now we want to do one step further and, looking at the polygonal billiards model, build a dynamical system that produces anomalous transport in absence of chaos. In this chapter we will introduce the classical dynamical system $(\hat{M}, \mu, S_\alpha^n)$ on which the new model is based, how it is constructed and some characteristics of it. The system is defined by means of a map S in which the vertical component is trivial. Nevertheless we preserve the bidimensional nature of the dynamics to stress the analogy with billiard model and in view of further developments (cf. Chap. 6).

4.1 System Details

We will start giving a sequence of definitions about the new model. We will denote the two spatial coordinates as x and y. As for multibaker map the phase space $\hat{M}$ of our dynamics will consist of a chain of identical square cells of linear side $a = 1$ and area $a \times a = 1$, i.e. $\hat{M} = [0, 1] \times [0, 1] \times \mathbb{Z}$. We will indicate the unit square with $M = [0, 1]^2$. The generic cell is identified by the set $M_m = M \times \{m\}$ with $m \in \mathbb{Z}$. Moreover each cell will be equipped with infinitely many 'slicers' partitioning it in subcells. At each temporal step

$n \in \mathbb{N}$ the dynamics will act in each cell activating, beyond the central one, two symmetric slicers depending on the cell index, and therefore dividing each cell into four vertical strips. Then the map will translate each strip within the neighbouring cells by means of the following map.

Definition 4.1. *Let l_m be a parameter in $[0, 1/2]$, $m \in \mathbb{Z}$. The map $S : \hat{M} \to \hat{M}$ such that*

$$S(x, y, m) = \begin{cases} (x, y, m-1) & \text{if } 0 \le x \le l_m \text{ or } \frac{1}{2} \le x \le 1 - l_m \\ (x, y, m+1) & \text{if } l_m < x < \frac{1}{2} \text{ or } 1 - l_m < x \le 1 \end{cases} \tag{4.1}$$

is called 'slicer map'. The vertical lines at $x = l_m$ and $x = 1 - l_m$ are called 'slicers'. Notice that l_m identifies both the two active symmetric slicers in the m-th cell, i.e. l_m and $1 - l_m$.

This map is invertible and its inverse is

$$S^{-1}(x, y, m) = \begin{cases} (x, y, m+1) & \text{if } 0 \le x \le l_m \text{ or } \frac{1}{2} \le x \le 1 - l_m \\ (x, y, m-1) & \text{if } l_m < x < \frac{1}{2} \text{ or } 1 - l_m < x \le 1 \end{cases} \tag{4.2}$$

In Fig. 4.1 the map is defined graphically starting from an initial condition concentrated and uniform in the generic cell $M_m \subset \hat{M}$. Moreover the following holds:

Theorem 4.1.1. *The slicer map S is time reversal invariant.*

Proof. To prove the time-reversability, according to Def. 2.14, it suffices to define an involution $i : \hat{M} \to \hat{M}$. To this end we can take an involution similar to the one used for the multibaker map (2.21), i.e.

$$i(x, y, m) := (1 - x, 1 - y, m) \tag{4.3}$$

Notice that for this map holds that $i^2 = Id$, in fact if we take $(x, y, m) \in \hat{M}$ it results:

$$(x, y, m) \overset{i}{\longmapsto} (1 - x, 1 - y, m) \overset{i}{\longmapsto} (1 - (1 - x), 1 - (1 - y), m) = (x, y, m).$$

Moreover $iS = S^{-1}i$. Indeed, if we take $0 \le x \le l_m$, it results

$$(x, y, m) \overset{S}{\longmapsto} (x, y, m - 1) \overset{i}{\longmapsto} (1 - x, 1 - y, m - 1)$$

and

$$(x, y, m) \overset{i}{\longmapsto} (1-x, 1-y, m) \overset{S^{-1}}{\longmapsto} (1-x, 1-y, m-1)$$

The same can be shown for the remaining three cases. □

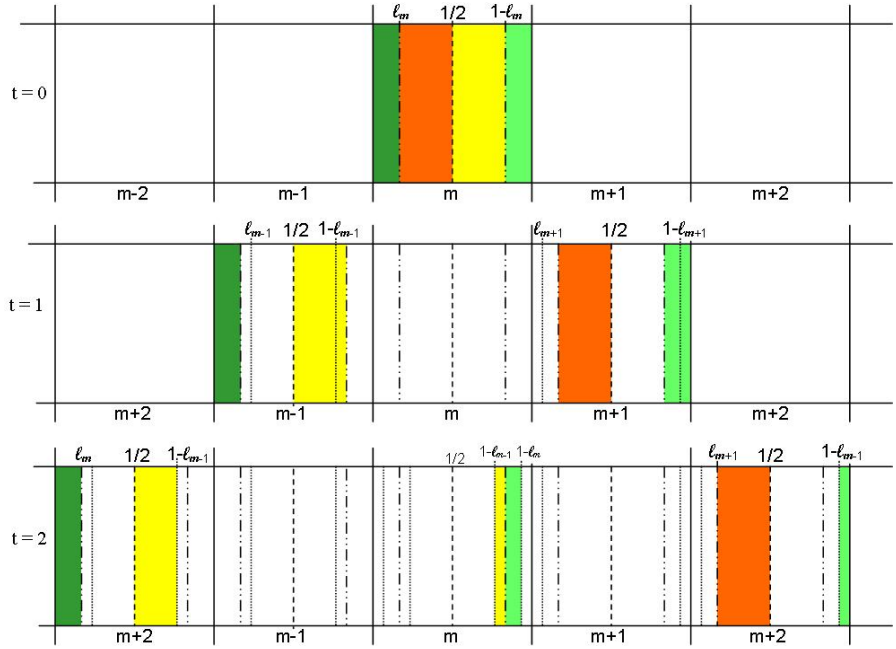

Figure 4.1: Slicer map action for initial conditions in a generic cell $M_m = M \times \{m\}$ in two time steps.

Let us now define a family of infinitely many slicers present in each square cell.

Definition 4.2. *Let $j \in \mathbb{Z}$ be an integer and $\alpha > 0$ a positive parameter in $\mathbb{R}$. The collection*

$$L_\alpha = \left\{ \frac{1}{(|j| + 2^{1/\alpha})^\alpha} := l_j, \ j \in \mathbb{Z} \right\} \tag{4.4}$$

is a family of α-slicers.

Let us introduce now a rule for the activation of the slicers in each cell.

Definition 4.3. *Let $m \in \mathbb{Z}$ be the cell index and $\alpha \in (0, \infty)$ a parameter. Let $l_m : \mathbb{Z} \to [0, 1]$ act as follows:*

$$l_m = \left(\frac{1}{|m| + 2^{1/\alpha}} \right)^{\alpha} \tag{4.5}$$

l_m is called slicer cell position.

Altogheter we introduce a slicers dynamics governed by the mapping S_α which is the map (4.1), where l_m is given by (4.5). Namely

$$S_\alpha(x, y, m) = \begin{cases} (x, y, m-1) & \text{if } 0 \leq x \leq \frac{1}{\left(|m|+2^{1/\alpha}\right)^{\alpha}} \text{ or } \frac{1}{2} \leq x \leq 1 - \frac{1}{\left(|m|+2^{1/\alpha}\right)^{\alpha}} \\ (x, y, m+1) & \text{if } \frac{1}{\left(|m|+2^{1/\alpha}\right)^{\alpha}} < x < \frac{1}{2} \text{ or } 1 - \frac{1}{\left(|m|+2^{1/\alpha}\right)^{\alpha}} < x \leq 1 \end{cases} \tag{4.6}$$

This dynamics is nonchaotic, since it presents zero Lyaponuv exponents and it preserves phase space volumes analogously to polygonal billiards. Indeed different point neither separate nor converge, in time, except when separated by an active slicer. In that case their distance jumps discontinuously, which is analogous to the dynamics of polygonal billiards [23], [24].

The equations of motion of the dynamical system, given an initial condition $\hat{X}_0 \in \hat{M}$, are:

$$\hat{X}_n = S_\alpha^n \left(\hat{X}_0 \right) \tag{4.7}$$

In particular, given $\hat{X}_0 = (x_0, y_0, m_0) \in \hat{M}$, then after n time steps, it results:

$$S_\alpha^n(x_0, y_0, m_0) = \left(x_0, y_0, m_0 + \sum_{i=1}^{n} k_i(x_0) \right)$$

where $k_i \in \{-1, +1\}$.

Let us now define a probability measure $\hat{\delta}_n$ that evolves with the dynamics S_α^n. First of all, let δ_0 be the Lebesgue measure in M and $\delta_\mathbb{Z}$ the Delta measure on the integers $\mathbb{Z}$, i.e. $\forall Z \subset \mathbb{Z}$, $\delta_\mathbb{Z}(Z) = card(Z)$. Then we take as measure on the phase-space $\hat{M}$ the product measure $\hat{\delta}_0 = \delta_0 \times \delta_\mathbb{Z}$, such that, given $\hat{G} \subset \hat{M}$, measurable set such that $\hat{G} = R \times \{z\}$, with $R \subset M$ and $z \in \mathbb{Z}$, we have

$$\begin{aligned} \hat{\delta_0} \left(\hat{G} \right) &= (\delta_0 \times \delta_\mathbb{Z}) (R \times \{z\}) = \\ &= \delta_0 (R) \, \delta_\mathbb{Z} (\{z\}) \end{aligned} \tag{4.8}$$

Notice that $\delta_{\mathbb{Z}}(\{z\}) = 1$ for all $z \in \mathbb{Z}$. Therefore

$$\hat{\delta}_0\left(\hat{G}\right) = \delta_0(R) \tag{4.9}$$

Remark 1. Any measurable set in $\hat{M}$ can be written as union of set like $\hat{G}$, namely $\hat{E} = \bigcup_{z\in Z} F_z \times \{z\}$, with $F_z \in M$ and $Z \subset \mathbb{Z}$ a set of indexes. Then it results

$$\hat{\delta}_0\left(\hat{E}\right) = \sum_{z\in Z} \delta_0(F_z)\,\delta_z(\{z\}) = \sum_{z\in Z} \delta_0(F_z) \tag{4.10}$$

Accordingly to this we give the following:

Definition 4.4. *Let $\hat{E} \subset \hat{M}$ be a measurable set. Then the evolving measure $\hat{\delta}_n$ defined by:*

$$\hat{\delta}_n(\hat{E}) = \hat{\delta}_0\left(S_\alpha^{-n}(\hat{E})\right) \tag{4.11}$$

is called slicer probability measure.

Remark 2. Taking as initial condition the unit square $M_0 = M \times \{0\}$, after n time steps the dynamics reaches a finite number of rectangles distributed in the cells. The farthest cell achieved at time step n is the n-th. Moreover if this n-th cell is odd the rectangles fall only in odd cells whereas if the n-th cell is even the rectangles fall only in even cells. Namely, let P and D respectively be the set of even and odd numbers smaller or equal to n, then if $n \in P$ we have

$$S_\alpha^n(M_0) = \bigcup_{j\in P} (R_j \times \{j\}) \tag{4.12}$$

and if $n \in D$

$$S_\alpha^n(M_0) = \bigcup_{j\in D} (R_j \times \{j\}) \tag{4.13}$$

where R_j is a rectangle in M_j.

In Fig. 4.2 is reported the behavior of the map S_α for a particular choice of α, starting from the initial condition mentioned above.

This kind of initial condition is fundamental for the subsequent results relating to the dynamics (4.6), therefore from now on we assume as initial condition the unit square M_0. We want to stress that the study of the model

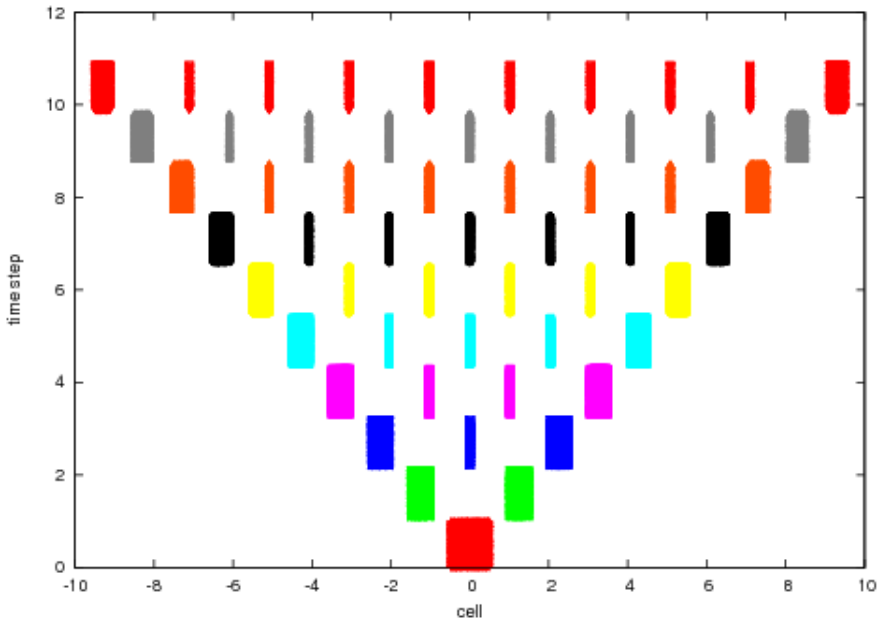

Figure 4.2: Behavior of map S for $\alpha = 1/3$, in 10 time steps, for a choice of $N = 10^4$ points.

under the choice of a particular initial condition do not affect the generality of it. We are in a situation analogous to the classical study of diffusion where the Gaussian behavior of the particles concentration is obtained from a particular choice of the initial condition, that is a Dirac δ-function representing an infinite concentration of particles at zero position. Moreover we want to underlined that the choice of the zero unit square is to simplify the analytical calculations. Infact choosing as an initial condition a generic cell m do not change the asymptotic results. In this case the only variation is the presence of a translation of m positions on the analytical expressions of the different involved quantities. According to all these observations let us proceed considering the following probability distribution $\hat{\rho}_0$, uniform and concentrated on the 0-th cell M_0:

$$\hat{\rho}_0\left(\hat{X}\right) = \begin{cases} 1, & \text{if } \hat{X} \in M_0 \\ 0, & \text{otherwise} \end{cases} \tag{4.14}$$

Then the probability distribution at time step n is given by:

$$\rho_n(\hat{X}) = \begin{cases} 1, & \text{if } \hat{X} \in S_\alpha^n(M_0) \\ 0 & \text{otherwise} \end{cases} \tag{4.15}$$

Observe that

$$\begin{aligned} \hat{\delta}_n\left(\hat{R}_j \times \{j\}\right) &= \hat{\delta}_0\left(S_\alpha^{-n}\left(\hat{R}_j \times \{j\}\right)\right) = \\ &= \delta_0(R_j) := A(j) \end{aligned} \tag{4.16}$$

with $R_j = I_j \times [0,1]$, $I_j \subset [0,1]$. $A(j)$ is nothing but the area of the rectangle R_j. Therefore we give the following:

Definition 4.5. *Let $\hat{X} \in \hat{M}$ and $n \in \mathbb{N}$, $n \in P$ (or $n \in D$). Then*

$$\rho_n^G(\hat{X}) = \begin{cases} A(j) & \text{if } \hat{X} \in M_j, \text{ for } j \in P \ \ (\text{or } j \in D) \\ 0 & \text{otherwise} \end{cases} \tag{4.17}$$

is the coarse grained probability distribution for map S_α at time instant n. Moreover, the quantity $A(j)$ is called travelling area, and indicated by A_v, when $j = \pm n$ wheras it is called sub-travelling area, and is indicated by A_p, when $|j| < n$.

The graining is constituted by the unit squares of the whole chain. Observe that the generic area $A(j)$ depends only on the width of the interval I_j which is directely determined by the position of the slicers in the j-th cell, therefore

$$A_v(\pm n) = l_{|\pm n|-1} = \left(\frac{1}{|\pm n| - 1 + 2^{1/\alpha}}\right)^\alpha \tag{4.18}$$

and

$$A_p(|j|) = l_{|j|-1} - l_{|j|+1} = \frac{1}{(|j| - 1 + 2^{1/\alpha})^\alpha} - \frac{1}{(|j| + 1 + 2^{1/\alpha})^\alpha} \tag{4.19}$$

for $j = -n+1, \ldots, n-1$ As far as the sub-travelling area are concerned we can further distinguish two expressions depending on whether the farthest cell reached is even or odd. More precisely, if the farthest cell n is odd, we have

$$A_p(j) = \begin{cases} l_{|j|-1} - l_{|j|+1} & \forall j \in D \ \ j \neq n \\ 0 & \forall j \in P \end{cases} \tag{4.20}$$

Conversely, if n is even it results

$$A_p(j) = \begin{cases} 0 & \forall j \in D \\ l_{|j|-1} - l_{|j|+1} & \forall j \in P \quad j \neq n \end{cases} \tag{4.21}$$

Therefore the expression of the coarse-grained probability $\hat{\rho}_n^G$ for the positive part of the real line, if $n \in P$ is given by:

$$\hat{\rho}_n^G(\hat{X}) = \begin{cases} l_0 - l_1, & \text{for } \hat{X} \in M_0 \\ l_{2k-1} - l_{2k+1}, & \text{for } \hat{X} \in M_{2k},\ k = 1, \ldots, \frac{n-2}{2} \\ l_{n-1} & \text{for } \hat{X} \in M_n \\ 0, & \text{otherwise} \end{cases} \tag{4.22}$$

Whereas, if $n \in D$ is:

$$\hat{\rho}_n^G(\hat{X}) = \begin{cases} l_{2k} - l_{2k+2}, & \text{for } \hat{X} \in M_{2k+1},\ k = 0, \ldots, \frac{n-3}{2} \\ l_{n-1} & \text{for } \hat{X} \in M_n \\ 0, & \text{otherwise} \end{cases} \tag{4.23}$$

For the simmetry of ρ_n^G, it results the same on the negative part of the chain. From numerical results reported below in the examples section, we evince that we can approximate the marginal probability distribution $\rho_n^G(m)$ with the following continuous function extended to $\mathbb{R}$:

$$\rho_t^\alpha(x) = \begin{cases} C\dfrac{1}{(x + 2^{1/\alpha})^{1+\alpha}} & \text{if } x < t, \\ 0, & \text{otherwise} \end{cases} \tag{4.24}$$

where C is the normalization constant and t is the time variable.

4.2 Generalized Diffusion Coefficient

As we have seen in a previous chapter, the generalized diffusion coefficient is given by the following relation, cf. 1.14:

$$T(\gamma) = \lim_{n \to \infty} \frac{\langle \Delta x^2(n) \rangle}{n^\gamma} \tag{4.25}$$

where $\gamma \in [0,2]$. The expression in angular brackets represents the mean square displacement (MSD) calculated for discrete times accordingly to the coarse grained probability distribution defined in (4.17). Namely

$$\begin{aligned} \langle \Delta \hat{X}_n^2 \rangle &= \sum_{\hat{X} \in \hat{M}} \rho_n^G \left(\hat{X} \right) \cdot \left| \hat{X} - \hat{X}_0 \right|^2 = \\ &= \sum_{j=-n}^{n} A(j) j^2 \end{aligned} \tag{4.26}$$

where with $|\cdot|$ we indicate the euclidean distance.

Let us now give the first result for the dynamics S_α.

Theorem 4.2.1. *For $\alpha \in (0,2)$ the generalized diffusion coefficient for the dynamics S_α, i.e. map (4.6) with an initial condition concentrated and uniform in the 0-th cell, is given by*

$$T_\alpha(\gamma) = \begin{cases} +\infty & \text{if } 0 \leq \gamma < 2-\alpha \\ \frac{4}{2-\alpha} & \text{if } \gamma = 2-\alpha \\ 0 & \text{if } 2-\alpha < \gamma \leq 2 \end{cases} \tag{4.27}$$

Therefore the transport exponent (cf. Def. 1.1) results to be $\gamma = 2-\alpha$.

Proof. Since the map is symmetric, we will give the proof only for the positive side of the cells' chain calculating the generalized diffusion coefficient for $j > 0$, i.e. $T_\alpha^R(\gamma)$. Then $T_\alpha = 2T_\alpha^R(\gamma)$.
For (1.14) and (4.26) one has:

$$T_\alpha^R(\gamma) = \lim_{n\to\infty} \frac{1}{n^\gamma} \sum_{j=0}^{n} A(j) j^2 \tag{4.28}$$

Since we have distinguished the area in travelling and sub-travelling we have that

$$T_\alpha^R(\gamma) = \lim_{n\to\infty} \frac{1}{n^\gamma} \left(\sum_{j=0}^{n-1} A_p(j) j^2 + A_v(n) n^2 \right) \tag{4.29}$$

Let's focus first on the sub-travelling area. If we introduce the quantity:

$$Q_n = \sum_{j=0}^{n-1} A_p(j) j^2 \tag{4.30}$$

then the Lemma 4.2.2 proved below implies

$$\lim_{n\to\infty}\frac{Q_n}{n^\gamma}=\begin{cases}\infty & \text{if } 0\le\gamma<2-\alpha\\ \frac{2}{2-\alpha}-1 & \text{if } \gamma=2-\alpha\\ 0 & \text{if } 2-\alpha<\gamma\le 2\end{cases} \tag{4.31}$$

Let's calculate now the limit of the travelling area:

$$\lim_{n\to\infty}\frac{n^2}{(n+2^{1/\alpha}-1)^\alpha}\cdot\frac{1}{n^\gamma}=\begin{cases}+\infty & \text{if } 0\le\gamma<2-\alpha\\ 1 & \text{if } \gamma=2-\alpha\\ 0 & \text{if } 2-\alpha<\gamma\le 2\end{cases} \tag{4.32}$$

Summing the two limits as in (4.29) we conclude that the generalized diffusion coefficient for the map S_α concerning the positive part of the chain ($j>0$) is given by:

$$T_\alpha^R(\gamma)=\begin{cases}\infty & \text{if } 0\le\gamma<2-\alpha\\ \frac{2}{2-\alpha} & \text{if } \gamma=2-\alpha\\ 0 & \text{if } 2-\alpha<\gamma\le 2\end{cases} \tag{4.33}$$

As we already said to have the coefficient for the whole map it suffices multiply by a factor 2 since j^2 takes same values for positive and negative j. Therefore we conclude that the transport exponent is given by $\gamma=2-\alpha$. □

Remark 3. From the result of the theorem we evince that the mean square displacement of the map (4.6) has the following asymptotic behavior:

$$\langle\Delta\hat{X}_n^2\rangle\sim n^{2-\alpha} \tag{4.34}$$

Therefore, according to Def. 1.1, we can say that the map S_α presents a wide range of transport behaviors, when α varies in $(0,2)$. Precisely, S_α is sub-diffusive when $1<\alpha<2$, diffusive when $\alpha=1$ and super-diffusive when $0<\alpha<1$.

Lemma 4.2.2. *Let Q_n be the quantity*

$$Q_n=\sum_{j=0}^{n-1}A_p(j)j^2 \tag{4.35}$$

where A_p is the sub-travelling area defined by (4.19). Then

$$\lim_{n\to\infty}\frac{Q_n}{n^\gamma}=\begin{cases}\infty & \text{if } 0\le\gamma<2-\alpha\\ \frac{2}{2-\alpha}-1 & \text{if } \gamma=2-\alpha\\ 0 & \text{if } 2-\alpha<\gamma\le 2\end{cases} \tag{4.36}$$

for $\alpha\in(0,2)$.

Proof. As noted previously, the series Q_n assumes a different form depending on wheter n is even or odd, therefore we proceed by calculating separately the limits for the two cases, proving that they are equal.
Let's begin from the even series, so that $n\in P$, $n>2$. Then

$$Q_n=\sum_{j=1,j\in P}^{n-1}A_p(j)j^2=4\sum_{j=1}^{\frac{n}{2}-1}\left[\frac{1}{(2j+2^{1/\alpha}-1)^\alpha}-\frac{1}{(2j+2^{1/\alpha}+1)^\alpha}\right]j^2 \tag{4.37}$$

Observe that this is a sort of telescopic sum, indeed, let's analyze its behaviour for a fixed n, for example $n=8$:

$$\begin{aligned}Q_8 &= 4\left[\frac{1}{(1+2^{1/\alpha})^\alpha}-\frac{1}{(3+2^{1/\alpha})^\alpha}+\frac{4}{(3+2^{1/\alpha})^\alpha}-\frac{4}{(5+2^{1/\alpha})^\alpha}+\right.\\ &\quad\left.+\frac{9}{(5+2^{1/\alpha})^\alpha}-\frac{9}{(7+2^{1/\alpha})^\alpha}\right]=\\ &= 4\left[\frac{1}{(1+2^{1/\alpha})^\alpha}+\frac{3}{(3+2^{1/\alpha})^\alpha}+\frac{5}{(5+2^{1/\alpha})^\alpha}-\frac{9}{(7+2^{1/\alpha})^\alpha}\right]\end{aligned}$$

It can be showed by induction that the recurrence evinced from the example with $n=8$ can be set in the following general form:

$$Q_n=4\cdot\sum_{j=1}^{\frac{n}{2}-1}\frac{2j-1}{(2j-1+2^{1/\alpha})^\alpha}-\frac{(n-2)^2}{(n-1+2^{1/\alpha})^\alpha} \tag{4.38}$$

Let R_n be defined by

$$R_n=4\cdot\sum_{j=1}^{\frac{n}{2}-1}\frac{2j-1}{(2j-1+2^{1/\alpha})^\alpha} \tag{4.39}$$

and consider first this term, introducing:

$$f(j) = \frac{2j-1}{(2j-1+2^{1/\alpha})^{\alpha}} \tag{4.40}$$

whose derivative is given by

$$f'(j) = \frac{2\left[2(1-\alpha)j + 2^{1/\alpha} + \alpha - 1\right]}{(2j+2^{1/\alpha}-1)^{\alpha+1}} \tag{4.41}$$

The sign of f' shows that f is always increasing for $0 < \alpha \leq 1$. For $1 < \alpha < 2$, f is increasing for $j < j(\alpha)$ and decreasing for $j > j(\alpha)$, where $j(\alpha) = (1-\alpha-2^{1/\alpha})/2(\alpha-1)$.
We treat separately the three cases $0 < \alpha < 1$, $1 < \alpha < 2$ and $\alpha = 1$.
First case: $0 < \alpha < 1$.
Because in this case f is monotonically increasing $\forall j > 0$, we can bound our sum from above and below, taking the upper sum and lower sum for the integral of f. This yields:

$$\int_0^{\frac{n}{2}-1} f(x)dx \leq \sum_{j=1}^{\frac{n}{2}-1} f(j) \leq \int_1^{\frac{n}{2}} f(x)dx \tag{4.42}$$

Taking the limit, we have:

$$\lim_{n\to\infty} \frac{1}{n^{\gamma}} \int_0^{\frac{n}{2}-1} f(x)dx \leq \lim_{n\to\infty} \frac{1}{n^{\gamma}} \sum_{j=1}^{\frac{n}{2}-1} f(j) \leq \lim_{n\to\infty} \frac{1}{n^{\gamma}} \int_1^{\frac{n}{2}} f(x)dx \tag{4.43}$$

Now let's consider the indefinit integral:

$$\int f(x)dx = \int \frac{2x-1}{\left(2x-1+2^{1/\alpha}\right)^{\alpha}} dx \tag{4.44}$$

It can be computed by the change of variable $\left(2x-1+2^{1/\alpha}\right)^{\alpha} =: t$, obtaining:

$$\int f(x)dx = \frac{1}{2}\left[\frac{(2x-1+2^{1/\alpha})^{2-\alpha}}{2-\alpha} - 2^{1/\alpha} \cdot \frac{(2x-1+2^{1/\alpha})^{1-\alpha}}{1-\alpha}\right] \tag{4.45}$$

Then the definite integrals, bounding the sum in (4.42) are respectively:

$$\int_0^{\frac{n}{2}-1} f(x)dx = \frac{1}{2}\left[\frac{(n-3+2^{1/\alpha})^{2-\alpha}}{2-\alpha} - 2^{1/\alpha}\cdot\frac{(n-3+2^{1/\alpha})^{1-\alpha}}{1-\alpha} + \right. \\ \left. + \left(2^{1/\alpha}-1\right)^{1-\alpha}\cdot\frac{2^{1/\alpha}-\alpha+1}{(2-\alpha)(1-\alpha)}\right] \tag{4.46}$$

and

$$\int_1^{\frac{n}{2}} f(x)dx = \frac{1}{2}\left[\frac{(n-1+2^{1/\alpha})^{2-\alpha}}{2-\alpha} - 2^{1/\alpha}\cdot\frac{(n-1+2^{1/\alpha})^{1-\alpha}}{1-\alpha} + \right. \\ \left. + (2^{1/\alpha}+1)^{1-\alpha}\cdot\frac{(2^{1/\alpha}+\alpha-1)}{(2-\alpha)(1-\alpha)}\right] \tag{4.47}$$

Now taking the $n\to\infty$ limit we have:

$$\lim_{n\to\infty}\frac{1}{n^\gamma}\int_0^{\frac{n}{2}-1} f(x)dx = \begin{cases} \infty & \text{if } 0\le\gamma<2-\alpha \\ \frac{1}{2(2-\alpha)} & \text{if } \gamma=2-\alpha \\ 0 & \text{if } 2-\alpha<\gamma\le 2 \end{cases} \tag{4.48}$$

and

$$\lim_{n\to\infty}\frac{1}{n^\gamma}\int_1^{\frac{n}{2}} f(x)dx = \begin{cases} \infty & \text{if } 0\le\gamma<2-\alpha \\ \frac{1}{2(2-\alpha)} & \text{if } \gamma=2-\alpha \\ 0 & \text{if } 2-\alpha<\gamma\le 2 \end{cases} \tag{4.49}$$

As these two limits coincide for (4.43) the sum converges to the same limits:

$$\lim_{n\to\infty}\frac{1}{n^\gamma}\sum_{j=1}^{\frac{n}{2}-1} f(j) = \begin{cases} \infty & \text{if } 0\le\gamma<2-\alpha \\ \frac{1}{2(2-\alpha)} & \text{if } \gamma=2-\alpha \\ 0 & \text{if } 2-\alpha<\gamma\le 2 \end{cases} \tag{4.50}$$

Therefore:

$$\lim_{n\to\infty}\frac{R_n}{n^\gamma} = \begin{cases} \infty & \text{if } 0\le\gamma<2-\alpha \\ \frac{2}{2-\alpha} & \text{if } \gamma=2-\alpha \\ 0 & \text{if } 2-\alpha<\gamma\le 2 \end{cases} \tag{4.51}$$

Second case: $1<\alpha<2$. In this case, f deacreses for $j>j(\alpha)$, for some value $j(\alpha)$.

Therefore, $\forall \alpha \in (1,2)$, introduce $\bar{j}_\alpha = \lfloor j(\alpha) \rfloor$, where $\lfloor x \rfloor$ is the integer part of x, and consider

$$R_n = 4 \left(\sum_{j=1}^{\bar{j}_\alpha} f(j) + \sum_{j=\bar{j}_\alpha+1}^{\frac{n}{2}-1} f(j) \right) \tag{4.52}$$

Observe that

$$\lim_{n\to\infty} \frac{1}{n^\gamma} \sum_{j=1}^{\bar{j}_\alpha} f(j) = 0 \tag{4.53}$$

for all $\gamma > 0$. Then, focus on the second term of the sum (4.52). Repeating the previous reasoning, we obtain:

$$\int_{\bar{j}_\alpha+1}^{\frac{n}{2}} f(x)dx < \sum_{j=\bar{j}_\alpha+1}^{\frac{n}{2}-1} f(j) < \int_{\bar{j}_\alpha}^{\frac{n}{2}-1} f(x)dx. \tag{4.54}$$

and passing to the limit as in the previous case, we have:

$$\lim_{n\to\infty} \frac{1}{n^\gamma} \int_{\bar{j}_\alpha+1}^{\frac{n}{2}} f(x)dx \leq \lim_{n\to\infty} \frac{1}{n^\gamma} \sum_{j=\bar{j}_\alpha+1}^{\frac{n}{2}-1} f(j) \leq \lim_{n\to\infty} \frac{1}{n^\gamma} \int_{\bar{j}_\alpha}^{\frac{n}{2}-1} f(x)dx. \tag{4.55}$$

Recalling the result of the indefinite integral previously calculated, we have:

$$\int_{\bar{j}_\alpha+1}^{\frac{n}{2}} f(x)dx = \frac{1}{2} \left[\frac{(n-1+2^{1/\alpha})^{2-\alpha}}{2-\alpha} - 2^{1/\alpha} \cdot \frac{(n-1+2^{1/\alpha})^{1-\alpha}}{1-\alpha} + cost_1(\alpha) \right] \tag{4.56}$$

and

$$\int_{\bar{j}_\alpha}^{\frac{n}{2}-1} f(x)dx = \frac{1}{2} \left[\frac{(n-3+2^{1/\alpha})^{2-\alpha}}{2-\alpha} - 2^{1/\alpha} \cdot \frac{(n-3+2^{1/\alpha})^{1-\alpha}}{1-\alpha} + cost_2(\alpha) \right] \tag{4.57}$$

The limits of the two integrals result the same as in (4.48) and (4.49) and yield :

$$\lim_{n\to\infty} \frac{1}{n^\gamma} \sum_{j=\bar{j}_\alpha+1}^{\frac{n}{2}-1} f(j) = \begin{cases} \infty & \text{if } 0 \leq \gamma < 2-\alpha \\ \frac{2}{2-\alpha} & \text{if } \gamma = 2-\alpha \\ 0 & \text{if } 2-\alpha < \gamma \leq 2 \end{cases} \tag{4.58}$$

Therefore, we have:

$$\lim_{n\to\infty}\frac{R_n}{n^\gamma}=\begin{cases}\infty & \text{if } 0\le\gamma<2-\alpha\\ \frac{2}{2-\alpha} & \text{if } \gamma=2-\alpha\\ 0 & \text{if } 2-\alpha<\gamma\le 2\end{cases} \tag{4.59}$$

for all $1<\alpha<2$.

Third case: $\alpha=1$.

In this case f is increasing for all $j>0$. Then, analogously to the first case, we have:

$$\int_0^{\frac{n}{2}-1} f(x)dx\le\sum_{j=1}^{\frac{n}{2}-1} f(j)\le\int_1^{\frac{n}{2}} f(x)dx \tag{4.60}$$

and taking the limit

$$\lim_{n\to\infty}\frac{1}{n^\gamma}\int_0^{\frac{n}{2}-1} f(x)dx\le\lim_{n\to\infty}\frac{1}{n^\gamma}\sum_{j=1}^{\frac{n}{2}-1} f(j)\le\lim_{n\to\infty}\frac{1}{n^\gamma}\int_1^{\frac{n}{2}} f(x)dx \tag{4.61}$$

Consider the indefinite integral:

$$\int f(x)dx=\int\frac{2x-1}{2x+1}dx=x-\log(2x+1) \tag{4.62}$$

Therefore the values of the two definite integrals result:

$$\int_0^{\frac{n}{2}-1} f(x)dx=\left(\frac{n}{2}-1\right)-\log(n-1) \tag{4.63}$$

and

$$\int_1^{\frac{n}{2}} f(x)dx=\frac{n}{2}-\log(n+1)+\log 3-1 \tag{4.64}$$

As above taking the $n\to\infty$ limit we have:

$$\lim_{n\to\infty}\frac{1}{n^\gamma}\int_0^{\frac{n}{2}-1} f(x)dx=\begin{cases}\infty & \text{if } 0\le\gamma<1\\ \frac{1}{2} & \text{if } \gamma=1\\ 0 & \text{if } 1<\gamma\le 2\end{cases} \tag{4.65}$$

and

$$\lim_{n\to\infty}\frac{1}{n^\gamma}\int_1^{\frac{n}{2}} f(x)dx=\begin{cases}\infty & \text{if } 0\le\gamma<1\\ \frac{1}{2} & \text{if } \gamma=1\\ 0 & \text{if } 1<\gamma\le 2\end{cases} \tag{4.66}$$

Therefore

$$\lim_{n\to\infty}\frac{R_n}{n^\gamma}=\begin{cases}\infty & \text{if } 0\le\gamma<1\\ 2 & \text{if } \gamma=1\\ 0 & \text{if } 1<\gamma\le 2\end{cases} \tag{4.67}$$

We can observe that the result of the limit of R_n/n^γ as n goes to infinity results equal in all the three cases. Therefore remembering Eq. (4.38) we have that:

$$\lim_{n\to\infty}\frac{Q_n}{n^\gamma}=\lim_{n\to\infty}\left[\frac{R_n}{n^\gamma}-\frac{(n-1)^2}{n^\gamma(n-1+2^{1/\alpha})^\alpha}\right] \tag{4.68}$$

and we eventually obtain

$$\lim_{n\to\infty}\frac{Q_n}{n^\gamma}=\begin{cases}\infty & \text{if } 0\le\gamma<2-\alpha\\ \frac{2}{2-\alpha}-1 & \text{if } \gamma=2-\alpha\\ 0 & \text{if } 2-\alpha<\gamma\le 2\end{cases} \tag{4.69}$$

for $\alpha\in(0,2)$.

For the case in which the farthest cell n is odd, one proceeds similarly. In this situation the expression of the sum is given by

$$Q_n=\sum_{j=0,j\in D}^{n-1}A_p(j)j^2=\sum_{j=0}^{\frac{n-3}{2}}\left[\frac{1}{(2j+2^{1/\alpha})^\alpha}-\frac{1}{(2j+2+2^{1/\alpha})^\alpha}\right](2j+1)^2 \tag{4.70}$$

The formula corrisponding to (4.38) is now given by:

$$Q_n=\frac{1}{2}+8\sum_{j=1}^{\frac{n-3}{2}}\frac{j}{(2j+2^{1/\alpha})^\alpha}-\frac{(n-2)^2}{(n-1+2^{1/\alpha})^\alpha} \tag{4.71}$$

and the resulting limit is again:

$$\lim_{n\to\infty}\frac{Q_n}{n^\gamma}=\begin{cases}\infty & \text{if } 0\le\gamma<2-\alpha\\ \frac{2}{2-\alpha}-1 & \text{if } \gamma=2-\alpha\\ 0 & \text{if } 2-\alpha<\gamma\le 2\end{cases} \tag{4.72}$$

for $\alpha\in(0,2)$.

□

We can now establish the following result.

Proposition 4.2.3. *For $\alpha = 2$ the generalized diffusion coefficient for the map (4.6), with an initial condition uniform and concentrated in the 0-th cell, is given by*

$$T_2(\gamma) = \begin{cases} +\infty & \text{if} \quad \gamma = 0 \\ 0 & \text{if} \quad 0 < \gamma \leq 2 \end{cases} \tag{4.73}$$

Proof. As for Theorem 4.2.1 the symmetry of the map requires the proof only for the positive side of the chain.
To calculate

$$T_2^R(\gamma) = \lim_{n\to\infty} \frac{1}{n^\gamma} \sum_{j=0}^{n} A(j) j^2 = \tag{4.74}$$

$$= \lim_{n\to\infty} \frac{1}{n^\gamma} \left(\sum_{j=0}^{n-1} A_p(j) j^2 + A_v(n) n^2 \right) \tag{4.75}$$

consider first the sub-travelling area A_p and let n be in P. Then

$$Q_n = \sum_{j=0, j\in P}^{n-1} A_p(j) j^2 = 4 \sum_{j=1}^{\frac{n}{2}-1} \left[\frac{1}{\left(2j + \sqrt{2} - 1\right)^2} - \frac{1}{\left(2j + \sqrt{2} + 1\right)^2} \right] j^2 =$$

$$= 4 \sum_{j=1}^{\frac{n}{2}-1} \frac{2j-1}{\left(2j + \sqrt{2} - 1\right)^2} - \frac{(n-2)^2}{(n + \sqrt{2} - 1)^2} \tag{4.76}$$

Analyze now the generic term of the first sum in (4.76):

$$f(j) = \frac{2j-1}{\left(2j + \sqrt{2} - 1\right)^2} \tag{4.77}$$

whose derivative is

$$f'(j) = \frac{2 + \sqrt{2} - 4j}{(2j + \sqrt{2} - 1)^3} \tag{4.78}$$

The sign of f' shows that f is decreasing for $j > (1 + \sqrt{2})/2$. So we rewrite Q_n as follow:

$$Q_n = \frac{4}{(1 + \sqrt{2})^2} + 4 \sum_{j=2}^{\frac{n}{2}-1} f(j) - \frac{(n-2)^2}{(n + \sqrt{2} - 1)^2} \tag{4.79}$$

Now, as in the (4.42) we have

$$\int_2^{\frac{n}{2}} f(x)dx \leq \sum_{j=2}^{\frac{n}{2}-1} f(j) \leq \int_{\frac{1+\sqrt{2}}{2}}^{\frac{n}{2}-1} f(x)dx \tag{4.80}$$

Operating the same change of variable as in the proof of Lemma 4.2.2 the indefinite integral results to be:

$$\int f(x)dx = \int \frac{2j-1}{\left(2j+\sqrt{2}-1\right)^2} = \frac{1}{2}\left[\log(2j-1+\sqrt{2}) + \frac{\sqrt{2}}{2j-1+\sqrt{2}}\right] \tag{4.81}$$

Then the two definite integrals bounding the sum in (4.80) are, respectively:

$$\int_2^{\frac{n}{2}} f(x)dx = \frac{1}{2}\left(\log\frac{n-1+\sqrt{2}}{3+\sqrt{2}} + \frac{\sqrt{2}}{n-1+\sqrt{2}} - \frac{\sqrt{2}}{3+\sqrt{2}}\right) \tag{4.82}$$

$$\int_{\frac{1+\sqrt{2}}{2}}^{\frac{n}{2}-1} f(x)dx = \frac{1}{2}\left(\log\frac{n-3+\sqrt{2}}{2\sqrt{2}} - \frac{1}{2}\right) \tag{4.83}$$

Now taking the $n \to \infty$ limit we have:

$$\lim_{n\to\infty} \frac{1}{n^\gamma} \int_2^{\frac{n}{2}} f(x)dx = \begin{cases} +\infty & \text{if } \gamma = 0 \\ 0 & \text{if } 0 < \gamma \leq 2 \end{cases} \tag{4.84}$$

$$\lim_{n\to\infty} \frac{1}{n^\gamma} \int_1^{\frac{n}{2}-1} f(x)dx = \begin{cases} +\infty & \text{if } \gamma = 0 \\ 0 & \text{if } 0 < \gamma \leq 2 \end{cases}. \tag{4.85}$$

Therefore

$$\lim_{n\to\infty} \frac{Q_n}{n^\gamma} = \begin{cases} +\infty & \text{if } \gamma = 0 \\ 0 & \text{if } 0 < \gamma \leq 2 \end{cases}. \tag{4.86}$$

Repaeting the same reasoning when $n \in D$ we obtain the very same result as in (4.86). Let's calculate now the limit for the travelling area that results to be:

$$\lim_{n\to\infty} \frac{n^2}{(n-1+\sqrt{2})^2} \cdot \frac{1}{n^\gamma} = \begin{cases} +\infty & \text{if } \gamma = 0 \\ 0 & \text{if } 0 < \gamma \leq 2 \end{cases} \tag{4.87}$$

Therefore the generalized diffusion coefficient is

$$T_2(\gamma) = \begin{cases} +\infty & \text{if } \gamma = 0 \\ 0 & \text{if } 0 < \gamma \leq 2 \end{cases} \tag{4.88}$$

□

In this case we can say that the dynamics is '*logarithmically diffusive*', meaning that

$$\langle \Delta \hat{X}_n^2 \rangle \sim \log n$$

asymptotically in n.

Theorem 4.2.4. *For $\alpha \in (0, 2]$ the moments $\langle \Delta \hat{X}_n^p \rangle$, $p > 2$, $p \in P$ for the dynamics S_α, i.e. map (4.6) with an initial condition concentrated and uniform in the 0-th cell, have the following asymptotic beahvior:*

$$\langle \Delta \hat{X}_n^p \rangle \sim n^{p-\alpha}.$$

The moments for $p \in D$ all equal zero.

We want to calculate the following limit

$$\lim_{n\to\infty} \frac{\langle \Delta \hat{X}_n^p \rangle}{n^\gamma} := L(\alpha, p) \tag{4.89}$$

Since the map is symmetric we give the proof only for the positive side of the chain. Then, the even moments are given by multipling for a factor two, whereas the odd moments result all zero because of the simmetry. As in (4.26) one has:

$$\langle \Delta \hat{X}_n^p \rangle = \sum_{\hat{X} \in \hat{M}} \rho_n^G \left(\hat{X} \right) \left| \hat{X} - \hat{X}_0 \right|^p = \sum_{j=-n}^{n} A(j) j^p \tag{4.90}$$

Therefore we will consider

$$L(\alpha, p) = \lim_{n\to\infty} \frac{1}{n^\gamma} \sum_{j=0}^{n} A(j) j^p \tag{4.91}$$

Also in this case we have to consider the distinction of the area in two groups, therefore we write

$$L(\alpha, p) = \lim_{n\to\infty} \frac{1}{n^\gamma} \left(\sum_{j=0}^{n-1} A_p(j) j^p + A_v(n) n^p \right) \tag{4.92}$$

Let us focus first on the sub-travelling area. If we introduce the quantity:

$$P_n = \sum_{j=0}^{n-1} A_p(j) j^p \tag{4.93}$$

then for the Lemma 4.2.5 it results that:

$$\lim_{n\to\infty}\frac{1}{n^{\gamma}}\sum_{j=0}^{n-1}A_p(j)j^2=\begin{cases}\infty & \text{if } 0\leq\gamma<p-\alpha\\ \dfrac{\alpha}{p-\alpha}>0 & \text{if } \gamma=p-\alpha\\ 0 & \text{if } \gamma>p-\alpha\end{cases}\tag{4.94}$$

Then the limit of the travelling area is given by:

$$\lim_{n\to\infty}\frac{n^p}{(n+2^{1/\alpha}-1)^{\alpha}}\cdot\frac{1}{n^{\gamma}}=\begin{cases}+\infty & \text{if } 0\leq\gamma<p-\alpha\\ 1 & \text{if } \gamma=p-\alpha\\ 0 & \text{if } \gamma>p-\alpha\end{cases}\tag{4.95}$$

Therefore, summing togheter the results as in the formula (4.92) we conclude that

$$L(\alpha,p)=\begin{cases}\infty & \text{if } 0\leq\gamma<p-\alpha\\ \dfrac{\alpha}{p-\alpha}+1 & \text{if } \gamma=p-\alpha\\ 0 & \text{if } \gamma>p-\alpha\end{cases}\tag{4.96}$$

To have the limit for the whole map, for $p\in P$, it suffices multiply by a factor 2 since j^p takes same values for positive and negative j. Therefore we conclude that the asymptotic behavior of the moments as $n\to\infty$ is

$$\langle\Delta\hat{X}_n^p\rangle\sim n^{p-\alpha}\tag{4.97}$$

Lemma 4.2.5. *Let P_n be the quantity defined by*

$$P_n=\sum_{j=0}^{n-1}A_p(j)j^p\tag{4.98}$$

where A_p is the sub-travelling area defined by (4.19).Then

$$\lim_{n\to\infty}\frac{P_n}{n^{\gamma}}=\begin{cases}\infty & \textit{if } 0\leq\gamma<p-\alpha\\ \dfrac{\alpha}{p-\alpha} & \textit{if } \gamma=p-\alpha\\ 0 & \textit{if } \gamma>p-\alpha\end{cases}\tag{4.99}$$

for $\alpha\in(0,2]$.

Proof. As noted previously, the series P_n assumes a different form depending on whether n is even or odd, therefore we proceed by calculating separately the limits for the two cases proving that they are equal.
Let's begin with $n \in P$. Then

$$\begin{aligned} P_n &= \sum_{j=0, j\in P}^{n-1} A_p(j) j^p = \\ &= 2^p \sum_{j=1}^{\frac{n}{2}-1} \left[\frac{1}{(2j + 2^{1/\alpha} - 1)^\alpha} - \frac{1}{(2j + 2^{1/\alpha} + 1)^\alpha} \right] j^p \end{aligned} \tag{4.100}$$

Observe that this is a sort of telescopic sum, indeed, let's analyze its behaviour for a fixed n, for example $n = 8$:

$$\begin{aligned} P_8 &= 2^p \left[\frac{1}{(1 + 2^{1/\alpha})^\alpha} - \frac{1}{(3 + 2^{1/\alpha})^\alpha} + \frac{2^p}{(3 + 2^{1/\alpha})^\alpha} - \frac{2^p}{(5 + 2^{1/\alpha})^\alpha} + \right. \\ &\quad \left. + \frac{3^p}{(5 + 2^{1/\alpha})^\alpha} - \frac{3^p}{(7 + 2^{1/\alpha})^\alpha} \right] = \\ &= 2^p \left[\frac{1}{(1 + 2^{1/\alpha})^\alpha} + \frac{2^p - 1}{(3 + 2^{1/\alpha})^\alpha} + \frac{3^p - 2^p}{(5 + 2^{1/\alpha})^\alpha} - \frac{3^p}{(7 + 2^{1/\alpha})^\alpha} \right] \end{aligned}$$

It can be shown by induction that the recurrence evinced from the example can be set in the following general form:

$$P_n = 2^p \cdot \sum_{j=0}^{\frac{n}{2}-2} \frac{(j+1)^p - j^p}{(2j + 1 + 2^{1/\alpha})^\alpha} - \frac{(n-2)^p}{(n - 1 + 2^{1/\alpha})^\alpha} \tag{4.101}$$

Let R_n be defined by

$$R_n = 2^p \cdot \sum_{j=0}^{\frac{n}{2}-2} \frac{(j+1)^p - j^p}{(2j + 1 + 2^{1/\alpha})^\alpha} \tag{4.102}$$

and consider first this term, negleting the last term in (4.101). We proceed analyzing the generic term of R_n:

$$\begin{aligned} f(j) &= \frac{(j+1)^p - j^p}{(2j + 1 + 2^{1/\alpha})^\alpha} = \\ &= \sum_{k=1}^{p} \binom{p}{k} \frac{j^{p-k}}{(2j + 1 + 2^{1/\alpha})^\alpha} \end{aligned} \tag{4.103}$$

whose derivative is given by:

$$f'(j) = \sum_{k=1}^{p} \binom{p}{k} \frac{\left[2(p-k-\alpha)j + (p-k)(1+2^{1/\alpha})\right]}{(2j+1+2^{1/\alpha})^{\alpha+1}} j^{p-k-1} \tag{4.104}$$

Let be

$$f_k(j) = \binom{p}{k} \frac{\left[2(p-k-\alpha)j + (p-k)(1+2^{1/\alpha})\right]}{(2j+1+2^{1/\alpha})^{\alpha+1}} j^{p-k-1} \tag{4.105}$$

And let us study the sign of these functions f_k. We should distinguish two cases, for $0 < \alpha \leq 1$ or for $1 < \alpha \leq 2$.
If $0 < \alpha \leq 1$, we can write

$$f'(j) = \sum_{k=1}^{p-1} f_k(j) + f_p(j) \tag{4.106}$$

where all the functions in the sum are positive, i.e. $f_k(j) > 0$ for all $k = 1, \ldots, p-1$ and for all $j > 0$. Therefore the only negative contribute to the derivative is given by $f_p(j)$. Now observe that

$$f_p(j) = -\frac{2\alpha}{(2j+1+2^{1/\alpha})^{\alpha+1}} \overset{j\to\infty}{\longrightarrow} 0 \tag{4.107}$$

therefore we can conclude that the derivative, in the case of $\alpha \leq 1$, is positive and therefore the function f is increasing for all $j > 0$.
Now let us consider the case $1 < \alpha \leq 2$. In this case we can write:

$$f'(j) = \sum_{k=1}^{p-2} f_k(j) + f_{p-1}(j) + f_p(j) \tag{4.108}$$

As before also now all the functions in the sum are positive, i.e. $f_k(j) > 0$ for all $k = 1, \ldots, p-2$ and for all $j > 0$. Therefore the negative contributes to the derivative are given by $f_{p-1}(j)$ and $f_p(j)$, for all $j > j_\epsilon > 0$, where $j_\epsilon = \left\lfloor (1+2^{1/1+\epsilon})/2\epsilon \right\rfloor$. Now observe that

$$f_{p-1}(j) = p\frac{2(1-\alpha)j + 1 + 2^{1/\alpha}}{(2j+1+2^{1/\alpha})^{\alpha+1}} \overset{j\to\infty}{\longrightarrow} 0 \tag{4.109}$$

and $f_p(j)$ have the same behavior as above. Therefore, also in this case we can conclude that the derivative is overall positive and the function f is

increasing for all $j > 0$.

Therefore we can bound our sum from above and below, taking it as the upper sum and lower sum for the integral of f. This yields:

$$\int_0^{\frac{n}{2}-2} f(x)dx < \sum_{j=0}^{\frac{n}{2}-2} f(j) < \int_1^{\frac{n}{2}-1} f(x)dx. \tag{4.110}$$

and passing to the limit as in the previous case we will have:

$$\lim_{n\to\infty} \frac{1}{n^\gamma} \int_0^{\frac{n}{2}-2} f(x)dx \leq \lim_{n\to\infty} \frac{1}{n^\gamma} \sum_{j=0}^{\frac{n}{2}-2} f(j) \leq \lim_{n\to\infty} \frac{1}{n^\gamma} \int_{j_1}^{\frac{n}{2}-1} f(x)dx. \tag{4.111}$$

Let's calculate, with the same change of variable as in Lemma 4.2.2, the indefinite integral, for the case $0 < \alpha < 2$, with $\alpha \neq 1$:

$$\begin{aligned}
\int f(x)dx &= \int \frac{(x+1)^p - x^p}{\left(2x+1+2^{1/\alpha}\right)^\alpha} dx = \\
&= \int \sum_{k=1}^{p} \binom{p}{k} \frac{x^{p-k}}{\left(2x+1+2^{1/\alpha}\right)^\alpha} dx = \\
&= \sum_{k=1}^{p} \binom{p}{k} \left\{ \sum_{s=0}^{p-k} \binom{p-k}{s} \frac{(-1)^s (1+2^{1/\alpha})^s}{2^{p-k+1}} \frac{\left(2x+1+2^{1/\alpha}\right)^{p-k-s+1-\alpha}}{p-k-s+1-\alpha} \right\}
\end{aligned}$$

Therefore

$$\begin{aligned}
\int_0^{\frac{n}{2}-2} f(x)dx &= \sum_{k=1}^{p} \binom{p}{k} \left\{ \sum_{s=0}^{p-k} \binom{p-k}{s} \frac{(-1)^s (1+2^{1/\alpha})^s}{2^{p-k+1}} \left[\frac{\left(n-3+2^{1/\alpha}\right)^{p-k-s+1-\alpha}}{p-k-s+1-\alpha} + \right.\right. \\
&+ \left.\left. \frac{c^1(k,s)}{p-k-s+1-\alpha} \right] \right\}
\end{aligned} \tag{4.112}$$

and

$$\begin{aligned}
\int_1^{\frac{n}{2}-1} f(x)dx &= \sum_{k=1}^{p} \binom{p}{k} \left\{ \sum_{s=0}^{p-k} \binom{p-k}{s} \frac{(-1)^s (1+2^{1/\alpha})^s}{2^{p-k+1}} \left[\frac{\left(n-1+2^{1/\alpha}\right)^{p-k-s+1-\alpha}}{p-k-s+1-\alpha} + \right.\right. \\
&+ \left.\left. \frac{c^2(k,s)}{p-k-s+1-\alpha} \right] \right\}
\end{aligned} \tag{4.113}$$

where $c^1(k,s) = -(1+2^{1/\alpha})^{p-k-s+1-\alpha}$ and $c^2(k,s) = -(5+2^{1/\alpha})^{p-k-s+1-\alpha}$.

For $\alpha = 1$ the indefinite integral is given by:

$$\begin{aligned}\int f(x)dx &= \int \frac{(x+1)^p - x^p}{2x+3}dx = \\ &= \sum_{k=1}^{p}\binom{p}{k}\int \frac{x^{p-k}}{2x+3}dx = \\ &= \sum_{k=1}^{p}\binom{p}{k}\frac{1}{2^{p-k+1}}\left\{\sum_{s=0}^{p-k-1}\binom{p-k-1}{s}(-3)^s\frac{(2x+3)^{p-k-s}}{p-k-s} + (-3)^{p-k}\log(2x+3)\right\}\end{aligned}$$

Therefore

$$\begin{aligned}\int_0^{\frac{n}{2}-2} f(x)dx &= \sum_{k=1}^{p}\binom{p}{k}\frac{1}{2^{p-k+1}}\left\{\sum_{s=0}^{p-k-1}\binom{p-k-1}{s}(-3)^s\frac{(n-1)^{p-k-s}}{p-k-s}+\right. \\ &+ \left.(-3)^{p-k}\log\frac{n-1}{3} - \sum_{s=0}^{p-k-1}\binom{p-k-1}{s}(-3)^s\frac{3^{p-k-s}}{p-k-s}\right\}\end{aligned} \tag{4.114}$$

and

$$\begin{aligned}\int_1^{\frac{n}{2}-1} f(x)dx &= \sum_{k=1}^{p}\binom{p}{k}\frac{1}{2^{p-k+1}}\left\{\sum_{s=0}^{p-k-1}\binom{p-k-1}{s}(-3)^s\frac{(n+1)^{p-k-s}}{p-k-s}+\right. \\ &+ \left.(-3)^{p-k}\log\frac{n+1}{5} + \sum_{s=0}^{p-k-1}\binom{p-k-1}{s}(-3)^s\frac{5^{p-k-s}}{p-k-s}\right\}\end{aligned} \tag{4.115}$$

For $\alpha = 2$ the indefinite integral is given by:

$$\begin{aligned}\int f(x)dx &= \int \frac{(x+1)^p - x^p}{(2x+1+\sqrt{2})^2}dx = \sum_{k=1}^{p}\binom{p}{k}\int \frac{x^{p-k}}{(2x+1+\sqrt{2})^2}dx = \\ &= \sum_{k=1}^{p}\binom{p}{k}\left\{\sum_{s=0,s\neq p-k-1}^{p-k}\binom{p-k}{s}(-1)^s(1+\sqrt{2})^s\frac{(2x+1+\sqrt{2})^{p-k-s-1}}{p-k-s-1}+\right. \\ &+ \left.(-1)^s(1+\sqrt{2})^s\log(2j+1+\sqrt{2})\right\}\end{aligned}$$

Therefore

$$\begin{aligned}\int_0^{\frac{n}{2}-2} f(x)dx &= \sum_{k=1}^{p}\binom{p}{k}\left\{\sum_{s=0,s\neq p-k-1}^{p-k}\binom{p-k}{s}(-1)^s(1+\sqrt{2})^s\frac{(n-3+\sqrt{2})^{p-k-s-1}}{p-k-s-1}+\right.\\ &+ (-1)^s(1+\sqrt{2})^s\log\frac{n-3+\sqrt{2}}{1+\sqrt{2}}+\\ &- \left.\sum_{s=0,s\neq p-k-1}^{p-k}\binom{p-k}{s}(-1)^s(1+\sqrt{2})^s\frac{1+\sqrt{2})^{p-k-s-1}}{p-k-s-1}\right\} \qquad (4.116)\end{aligned}$$

and

$$\begin{aligned}\int_1^{\frac{n}{2}-1} f(x)dx &= \sum_{k=1}^{p}\binom{p}{k}\left\{\sum_{s=0,s\neq p-k-1}^{p-k}\binom{p-k}{s}(-1)^s(1+\sqrt{2})^s\frac{(n-1+\sqrt{2})^{p-k-s-1}}{p-k-s-1}+\right.\\ &+ (-1)^s(1+\sqrt{2})^s\log\frac{n-1+\sqrt{2}}{3+\sqrt{2}}+\\ &- \left.\sum_{s=0,s\neq p-k-1}^{p-k}\binom{p-k}{s}(-1)^s(1+\sqrt{2})^s\frac{3+\sqrt{2})^{p-k-s-1}}{p-k-s-1}\right\} \qquad (4.117)\end{aligned}$$

In all the cases, i.e. for $0<\alpha\leq 2$ the limits of the integrals results to be :

$$\lim_{n\to\infty}\frac{1}{n^\gamma}\int_0^{\frac{n}{2}-2} f(x)dx = \begin{cases}\infty & \text{if } 0\leq\gamma<p-\alpha\\ \dfrac{p}{2^p(p-\alpha)} & \text{if } \gamma=p-\alpha\\ 0 & \text{if } \gamma>p-\alpha\end{cases} \qquad (4.118)$$

and

$$\lim_{n\to\infty}\frac{1}{n^\gamma}\int_1^{\frac{n}{2}-1} f(x)dx = \begin{cases}\infty & \text{if } 0\leq\gamma<p-\alpha\\ \dfrac{p}{2^p(p-\alpha)} & \text{if } \gamma=p-\alpha\\ 0 & \text{if } \gamma>p-\alpha\end{cases} \qquad (4.119)$$

for every $\alpha\in(0,2]$. Therefore

$$\lim_{n\to\infty}\frac{R_n}{n^\gamma} = \begin{cases}\infty & \text{if } 0\leq\gamma<p-\alpha\\ \dfrac{p}{2^p(p-\alpha)} & \text{if } \gamma=p-\alpha\\ 0 & \text{if } \gamma>p-\alpha\end{cases} \qquad (4.120)$$

At this point remembering Eq. (4.101) we finally have that

$$\lim_{n\to\infty}\frac{P_n}{n^\gamma}=\begin{cases}\infty & \text{if } 0\le\gamma<p-\alpha\\ \dfrac{\alpha}{p-\alpha} & \text{if } \gamma=p-\alpha\\ 0 & \text{if } \gamma>p-\alpha\end{cases} \tag{4.121}$$

for $\alpha\in(0,2]$.

For the case in which the farthest cell n is odd, series is given by:

$$P_n=\sum_{j=0}^{\frac{n-3}{2}}\left(\frac{1}{(2j+2^{1/\alpha})^\alpha}-\frac{1}{(2j+2+2^{1/\alpha})^\alpha}\right)(2j+1)^p \tag{4.122}$$

The corrispondent reduced sum is:

$$R_n \;=\; \frac{1}{2}+\sum_{j=1}^{\frac{n-3}{2}}\frac{(2j+1)^p-(2j-1)^p}{(2j+2^{1/\alpha})^\alpha}-\frac{(n-3)^p}{2^p(n-1+2^{1/\alpha})^\alpha} \tag{4.123}$$

At this point one can proceeds similarly to the even case, obtaining the very same results.

□

4.3 Numerical Results

In this last section we want to present two examples of the S_α and the related numerical results for two particular choices of α. In the numerical simulations we approximate the initial condition, equal to the unit square with the Lebesgue measure, by means of a uniform random distribution of point particles in it. Therefore, the mean square displacement (4.26) becomes:

$$\langle\Delta\hat{X}_n^2\rangle\approx\frac{1}{N}\sum_{i=1}^{N}\left(\hat{X}_n(i)-\hat{X}_0(i)\right)^2 \tag{4.124}$$

where N is the total number of point particles and $\hat{X}_k(i)$ is the position of the i-th particle at the time instant k.

Example 1. Let's take $\alpha = 1/2$.
In this case the family of slicers is the following:

$$L_{1/2} = \left\{ \frac{1}{(|j|+4)^{1/2}} = \frac{1}{\sqrt{j+4}},\ j \in \mathbb{Z} \right\} \tag{4.125}$$

From (4.34) we evince that the asymptotic behavior of the mean square displacement of the slicer dynamics $S_{1/2}$ is

$$\left\langle \Delta \hat{X}_n^2 \right\rangle \sim n^{\frac{3}{2}} \tag{4.126}$$

Therefore the map $S_{1/2}$ presents a super-diffusive behavior with $\gamma = 3/2$ (cf. Fig. 4.3) and generalized diffusion coefficient $T_{1/2} = \frac{8}{3}$ (cf. Fig. 4.4). Moreover from the Theorem 4.2.4 we can say that the moments higher than the second have the following behavior:

$$\langle \Delta \hat{X}_n^p \rangle \sim n^{p-\frac{1}{2}} \tag{4.127}$$

We illustrate this behavior in Fig. 4.5 where we show the numerical result for the sixth moment, i.e. $p = 6$, compared with the function $n^{11/2}$. Finally we can report even the analitically computed probability distribution for $S_{1/2}$, cf. (4.22) and (4.23). If $n \in P$:

$$\rho_n^G\left(\hat{X}\right) = \begin{cases} \frac{1}{2} - \frac{1}{\sqrt{5}}, & \text{for } \hat{X} \in M_0 \\ \frac{1}{\sqrt{2k+3}} - \frac{1}{\sqrt{2k+5}}, & \text{for } \hat{X} \in M_{2k},\ k = 2, \ldots, \frac{n-2}{2} \\ \frac{1}{\sqrt{n+3}} & \text{for } \hat{X} \in M_n \\ 0, & \text{otherwise} \end{cases} \tag{4.128}$$

and if $n \in D$:

$$\rho_n^G\left(\hat{X}\right) = \begin{cases} \frac{1}{\sqrt{2k+4}} - \frac{1}{\sqrt{2k+6}}, & \text{for } \hat{X} \in M_{2k+1},\ k = 2, \ldots, \frac{n-3}{2} \\ \frac{1}{\sqrt{n+3}} & \text{for } \hat{X} \in M_n \\ 0, & \text{otherwise} \end{cases} \tag{4.129}$$

In Fig. 4.6 we report the numerical result for the behavior of the marginal probability distribution function $\rho_n^G(m)$ for $\alpha = 1/2$ in the even case compared with the function $\rho^{1/2}(m) = \dfrac{1}{(m+4)^{3/2}}$ at a fixed time instant, cf. (4.24).

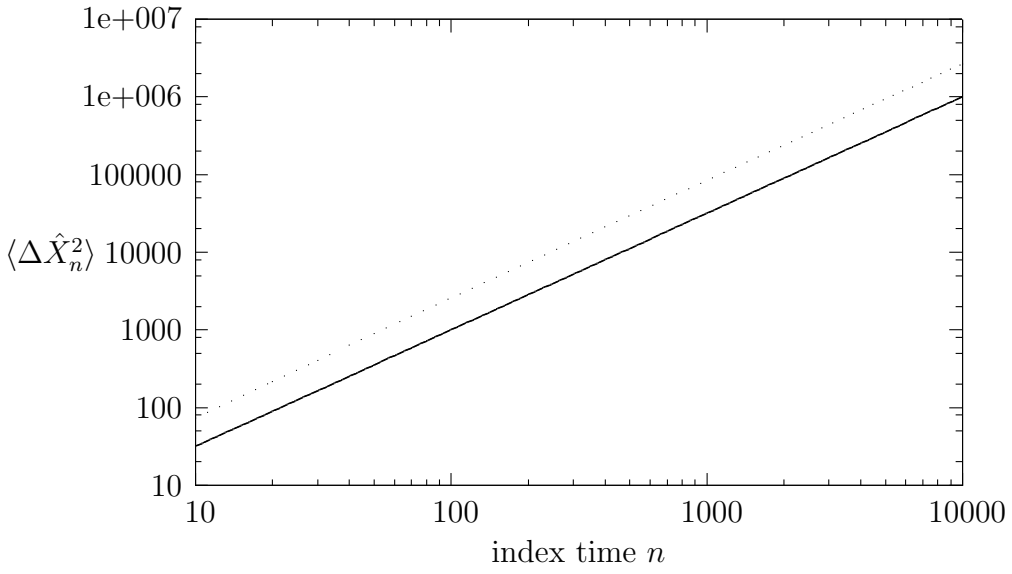

Figure 4.3: Behavior of mean square displacement of map $S_{1/2}$ (continuous line) for $n = 10^4$ and for a choice of $N = 10^4$ points, compared with $f(n) = n^{3/2}$ (dotted line).

Example 2. Let's take $\alpha = 1/3$.
In this case the family of slicers is the following:

$$L_{1/3} = \left\{ \frac{1}{(|j|+8)^{1/3}} = \frac{1}{\sqrt[3]{j+8}} \; j \in \mathbb{Z} \right\} \tag{4.130}$$

From (4.34) we evince that the asymptotic behavior of the mean square displacement of the slicer dynamics $S_{1/3}$ is

$$\langle \Delta \hat{X}_n^2 \rangle \sim n^{\frac{5}{3}} \tag{4.131}$$

Therefore also the map $S_{1/3}$ presents a super-diffusive behavior with $\gamma = 5/3$ (cf. Fig. 4.7) and generalized diffusion coefficient $T_{1/3} = \frac{12}{5}$ (cf. Fig. 4.8). From the Theorem 4.2.4 we can say that the moments higher then the second of the map $S_{1/3}$ have the following behavior:

$$\langle \Delta \hat{X}_n^p \rangle \sim n^{p-\frac{1}{3}} \tag{4.132}$$

We illustrate this behavior in Fig. (4.2).

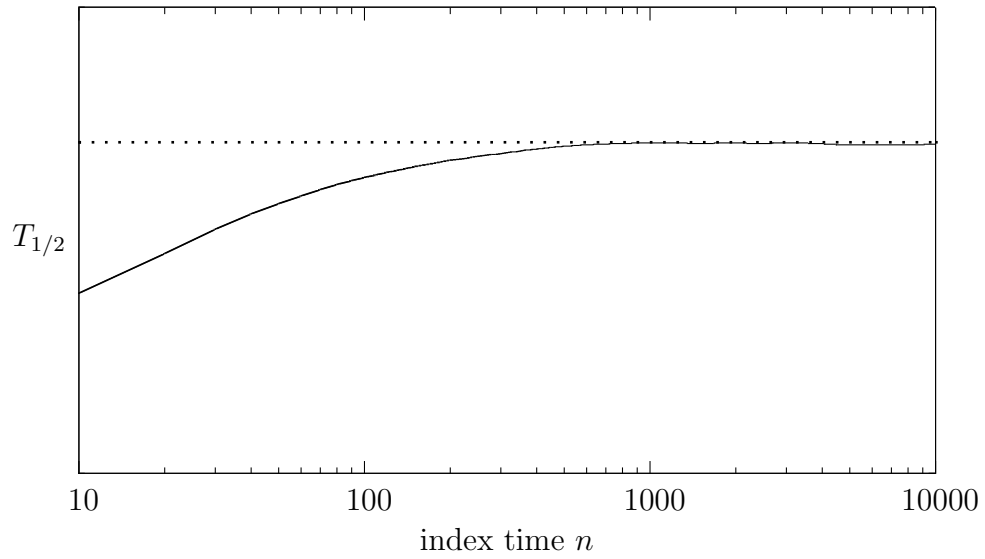

Figure 4.4: Behavior of the numerically estimated coefficient $T_{1/2}$ (continuous line) for $n = 10^4$ and for a choice of $N = 10^3$ points compared with $f(n) = \frac{8}{3}$ (dotted line).

Finally we report the probability probability distribution function for $S_{1/3}$, cf. (4.22) and (4.23). If $n \in P$:

$$\rho_n^G\left(\hat{X}\right) = \begin{cases} \frac{1}{2} - \frac{1}{\sqrt[3]{9}}, & \text{for } \hat{X} \in M_0 \\ \frac{1}{\sqrt{2k+7}} - \frac{1}{\sqrt{2k+9}}, & \text{for } \hat{X} \in M_{2k},\ k = 2, \ldots, \frac{n-2}{2} \\ \frac{1}{\sqrt{n+7}} & \text{for } \hat{X} \\ 0, & \text{otherwise} \end{cases} \tag{4.133}$$

and if $n \in D$:

$$\rho_n^G\left(\hat{X}\right) = \begin{cases} \frac{1}{\sqrt{2k+8}} - \frac{1}{\sqrt{2k+10}}, & \text{for } \hat{X} \in M_{2k+1},\ k = 2, \ldots, \frac{n-3}{2}, \\ \frac{1}{\sqrt{n+7}} & \text{for } \hat{X} \in M_n \\ 0, & \text{otherwise} \end{cases} \tag{4.134}$$

In the Fig. (4.9) we report the numerical result for the behavior of the marginal probability distribution function $\rho_n^G(m)$ for $\alpha = 1/3$ in the even case, compared with the function $\rho^{1/3}(m) = \dfrac{1}{(m+8)^{4/3}}$ at a fixed time instant, cf. (4.24).

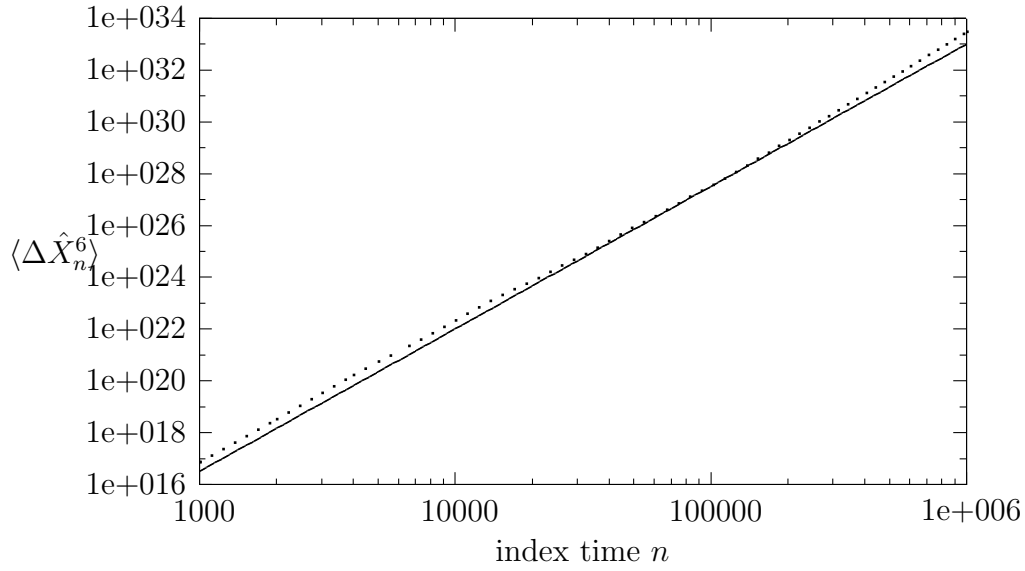

Figure 4.5: Behavior of moment with $p = 6$ for map $S_{1/2}$ (continuous line), estimated numerically with $n = 10^6$ and for a choice of $N = 10^4$ points, compared with $f(n) = n^{11/2}$ (dotted line).

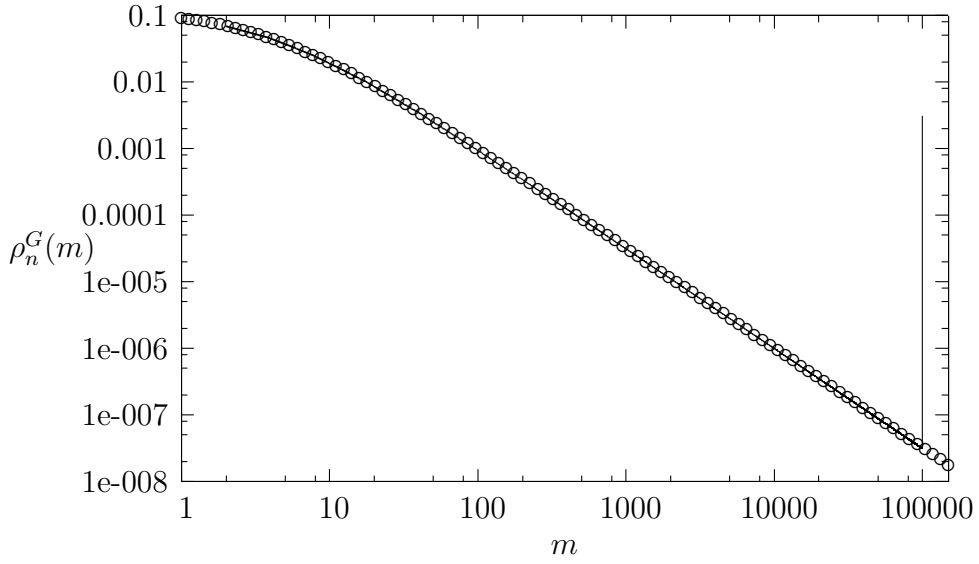

Figure 4.6: Behavior of marginal probability distribution function $\rho_n^G(m)$ (continuous line) for map $S_{1/2}$ compared with $\rho^{1/2}(m) = 1/(m+4)^{3/2}$ (circles) at fixed time $n = 10^5$.

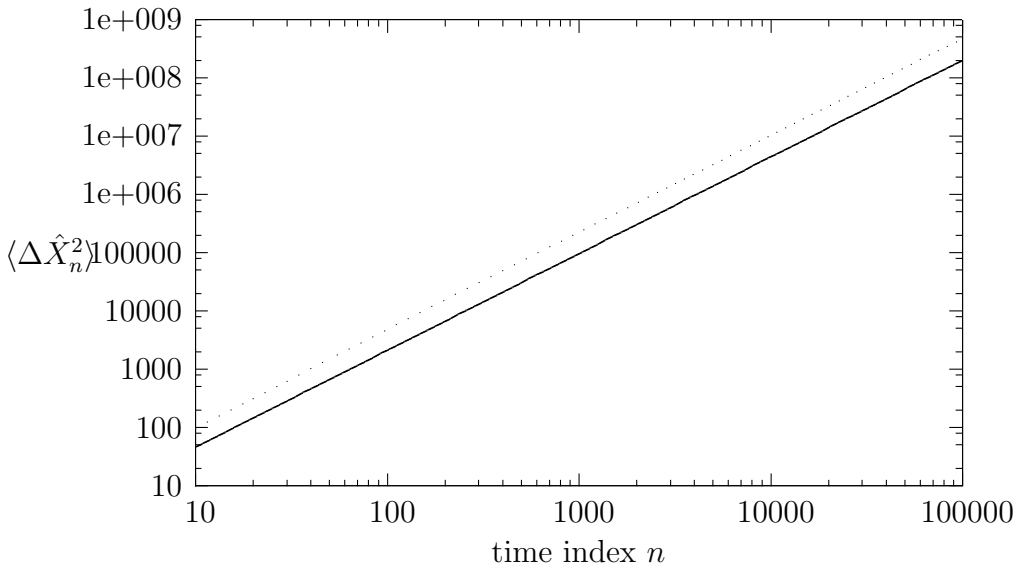

Figure 4.7: Behavior of mean square displacement of map $S_{1/3}$ (continuous line) for $n = 10^5$ and for a choice of $N = 10^5$ points, compared with $f(n) = n^{5/3}$ (dotted line).

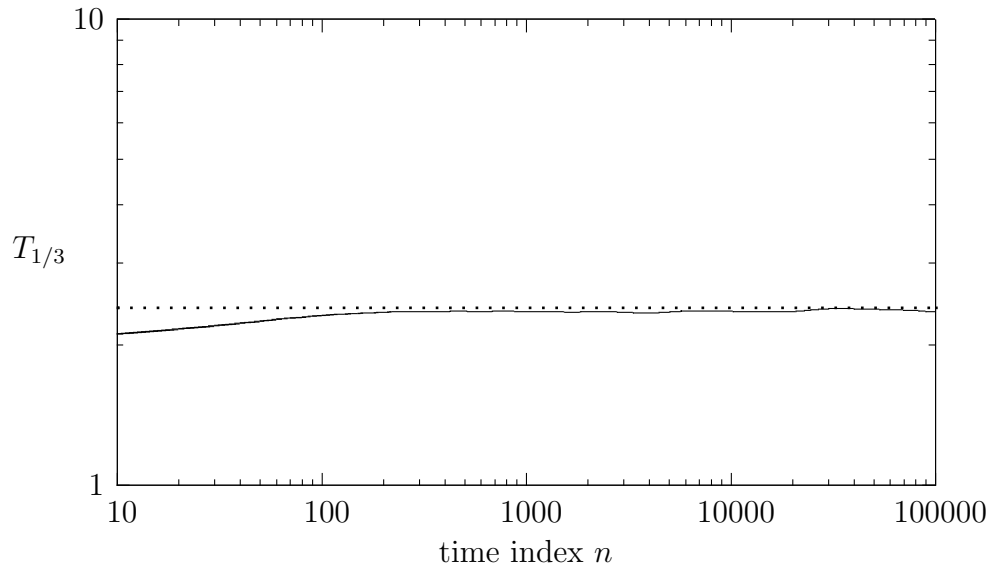

Figure 4.8: Behavior of the numerically estimated coefficient $T_{1/3}$ (continuous line) for $n = 10^5$ time steps and for a choice of $N = 10^5$ points, compared with $f(n) = \frac{12}{5}$ (dotted line).

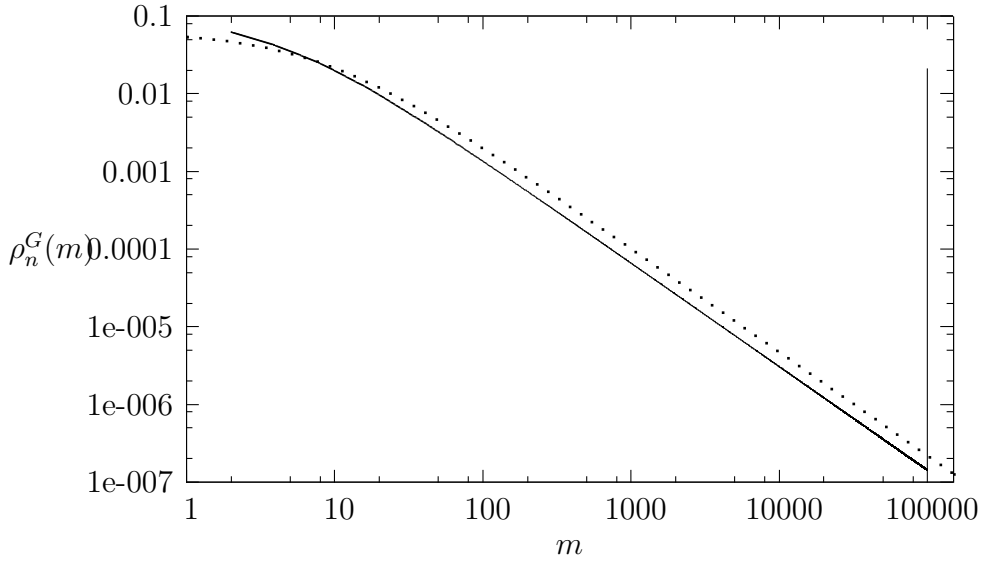

Figure 4.9: Behavior of marginal probability distribution function $\rho_n^G(m)$ for map $S_{1/3}$ (continuous line) compared with $\rho^{1/3}(m) = \dfrac{1}{(m+8)^{4/3}}$ (dotted line) at fixed time $n = 10^5$. Notice that the two function do not coincide perfeclty because we neglect the normalization constant.

Chapter 5

Slicer Map and Lévy Walks

In this section we compare our model with a model of a known sthocastic process, the Lévy walk, which yields anomalous diffusion [59]. We start from an introduction of the Lévy process and its properties. Then we define Lévy flights and Lévy walks in the framework of continuous time random walk. We find that the probability distribution characterizing our slicer dynamics is asymptotically closely related with the distribution of a Lévy walk.
Moreover, furhter analyzing these models, we may say that observations of the trivial dynamics described by our slicer maps cannot distinguish them from the highly complex evolutions of Lévy walks. Indeed, all moments of these dynamics coincide.

5.1 Lévy Stable Processes

We introduce a sequence of definitions about stable distributions and properties of random processes [60], to provide a proper framework for Lévy processes . Throughout this section, we denote by $X, X_1, X_2, \ldots$ and by $S_n = X_1 + \cdots + X_n$ mutually independent random variables with a common distribution F and their sum.

Definition 5.1. *The distribution F, not concentrated on the origin, is called*

stable if for all $n \in \mathbb{N}$ *there exists constants* $c_n > 0$ *and* γ_n *in* $\mathbb{R}$ *such that*

$$S_n \stackrel{d}{=} c_n X + \gamma_n \tag{5.1}$$

With $\stackrel{d}{=}$ *we mean that the random variables on the two side of the equality have the same distribution. If* $\gamma_n = 0$ *the distribution is called strictly stable.*

Definition 5.2. *A distribution* F *of a random variable* X *is infinitely divisible if for each* $n \in \mathbb{N}$ *there exists* $X_{1,n}; \ldots; X_{n,n}$ *independent and identically distributed random variables such that*

$$X \stackrel{d}{=} X_{1,n} + \ldots + X_{n,n} \tag{5.2}$$

Definition 5.3. *A process* $\{X(t), t \geq 0\}$ *is said to have independent increments if its increments* $X(t_{k+1}) - X(t_k)$ *are mutually independent for any finite set* $t_1 < \ldots < t_n$.

Definition 5.4. *A process* $\{X(t), t \geq 0\}$ *has stationary increments if the distribution of* $X_{s+t} - X_s$ *depends only on the length* t *of the time interval and not on* s.

Remark 4. Partition the time interval $(s, s+t)$ by $n+1$ equidistant points $s = t_0 < t_1 < \ldots < t_n = s+t$ and take $X_{k,n} = X(t_k) - X(t_{k-1})$. The random variable $X(s+t) - X(s)$ of a process X with independent stationary increments is the sum of n independent identically distributed random variables $X_{k,n}$. Hence $X(s+t) - X(s)$ has an infinitely divisible distribution.

We can now give the definition of a Lévy process [61].

Definition 5.5. *A continuous-time process* $\{X(t), t \geq 0\}$ *with values in* $\mathbb{R}$ *is called a Lévy process if its sample paths are right continuous, have left limits at every time* t *and if it has stationary independent increments. The default initial condition is* $X(0) = 0$.

Let us denote a Lévy process by $\{L(t), t \geq 0\}$. From an obvious decomposition it follows that [62]:

$$\begin{aligned} L(t) &= L\left(\frac{t}{n}\right) + \left[L\left(\frac{2t}{n}\right) - L\left(\frac{t}{n}\right)\right] + \\ &+ \ldots + \left[L\left(\frac{nt}{n}\right) - L\left(\frac{(n-1)t}{n}\right)\right] \end{aligned} \tag{5.3}$$

in other words the random variable $L(t)$ can be subdivided into the sum of an arbitrary number of independent and identically distributed random variables, hence its probability distribution belongs to the class of infinitely divisible distributions.

If we consider a strictly stable Lévy process, its characteristic function reads [63]:

$$\phi(k; \mu, \sigma, \alpha, \beta) = \exp\left[i\mu k - \sigma^{\alpha} |k|^{\alpha} \left(1 - i\beta \frac{k}{|k|} \omega(k, \alpha)\right)\right] \tag{5.4}$$

where

$$\omega(k, \alpha) = \begin{cases} \tan\frac{\pi\alpha}{2}, & \text{if } \alpha \neq 1 \\ -\frac{2}{\pi} \ln|k|, & \text{if } \alpha = 1 \end{cases} \tag{5.5}$$

Further, we can define the probability density function related to the same Lévy stable process, through this characteristic function. The density is the Fourier transform of the characteristic function:

$$p_{\alpha,\beta}(k; \mu, \sigma) = \mathcal{F}\left\{\phi(k; \mu, \sigma, \alpha, \beta)\right\} = \int_{-\infty}^{+\infty} \phi(x) \exp(ikx)\, dx \tag{5.6}$$

Thus one can see that, in general, the characteristic function and, respectively the Lévy stable probability density function are determined by four real parameters: α, β, μ and σ. The exponent $\alpha \in [0, 2]$ is the index of stability, $\beta \in [-1, 1]$ is the skewness parameter, μ is the shift parameter and $\sigma > 0$ is a scale parameter. Among these parameters the shift and scale ones play a lesser role in the sense that they can be eliminated by proper scale and shift transformations

$$p_{\alpha,\beta}(x; \mu, \sigma) = \frac{1}{\sigma} p_{\alpha,\beta}\left(\frac{x - \mu}{\sigma}; 0, 1\right) \tag{5.7}$$

Due to this property we can set $\mu = 0$ and $\sigma = 1$ and denote the Lévy stable distribution function by $p_{\alpha,\beta}(x)$. Notice that $\beta = 0$ if the distribution is

symmetric. Lévy stable laws are of interest in particular for their asymptotic behavior. For $x \to \pm\infty$ the symmetric stable density function scales as follows:

$$p_{\alpha,0}(x) \sim C_1(\alpha)\frac{1}{|x|^{1+\alpha}} \tag{5.8}$$

where $C_1 = \frac{1}{\pi}\sin\left(\frac{\pi\alpha}{2}\right)\Gamma(1+\alpha)$. Moreover the variance (i.e. mean square displacement) of all Lévy stable probability density functions diverges if $\alpha < 2$.

5.2 Lévy Flights and Lévy Walks

Now we want to introduce Lévy flights and Lévy walks in the framework of continuous time random walks [64], [65]. Let $p(x,t)$ be the probability distribution of being at position x at time t and let $\psi(x,t)$ be the probability distribution of making a step of lenght x in the time interval t to $t+dt$. The total transition probability in this time interval is

$$\psi(t) = \sum_x \psi(x,t) = \psi(k=0,t) \tag{5.9}$$

where $\psi(k,t)$ is the Fourier transform $x \to k$ of $\psi(x,t)$. If we denote by $\eta(x,t)$ the probability density of just arriving at x in the time interval t to $t+dt$, then [66], [67], [68]

$$\eta(x,t) = \sum_{x'}\int_0^t \eta(x',\tau)\psi(x-x',t-\tau)d\tau + \delta(t)\delta_{x,0} \tag{5.10}$$

Here we have assumed the initial condition of starting at $t=0$ from $x=0$. The relation between $p(x,t)$ and $\eta(x,t)$ is given through

$$p(x,t) = \int_0^t \eta(x,t-\tau')\phi(\tau')d\tau' \tag{5.11}$$

where

$$\phi(t) = 1 - \int_0^t \psi(\tau)d\tau \tag{5.12}$$

is the probability of not having left the original site up to time t. The Laplace transform of $\phi(t)$ yields

$$\phi(u) = \frac{1 - \psi(u)}{u} \tag{5.13}$$

Using (5.11) and changing the order of the integrations allows us to write (5.10) as an integral equation for $p(x,t)$ with kernel $\psi(x,t)$:

$$p(x,t) = \sum_{x'} \int_0^t p(x',\tau)\psi(x-x',t-\tau)d\tau + \phi(t)\delta_{x,0} \tag{5.14}$$

From this last equation one has in the Fourier-Laplace space

$$p(k,u) = p(k,u)\psi(k,u) + \phi(u) \tag{5.15}$$

from which follows

$$p(k,u) = \frac{1-\psi(u)}{u}\frac{1}{1-\psi(k,u)} \tag{5.16}$$

This quantity is the key to the determination of $p(x,t)$ through Fourier-Laplace inversion. Now let us consider two different cases. In the first case we take a distribution $\psi(x,t)$ in which x and t are decoupled [63], i.e.

$$\psi(x,t) = \lambda(x)\psi(t) \tag{5.17}$$

Hence (5.16) become

$$p(k,u) = \frac{1-\psi(u)}{u}\frac{1}{1-\lambda(k)\psi(u)} \tag{5.18}$$

Then assume $\psi(t) = \delta(t-t_0)$ and $\lambda(x)$ of Lévy stable form, with index $0 < \alpha < 2$. The resulting process is markovian, but with diverging variance. From (5.18) we obtain the Fourier image of the associated probability density function:

$$p(k,t) = exp\left[-K_\alpha |k|^\alpha t\right] \tag{5.19}$$

Comparing with (5.4) this is nothing but the characteristic function of a symmetric Lévy stable probability density function with index of stability

α. This type of random process is called Lévy flight. In the second case we consider a coupled form of $\psi(x,t)$. In this respect a suitable function is [64]

$$\psi(x,t) = A\,|x|^{-\xi}\,\delta(|x| - t^{\nu}) \tag{5.20}$$

where through the δ-function x and t are coupled. In this case steps of arbitrary lenght are allowed but long steps are penalized by required longer time to be performed. This process is called Lévy walk.

5.3 Lévy Walk in Quenched Disordered Media

In this section we take into consideration a particular model of Lévy walk in quenched disordered media, which is studied in Ref. [59]. In that work, the authors introduce a one-dimensional structure with a sequence of scatterers spaced according to a Lévy type distribution (cf. Fig. 5.1), so that the probability density for two consecutive scatterers to be at distance r is given by:

$$\lambda(r) \equiv \beta r_0^{\beta} \frac{1}{r^{\beta+1}}, \quad r \in [r_0, +\infty) \tag{5.21}$$

where $\beta > 0$ and r_0 is a cutoff fixing the characteristic length scale of the system. A continuous time random walk is naturally defined on this structure, which is to say that a walker moves ballistically (at constant velocity v) until it reaches one of the scatterers and then it is transmitted or reflected with probability 1/2. The authors of [59] derive an analytic expression for the asymptotic behavior of the mean square displacement $\langle r^2(t)\rangle$ when averaged over the scattering points. At first they introduce the most general scaling hypothesis for the probability distribution $P(r,t)$:

$$P(r,t) = l^{-1}(t) f\left(\frac{r}{l(t)}\right) + g(r,t) \tag{5.22}$$

where $l(t)$ is the characteristic length of P. The following convergences in probability are assumed:

$$\lim_{t\to+\infty}\int_0^{vt}\left|P(r,t)-l^{-1}(t)f\left(\frac{r}{l(t)}\right)\right|dr=0 \tag{5.23}$$

and

$$\lim_{t\to+\infty}\int|g(r,t)|\,dr=0 \tag{5.24}$$

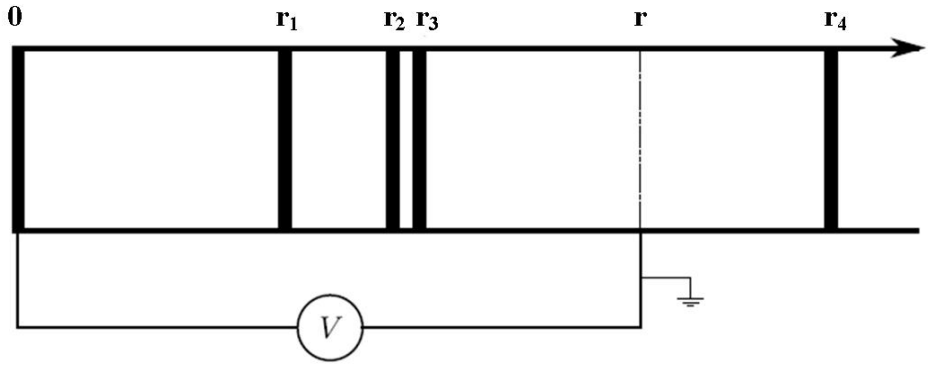

Figure 5.1: Model of the unidimensional structure of Burioni et al. model and related electric problem. At the locations r_1, r_2, ... we find the scatterers placed according to a Lévy type distribution.

The explicit expression of the mean square displacement now reads:

$$\langle r^2(t)\rangle=\int_0^{vt}l^{-1}(t)f\left(\frac{r}{l(t)}\right)r^2dr+\int_0^{vt}g(r,t)r^2dr \tag{5.25}$$

To get an analytic expression for this quantity, an electric problem equivalent to a random walk has been taken into consideration [69], allowing the calculation of the number $N(t)$ of scattering sites visited by the walker in a time t. More precisely, in the electrical analogy $N(t)$ is given by the resistance R of a segment of length $l(t)$. From [70], Burioni et al. calculated analitically the asymptotic behavior of R at large distances obtaining $R(r)\sim r^\beta$ for $\beta<1$ and $R(r)\sim r$ for $\beta>1$, and accordingly for $r\gg l(t)$:

$$N(t)\approx R(l(t))\sim\begin{cases}t^{\frac{\beta}{1+\beta}}, & \text{if } 0<\beta<1\\ t^{1/2}, & \text{if } \beta\geq 1\end{cases} \tag{5.26}$$

Another assumption made by the authors of [59] is the "single long jump" hypothesis, which amounts to neglect the possibility of multiple consecutive jumps of length larger then a given size. For $r \gg l(t)$ this yields:

$$P(r,t) \sim \frac{N(t)}{r^{1+\beta}} \tag{5.27}$$

According to this and recalling (5.26), the asymptotic (in t and r) probability density function for $\beta < 1$ is given by:

$$P(r,t) \sim t^{\frac{\beta}{1+\beta}} \frac{1}{r^{1+\beta}} \tag{5.28}$$

and for $\beta > 1$ is expressed by

$$P(r,t) \sim t^{\frac{1}{2}} \frac{1}{r^{1+\beta}} \tag{5.29}$$

Finally, the result for the mean square displacement is the following (cf. Fig. 5.2)

$$\langle r^2(t) \rangle \sim \begin{cases} t^{\frac{2+2\beta-\beta^2}{1+\beta}} & \text{if } 0 < \beta < 1 \\ t^{\frac{5}{2}-\beta} & \text{if } 1 \leq \beta \leq \dfrac{3}{2} \\ t & \text{if } \dfrac{3}{2} < \beta \end{cases} \tag{5.30}$$

More generally, one obtains an analytic result for the asymptotic behavior of the moments $\langle r^p(t) \rangle$ for all $p > 0$ that reads

$$\langle r^p(t) \rangle \sim \begin{cases} t^{\frac{p}{1+\beta}} & \text{if } \beta < 1,\ p < \beta \\ t^{\frac{p(1+\beta)-\beta^2}{1+\beta}} & \text{if } \beta < 1,\ p > \beta \\ t^{\frac{p}{2}} & \text{if } \beta > 1,\ p < 2\beta - 1 \\ t^{\frac{1}{2}+p-\beta} & \text{if } \beta > 1,\ p > 2\beta - 1 \end{cases} \tag{5.31}$$

5.4 Comparison

Now let us recall the result for the asymptotic behavior of the mean square displacement produced by our slicer model (4.34):

$$\langle \Delta \hat{X}^2(t) \rangle \sim t^{2-\alpha} \tag{5.32}$$

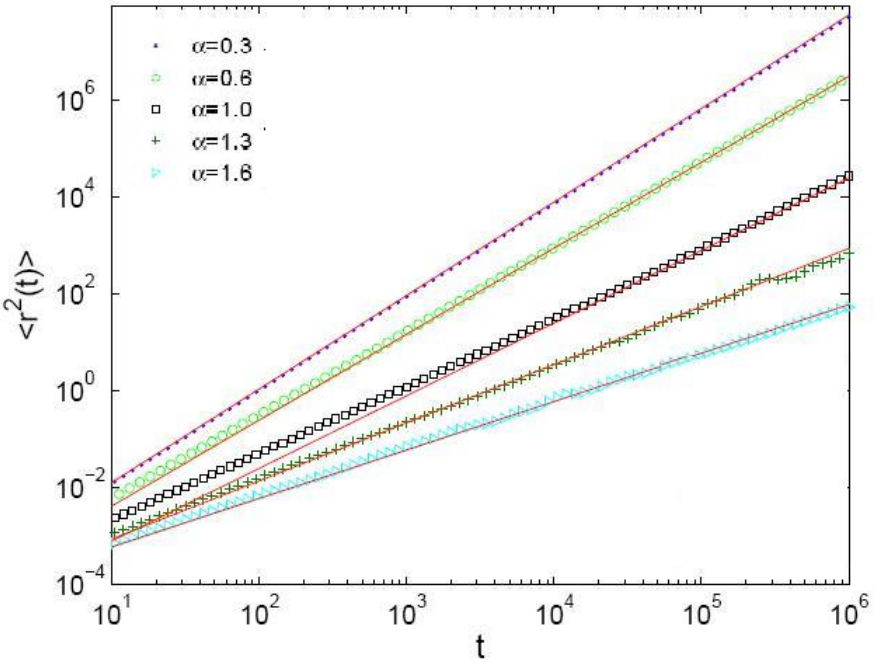

Figure 5.2: Asymptotic behavior of mean square displacement of Burioni et al. model for different choices of parameter β.

for $0 < \alpha \leq 2$, whereas the moments $\langle \Delta \hat{X}^p(t) \rangle$ for our slicer map for $p > 2$, asymptotically go like:

$$\langle \Delta \hat{X}^p(t) \rangle \sim t^{p-\alpha} \tag{5.33}$$

for $0 < \alpha \leq 2$ (cf. Theorem 4.2.4).

If we fix the Lévy walk parameter β, we can determine the value of our parameter α for which the second moments of the Lévy walk and of the slicer dynamics, (5.32) and (5.30), asymptotically coincide. We restrict the comparison to the case with $0 < \beta \leq \frac{3}{2}$, since the behavior of the two model is not comparable for $\beta > \frac{3}{2}$. Indeed, the Lévy model presents a constant diffusive trend for $\beta > \frac{3}{2}$, whereas the slicer map changes its transport properties for every variation of the parameter. This observation proves that the equivalence between Lévy walks and slicer dynamics is not trivial.

Therefore we obtain the following: for

$$\alpha = \begin{cases} \frac{\beta^2}{1+\beta} & \text{if } 0 < \beta \leq 1 \\ \beta - \frac{1}{2} & \text{if } 1 < \beta \leq \frac{3}{2} \end{cases} \tag{5.34}$$

the variances of the slicer dynamics and Lévy walk coincide asymptotically in t. Now let us consider the moments related to the two models for $p > 2$, $p \in P$. Consider the case of $0 < \beta < 1$ first. Take the value of α from (5.34) and substitute it in (5.33). This yields

$$\langle \Delta \hat{X}^p(t) \rangle \sim t^{\frac{p(1+\beta)-\beta^2}{1+\beta}} \tag{5.35}$$

for the asymptotic behavior in t of the slicer dynamics. If we do the same for the case $1 \leq \beta \leq \frac{3}{2}$ the moments of the slicer model are given by:

$$\langle \Delta \hat{X}^p(t) \rangle \sim t^{p-\beta+\frac{1}{2}} \tag{5.36}$$

for all $p > 2$. We notice that, comparing with (5.31), we obtain the same values of the Lévy walk model. In other words, fixing α and β so that the second moment are asymptotically equal, one obtains the asymptotic equality of all moments of order $p > 2$ as well. We have thus proved the following:

Theorem 5.4.1. *For all $0 < \beta \leq \frac{3}{2}$, $\beta \neq 1$, of a Lévy walk $\exists\ \alpha \in (0, 2]$ such that all moments of order ≥ 2 of the slicer map and of the Lévy walk asymptotically coincides. The value α is given by (5.34).*

Therefore our trivial deterministic model defined in the previous chapter seems to be asymptotically indistiguishable from a Lévy walk for $\beta \leq \frac{3}{2}$. To obtain this equivalence it suffices to fix α so that the second moments asymptotically coincide. This is confirmed also from the fact that the probability distribution of the slicer model is a Lévy-type density, for $\beta \leq \frac{3}{2}$, i.e. $\alpha \in [0, 3/2]$. However, for completeness, one should check the correlations to confirm this conjecture.

We have to precise that we are not looking at all moments of Lévy distribution as a function of two variables, which in general involve $t^p r^q$. Therefore the equality of all moments we considered des not imply the equality of the

probability distributions. This can be obtain only for special choice of r and t. This reinforces the non triviality of the observational indistinguishability. Let us now compare the two dynamics for a particular choice of the parameters: $\alpha = \dfrac{1}{3}$ and consequently $\beta = \dfrac{1+\sqrt{13}}{6}$, cf. (5.34). This yields

$$\langle \Delta \hat{X}^2(t) \rangle \sim t^{\frac{5}{3}} \tag{5.37}$$

for both systems (cf. Fig. 5.3). Similarly if we substitute $\alpha = 1/3$ and $\beta = (1+\sqrt{13})/6$ respectively in (5.33) and (5.31), the moments for $p > 2$, $p \in P$, have the following behavior:

$$\langle \Delta \hat{X}^p(t) \rangle \sim t^{\frac{3p-1}{3}} \tag{5.38}$$

The value $\alpha = \frac{1}{3}$ is of interest because $t^{5/3}$ is the numerically computed asymptotic value of the mean square displacement for the polygonal billiards with parallel walls which make angle of 90 degrees in [23], [24].

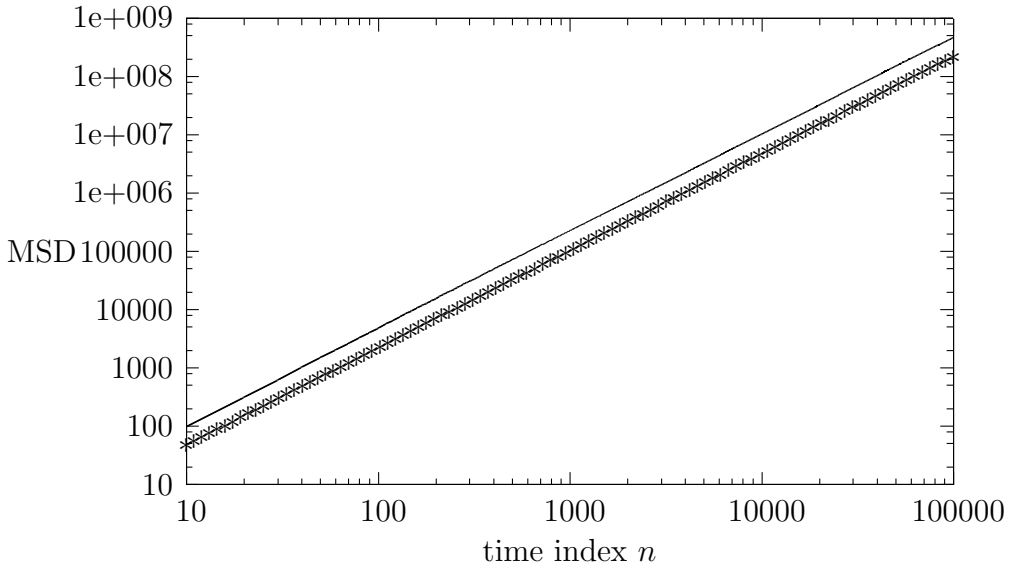

Figure 5.3: Behavior of the mean square displacement of map $S_{1/3}$ (stars line) up to a time $n = 10^5$ and for a choice of $N = 10^4$ points, compared with mean square displacement of Burioni et al. Lévy walk model (continuous line) where α and β are related by Eq. (5.34).

Chapter 6

Variations on the Slicer Map

In this section we introduce some variations of the slicers dynamics, with the purpose of increasing its similarity with the dynamics of polygonal billiards. To get closer, for instance, to the 2-dimensional nature of the dynamics of billiard map we introduce a second slicer so that the second coordinate of the slicer dynamics is not trivial anymore. These changes are just attempts and leave many open question to be investigated in the future. For each variation of the original slicer model, we analyze in particular the behavior of mean square displacement as a function of time.
For all the variations, we keep the same phase space of the original model, as described in Chapter 4, i.e. a chain of identical square cells, $\hat{M} = [0,1]^2 \times \mathbb{Z}$. We also indicate with $M_0 = [0,1]^2 \times \{0\}$ the 0-th cell. Analytically these models are very complex to deal with, therefore the results we present here are mainly of numerical nature.

6.1 Translating Slicer Map

In the first variation we consider the same slicer map S as in the slicer dynamics, cf. (4.1), but we introduce a different law to obtain infinitely many scales. Indeed, rather than introducing by hand infinitely many scales

by properly placing the family of slicers $\{l_j, j \in \mathbb{Z}\}$ in the generic cell of the chain and activating a pair of them by means of a particular rule (4.5), here we use an ergodic translation on the 1-dimensional torus to generate the slicers.
Let us recall the definition of the slicer map

$$S_{l_\alpha}(x,y,m) = \begin{cases} (x,y,m-1) & \text{if } 0 \le x \le l_\alpha \text{ or } \frac{1}{2} \le x \le 1-l_\alpha \\ (x,y,m+1) & \text{if } l_\alpha < x < \frac{1}{2} \text{ or } 1-l_\alpha < x \le 1 \end{cases} \tag{6.1}$$

We want to stress that now we do not have anymore the dependence of the active slicers from the cell index, but we have just two symmetric slicers l_α and $1-l_\alpha$ active at each time step, equal for all the cells.
Let us now introduce a temporal evolution for the slicers.

Definition 6.1. *Let $n \in \mathbb{N}$ be the temporal index and $\alpha \in (0,1]$ a parameter. $l_\alpha : \mathbb{N} \to [0,1]$ is a map such that:*

$$l_\alpha(n) = (l_\alpha(n-1) - \alpha)\, MOD_{1/2}. \tag{6.2}$$

The function $(x)MOD_{1/2}$ acts as follow:

$$(x)MOD_{1/2} = \begin{cases} x, & \text{if } 0 \le x \le \frac{1}{2} \\ x + \frac{1}{2}, & \text{if } x < 0 \end{cases} \tag{6.3}$$

If $\alpha \notin \mathbb{Q}$ the dynamical slicer (6.2) explores (ergodically) densely the interval $[0, 1/2]$. If $\alpha \in \mathbb{Q}$, the motion of l_α is periodic.
Altogheter the translating slicer dynamics is thus governed by the mapping $S_T = S_{l_\alpha}$ where l_α is given by (6.2) and defines at each time step the pairs of slicers l_α and $1-l_\alpha$ in the map S_{l_α} (4.1), starting from the central slicer $l(0) = 1/2$. More precisely at time step n we have

$$S_T^n = S_{l_\alpha(n-1)} \circ S_{l_\alpha(n-2)} \circ \ldots \circ S_{l_\alpha(1)} \circ S_{l_\alpha(0)} \tag{6.4}$$

We give now some examples. The first two results are about the case of a rational α, for which we can also do some analytical evaluations.

Example 3. Let $\alpha = \frac{1}{6}$. The time evolution $l_{1/6}$, (6.2), generates the following periodic sequence of slicers $\left\{\frac{1}{2}, \frac{1}{3}, \frac{1}{6}, 0, \frac{1}{3}, \frac{1}{6}, 0, \dots\right\}$ in time, whereas the complete dynamics S_T is described by Fig. 6.1.

We can obtain at this point some analytical results. Recalling the notion

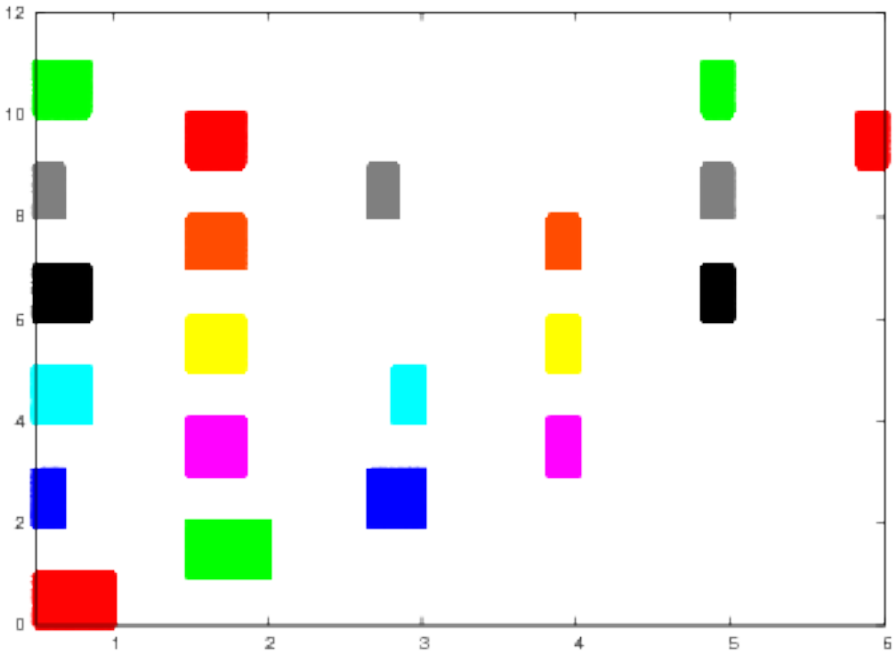

Figure 6.1: Behavior of map S_T for $\alpha = 1/6$ in the positive part of the chain, in 10 time steps, for a choice of $N = 10^5$ points. In the horizontal direction there is the cell index, in the vertical direction there is the time index.

of travelling and subtravelling area we notice that the sub-travelling area becomes periodic, and the travelling area makes a step forward in the chain every third step. Hence the only significant contribution to the mean square displacement (4.26) is given by the travelling aerea. Therefore the mean square displacement at time step $n = 3t$, with $t = 1, 2, \dots$, results:

$$\langle \Delta \hat{X}^2_{3t} \rangle = \frac{(t+2)^2}{6} \tag{6.5}$$

In the two temporal steps, right before a multiple of three, the dynamics follow a slightly different recurrence law for the mean square displacement,

but always dominated by a power of two. In fact, let the last time step be $n = 3t - 1$, with $t = 1, 2, \ldots$ then

$$\langle \Delta \hat{X}^2_{3t-1} \rangle = \frac{(t+3)^2}{6} \tag{6.6}$$

And finally, if the last time step is $n = 3t - 2$, with $t = 1, 2, \ldots$ then

$$\langle \Delta \hat{X}^2_{3t-2} \rangle = \frac{(t+4)^2}{6} \tag{6.7}$$

In each of the three cases, the limit of the mean square displacement as $n \to +\infty$ is asymptotically given by:

$$\langle \Delta \hat{X}^2_n \rangle \sim n^2 \tag{6.8}$$

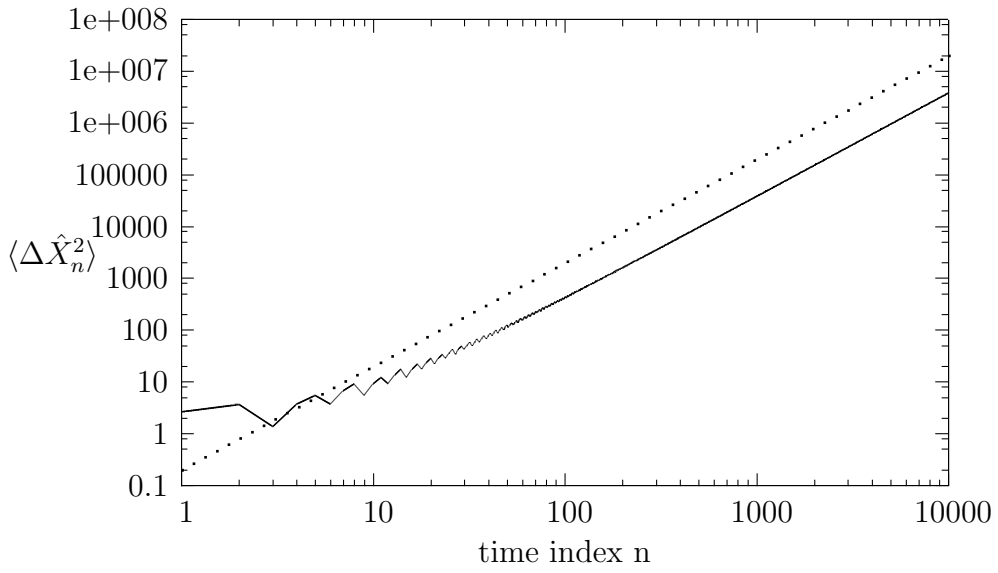

Figure 6.2: Behavior of mean square displacement of map S_T for $\alpha = \frac{1}{6}$ (continuous line), for a time of $n = 10^5$ and for a choice of $N = 10^4$ points, compared with n^2 (dotted line).

This case is illustrated by Fig. 6.2 where the behavior of the mean square displacement is reported for the map S_T with $\alpha = 1/6$ for a total number of time steps $n = 10^5$, togheter with the function $f(n) = n^2$.

Example 4. Let us choose $\alpha = \frac{1}{7}$. In this case the evolution rule (6.2) generates another periodic sequence of slicers $L_\alpha = \left\{\frac{1}{2}, \frac{3}{7}, \frac{2}{7}, \frac{1}{7}, 0, \frac{3}{7}, \frac{2}{7}, \frac{1}{7}, 0, \ldots\right\}$ in time, with longer period with respect to the previous case. Fig. 6.3 describes the dynamics of S_T for this choice of α.

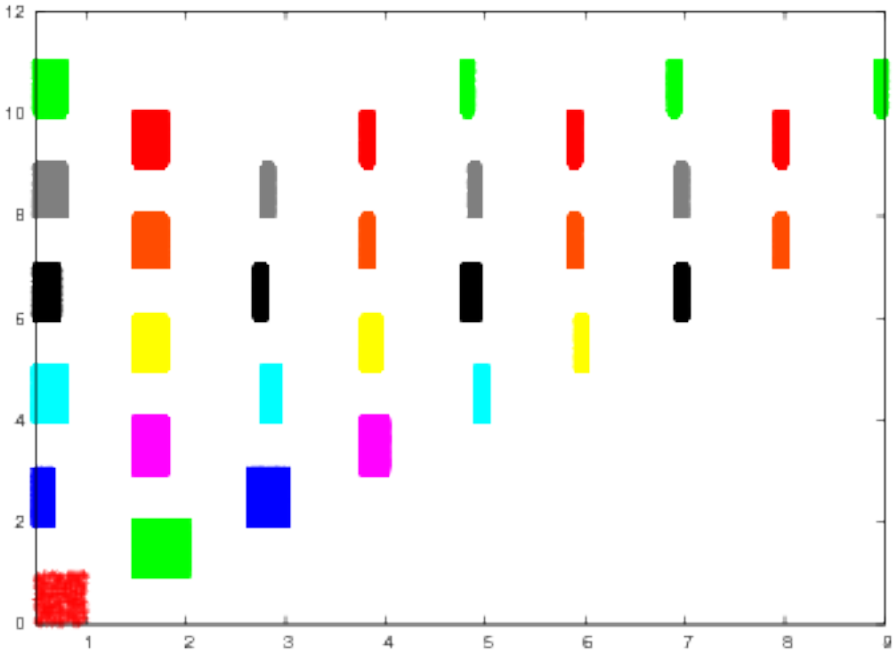

Figure 6.3: Behavior of map S_T for $\alpha = 1/7$ for the positive part of the chain, in 10 time steps, for a choice of $N = 10^5$ points. In the horizontal direction there is the cell index, in the vertical direction there is the time index.

Fig. 6.4 illustrates the asymptotic behavior of mean square displacement for the map S_T with $\alpha = 1/7$ and $n = 10^5$, togheter with the function $f(n) = n^2$.

To complete this brief analysis of the rational case, we also report in Fig. 6.5 the comparison between the asymptotic behavior of the mean square displacement concerning the two cases addressed above, i.e. $\alpha = \frac{1}{6}$ and $\alpha = \frac{1}{7}$.

Let us consider now an irrational choice of α. In this case, it is very

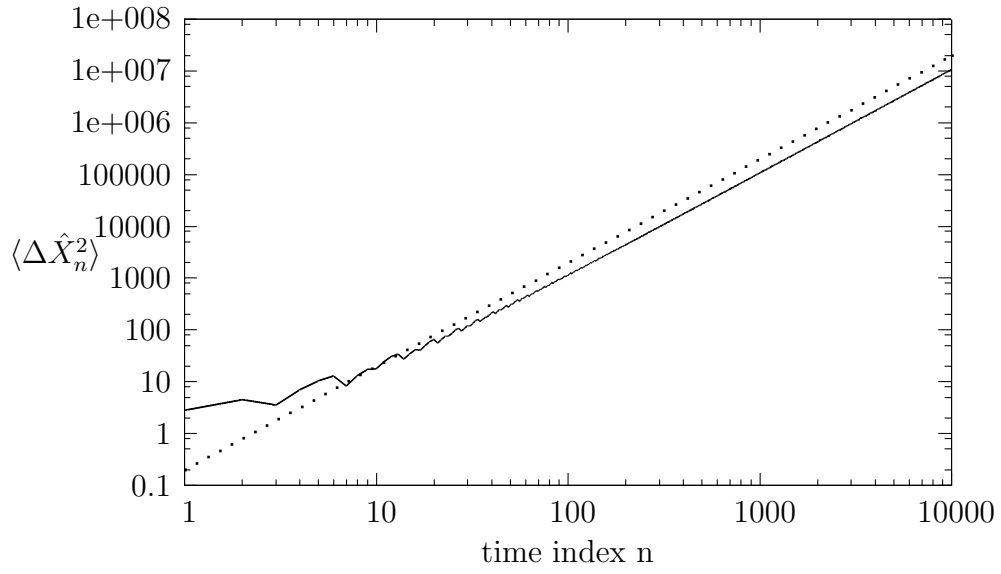

Figure 6.4: Behavior of mean square displacement of map S_T for $\alpha = \frac{1}{7}$ (continuous line), for a time of $n = 10^5$ and for a choice of $N = 10^4$ points, compared with n^2 (dotted line).

difficult to do analytical calculations, therefore we present numerical results. In Fig. 6.6 we observe the behavior of the map S_T for $\alpha = \dfrac{1}{\sqrt{7}}$. The only analytical result we obtained is the following. Consider the positive part of the chain. The dynamical slicer moves on the interval $[0, 1/2]$ never passing again in the same point because we are considering a ratio between the cell width, which is $1/2$ and the traslation parameter α that is irrational. In other words l_α moves on the interval $[0, 1/2]$ for a certain number of steps P, then, because of the modulo operation, it re-enters the same interval in an onother point and moves forward for another number of steps Q. Q and P do not necessarily coincide. In this case the travelling area diminishes during the first P steps, then it remains constant for the successive Q steps and so on, with fractions of times always different. These kinds of considerations do not suffice to clarify the behavior of the dynamics. From the numerical results we can reasonably deduce that the asymptotic behavior of the mean

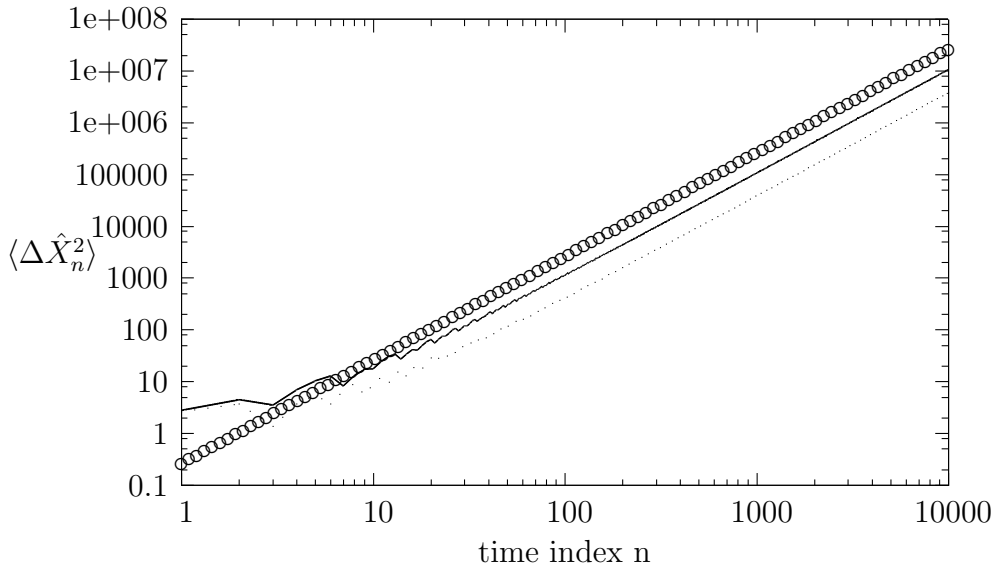

Figure 6.5: Behavior of mean square displacement of map S_T for $n = 10^5$ time steps and for a choice of $N = 10^4$ points. The dotted line is for $\alpha = 1/6$, the continuous line is for $\alpha = 1/7$ and the circles are for $f(n) = n^2$.

square displacement is, as above

$$\langle \Delta \hat{X}_n^2 \rangle \sim n^2 \tag{6.9}$$

In Fig. 6.7 we report these results for $\alpha = \dfrac{1}{\sqrt{7}}$ and $\alpha = 2.846 \cdot 10^{-4}$ togheter with $f(n) = n^2$.

6.2 Double Traslating Slicer Map

In this section we try to improve the previous model adding a second floating slicer, normal to the first one, in order to slow down the particles motion.

Definition 6.2. *Let* $S_{lv} : \hat{M} \to \hat{M}$ *such that*

$$S_{lv}(x, y, m) = \begin{cases} (x, y, m+1), & \text{if } (l_\alpha \leq x \leq 1) \text{ and } (0 \leq y < v_\beta) \\ (x, y, m-1) & \text{otherwise} \end{cases} \tag{6.10}$$

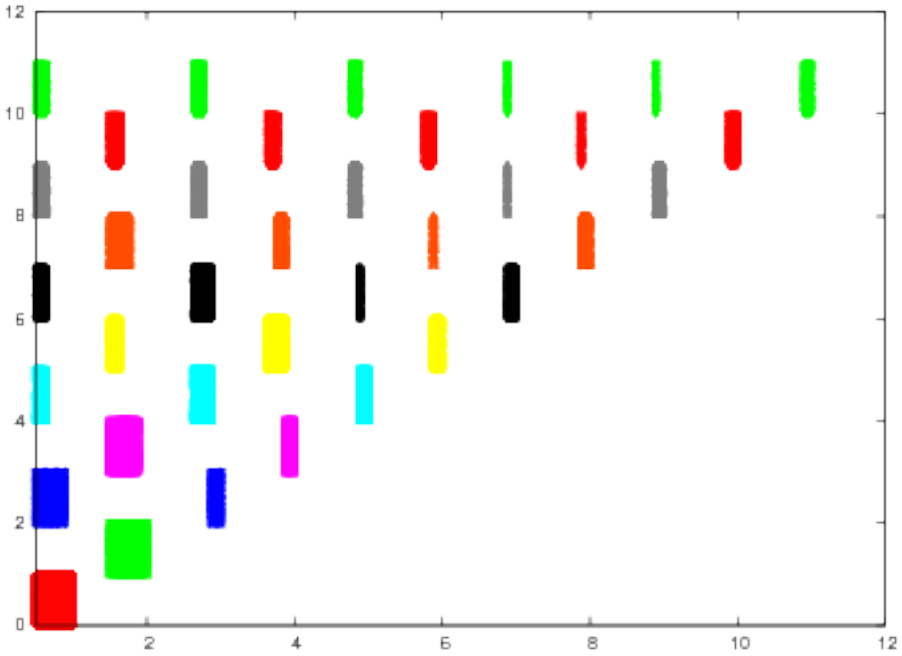

Figure 6.6: Behavior of map S_T for $\alpha = 1/\sqrt{7}$ for the positive part of the chain, in 10 time steps, for a choice of $N = 10^4$ points. In the horizontal direction there is the cell index, in the vertical direction there is the time index.

S_{lv} is called double slicers map. l_α is a vertical slicer and v_β is a horyzontal one.

We apply the same temporal evolution given in Def. 6.1 to the vertical slicer l_α, whereas for the horyzontal slicer v_β we define a slightly different translation rule:

Definition 6.3. *Let $n \in \mathbb{N}$ and $\beta \in [0,1]$, then $v_\beta : \mathbb{N} \to [0,1]$ acts as follows:*

$$v_\beta(n) = (v_\beta(n-1) - \beta)\, MOD_1 \tag{6.11}$$

The function $(x)MOD_1$ is such that:

$$(x)MOD_1 = \begin{cases} x, & \text{if } 0 \leq x \leq 1 \\ x-1, & \text{if } x > 1 \end{cases} \tag{6.12}$$

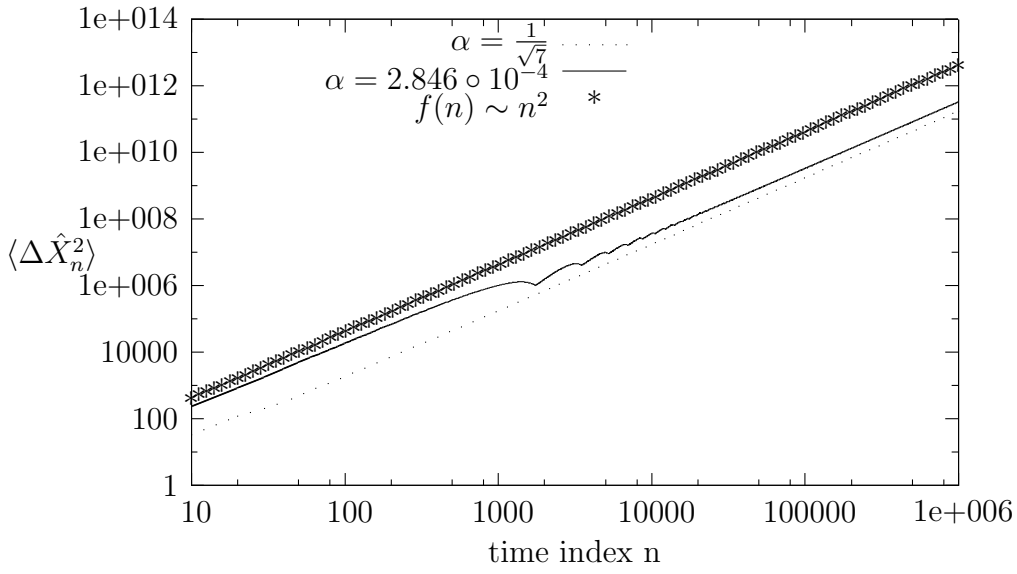

Figure 6.7: Asymptotic behavior of mean square displacement of map S_T for two different choices of irrational α, for a time of 10^6 steps and for a choice of $N = 10^3$ points compared with n^2.

The dynamics of the new system is therefore determined by the map $S_{\alpha\beta} := S_{l_\alpha v_\beta}$ where l_α is given by (6.2) and v_β is given by (6.11). More precisely at time step n we have

$$S^n_{\alpha\beta} = S_{l_\alpha(n-1)v_\beta(n-1)} \circ S_{l_\alpha(n-2)v_\beta(n-2)} \circ \ldots \circ S_{l_\alpha(1)v_\beta(1)} \circ S_{l_\alpha(0)v_\beta(0)} \qquad (6.13)$$

The initial conditions for the evolution of the vertical and the horyzontal slicers are respectively $l_\alpha(0) = 1/2$ and $v_\beta(0) = 1$.
In Fig. 6.8 we can observe the action of the map $S_{\alpha\beta}$, for $\alpha = 2.65 \cdot 10^{-2}$ and $\beta = 2.65 \cdot 10^{-3}$ and for a choice of 10^3 points. We report the numerical results related to mean square displacement of $S_{\alpha\beta}$ for these choices of α and β in Fig. 6.9. We choose very small parameters to make slower the decrease of the travelling area, but we evince that this is not enough to obtain a mean square displacement slower then ballistic although the behavior of the mean square displacement appears to be more complex than in the previous cases. The parameter are $\alpha = 2.65 \cdot 10^{-2}$ and $\beta = 2.65 \cdot 10^{-3}$ for the dotted line and

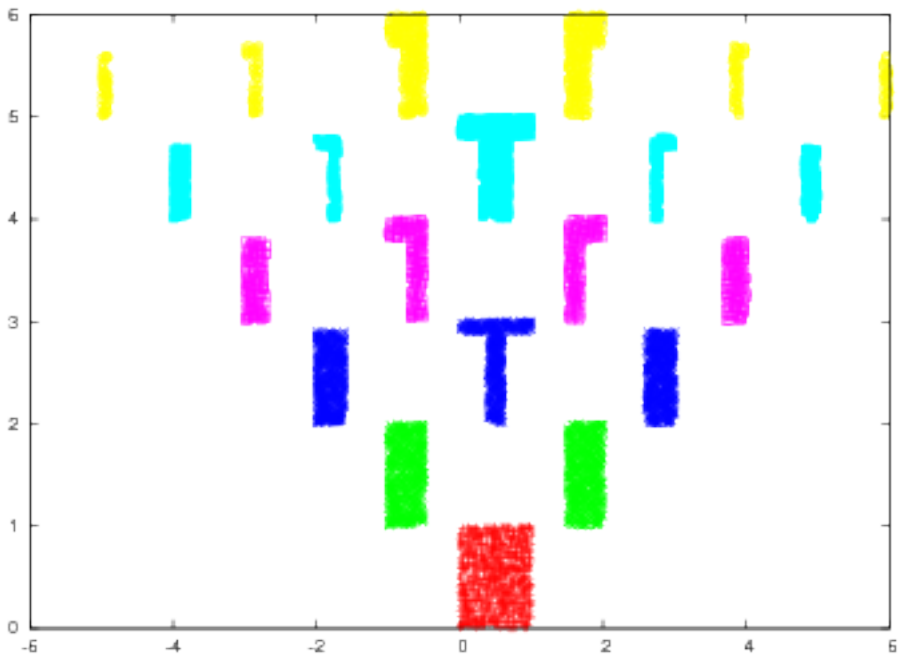

Figure 6.8: Behavior of map $S_{\alpha\beta}$ for $\alpha = 2.65 \cdot 10^{-2}$ and $\beta = 2.65 \cdot 10^{-3}$, in 10 time steps. In the horizontal direction there is the cell index, in the vertical direction there is the time index. The low resolution of the image is due to the choice of a low amounts of initial points ($N = 10^3$).

$\alpha = 8.37 \cdot 10^{-2}$ and $\beta = 8.37 \cdot 10^{-5}$ for the continuous line. In both case we start with from the 0-th cell with 10^5 points for $n = 10^7$. We compare these results with the function $f(n) = n^2$.

Moreover, in Fig. 6.10 we report the behavior of the only travelling area, for the same values of parameters α and β . Observing these results we notice that the travelling area seems to present a linear behavior, so that we can deduce that the travelling area alone does not determine the ballistic behavior of the mean square displacement, but also sub-travelling areas give a significant contribution to this trend.

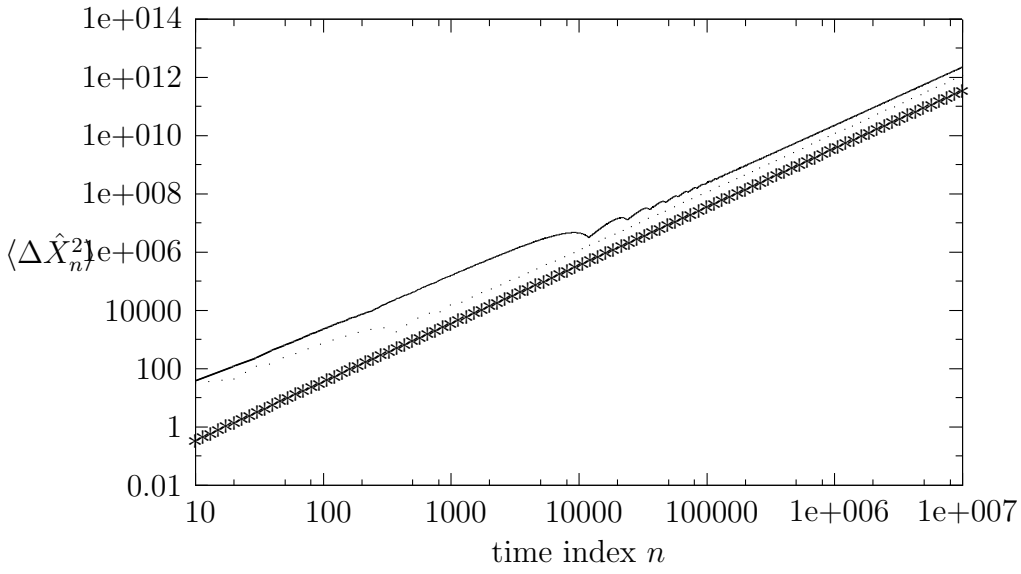

Figure 6.9: Behavior of mean square displacement of map $S_{\alpha\beta}$ for two different choices of α and β, for $n = 10^7$ and for a choice of $N = 10^5$ points. The dotted line is for $\alpha = 2.65 \cdot 10^{-2}$ and $\beta = 2.65 \cdot 10^{-3}$ and the continuous line is for $\alpha = 8.37 \cdot 10^{-2}$ and $\beta = 8.37 \cdot 10^{-5}$, whereas the stars line is for $f(n) = n^2$.

6.3 Fix Slicer and Traslating Points

The third attempt we make is to consider a fixed slicer and apply to points of the phase space an additional translational dynamics.
Let us recall again the definition of the slicer map

$$S_l(x, y, m) = \begin{cases} (x, y, m-1) & \text{if } 0 \leq x \leq l \text{ or } \frac{1}{2} \leq x \leq 1-l \\ (x, y, m+1) & \text{if } l < x < \frac{1}{2} \text{ or } 1-l < x \leq 1 \end{cases} \tag{6.14}$$

This time we want to stress that now we do not have any dependence of the active slicers from the cell index neither from the time index. We have just two fixed symmetric slicers l and $1-l$ in all the cells.
Let us now define a translation for the points:

Definition 6.4. *Let $\alpha \in [0, 1]$ be a parameter. $T : \hat{M} \to \hat{M}$ acts as follow*

$$T(x, y, m) = ((x + \alpha) MOD_1, y, m) \tag{6.15}$$

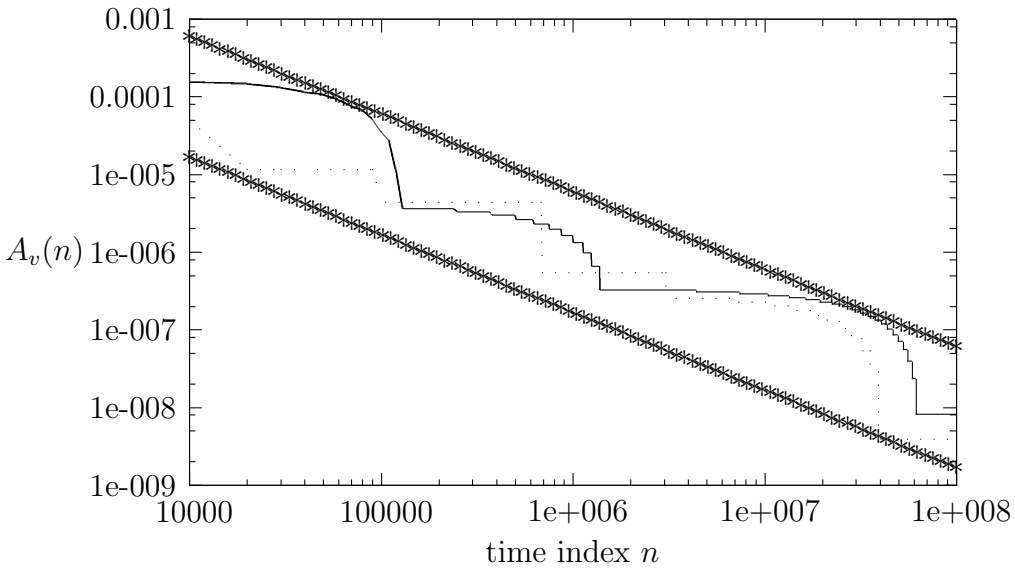

Figure 6.10: Behavior of travelling area of map $S_{\alpha\beta}$ for two diferent choices of α and β, for $n = 10^7$ and for a choice of $N = 10^5$ points. The dotted line is for $\alpha = 2.65 \cdot 10^{-2}$ and $\beta = 2.65 \cdot 10^{-3}$ and the continuous line is for $\alpha = 8.37 \cdot 10^{-2}$ and $\beta = 8.37 \cdot 10^{-5}$ whereas the stars lines are for the same $f(n) = n^2$ at two different quotes.

where $(x)MOD_1$ *is the same operation defined in (6.12).*

Definition 6.5. *The map* $S_{TP} : \hat{M} \to \hat{M}$ *such that* $S_{TP} = S_l \circ T$ *is called translated points slicer map.* S_l *is the map defined in (6.14) with* $l \in (0, 1]$ *fixed.*

Below we report the result related to this dynamics for $l = \frac{1}{2}$, $\alpha = \frac{1}{\sqrt{7}}$ for a choice of 100 points and $n = 9 \cdot 10^7$.

In Fig. 6.11 we can observe a view of the dynamics that seems quite similar to almost all the other maps presented above, but in Fig. 6.12 surprisingly we notice an apparent sub-diffusive trend of the mean square displacement. Obviously we wonder if we can trust this result or not. The number of points is quite low, therefore the first step should be to retry the simulation with an higher number of points. Then it should be possible, despite the complexity

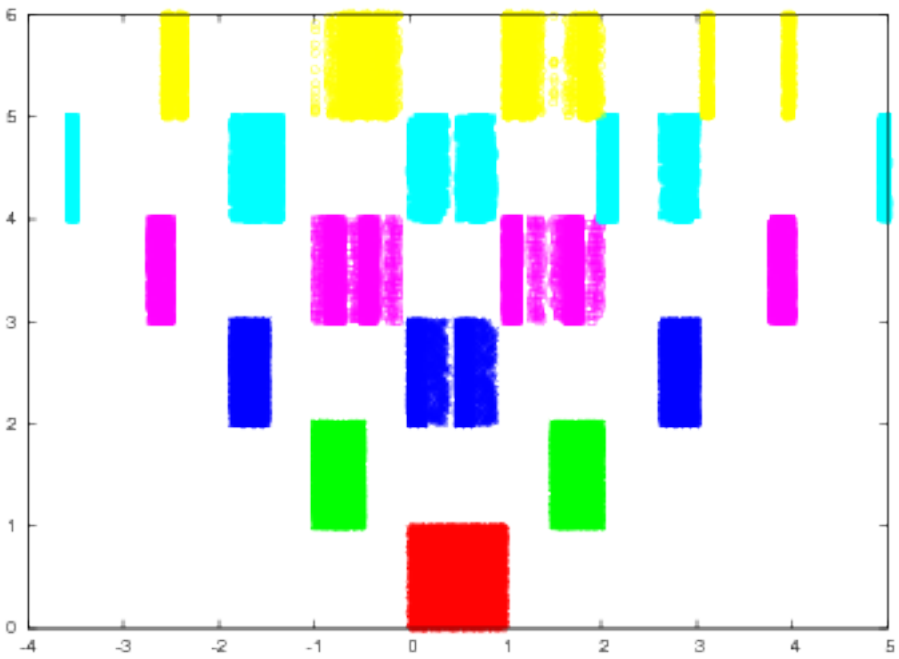

Figure 6.11: Behavior of map S_{TP} for $\alpha = 1/\sqrt{7}$, in 10 time steps. In the horizontal direction there is the cell index, in the vertical direction there is the time index. The low resolution of the image is due to the choice of a low amounts of initial points ($N = 10^3$).

of the problem, to do at least some general analytical considerations about the trend of the areas. At least the travelling one.

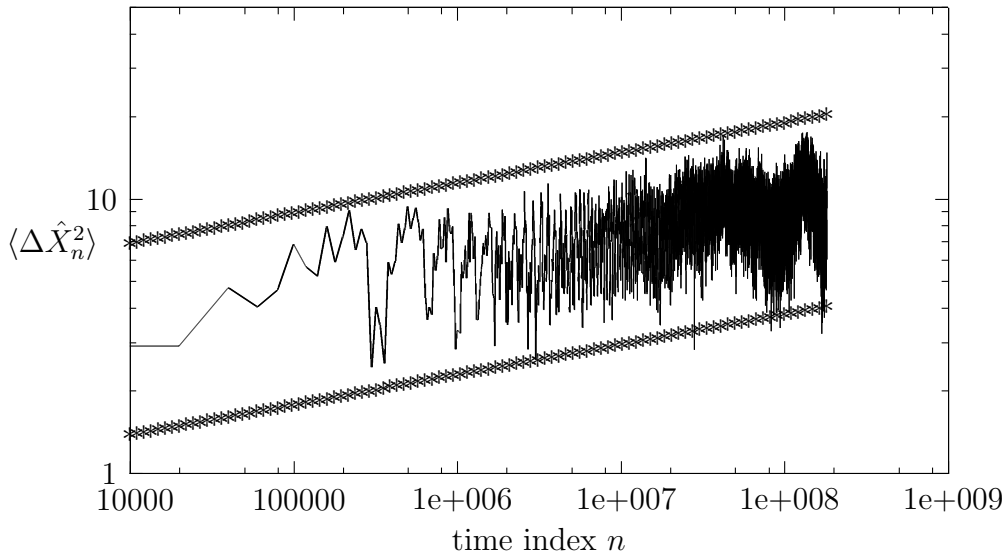

Figure 6.12: Behavior of mean square displacement of map S_{TP} for $\alpha = 1/\sqrt{7}$ (continuous line), $n = 9 \cdot 10^7$ and for a choice of $N = 10^2$ points, compared with $f(n) \approx n^{-0.11}$ (stars lines).

Chapter 7

Concluding remarks

In this thesis, in order to provide mathematically tractable models of anomalous diffusion, for the phenomenon of transient osmosis a new deterministic map, called slicer map, has been introduced. To this end we have also tried to reproduce features of the polygonal billiards dynamics. We have tried to go one step closer to such dynamics, than in the current literature. Indeed we have adopted area-preserving, non-chaotic dynamics. Results both of analytical and numerical nature related to this model have been presented. In particular two theorems have been obtained, which establish the asymptotic beahvior respectively of the mean square displacement and of the other moments of the map. A coarse grained probability density function has been introduced for the model, which enabled us to compare our model with stochastic models frequently used in the approach to the problem of anomalous transport. The analytical results for the mean square displacement presented a perfect agreement with a stochastic model of Lévy walks. Our conclusion is that a trivial deterministic area preserving and non-chaotic model, such as our slicer map results indistiguishable from Lévy walks, beacuse of the equality of the asymptotic behaviour of all moments once the mean square displacements agree. Nevertheless for completeness one should check also the behavior of correlations. The infinitely many scales that characterize our slicer map seem to be indispensable to obtain anomalous behavior. The

triviality of the proposed slicer model is unquestionable, but it is interesting precisely for that. The detailed mathematical study provided in this work opens the way to evolutions of the model, and give at the same time some hints about how to set up the mathematical framework in which it is possible to continue the work. In this work, some possible modifications of the model have been already outlined, pointing out the limits and the potentialities that they present. In particular to get closer to the 2-dimensional dynamics of billiard maps, a horyzontal slicer, which moves along the y axis, has been introduced. The first two modifications, obtained by means of a translational dynamics applied to the slicer, pose the limit of the exponential growth of the analytical tractability of the problem. At the same time the numerical results concerning these variations do not seem to give hope to find transport behaviors different from the ballistic one. Conversely the addition of a translational dynamics to the areas of the maps, fixing the slicer, at least in the numerical simulation, has provided some interesting results, with an exponent for the mean square displacement asymptotic trend $\gamma \approx 0.11$, which identifies a sub-diffusive transport behavior. This makes us think that further insight in this direction could bring same deeper and interesting results. In particular, one feature of polygonal billiards, which has not been introduced in the above models is the presence of rotations within the elementary cell. This ingredient seems essential to fully exploit the 2 dimensions of the phase space.

Appendix A

Numerical Codes

A.1 Slicer Map $S_{1/2}$

```
c**********************************************************************
c       NON-EXPANDING MULTI-BAKER MAP   alfa=1/2
c       SOURCE CODE FOR MSD CALCULATION
c**********************************************************************

      IMPLICIT NONE
      integer*8 i,j,mm(30000000),Npoint,Np,Ntot,Niter,Nitdon,Nmil,wstep
      integer Icont,iseed
      double precision X(30000000),Y(30000000),deltax
      double precision slice
      real r

      OPEN(8,file='Parameters',form='formatted',status='old')
           READ(8,*) slice,Npoint,Ntot
           READ(8,*) iseed,r,Icont,wstep
      CLOSE(8)
```

```
      Nmil= wstep

      OPEN(7,file='IC',form='formatted',status='unknown')
      DO i = 1,Npoint
         CALL rand(iseed,r)
              X(i) = r
         CALL rand(iseed,r)
              Y(i) = r
         WRITE(7,*) i,X(i),Y(i)
         mm(i) = 0
      ENDDO
      CLOSE(7)

  785 CONTINUE

      OPEN(8,file='msd',form='formatted',status='unknown')
      Niter = 0
  786 CONTINUE

      deltax = 0.0D0

      DO Np = 1,Npoint
        slice = 1.0D0/((DABS(DFLOAT(mm(Np)))+4)**0.5)
        IF(mm(Np) .GT. 0) THEN
           IF(X(Np) .LE. 1.0D0 - slice) mm(Np) = mm(Np) - 1
           IF(X(Np) .GT. 1.0D0 - slice) mm(Np) = mm(Np) + 1
        ELSEIF(mm(Np) .LT. 0) THEN
           IF(X(Np) .LE. slice) mm(Np) = mm(Np) - 1
           IF(X(Np) .GT. slice) mm(Np) = mm(Np) + 1
        ELSE
           IF(X(Np) .LE. 0.50D0) mm(Np) = mm(Np) - 1
```

```
           IF(X(Np) .GT. 0.50D0) mm(Np) = mm(Np) + 1
        ENDIF
        deltax = deltax + mm(Np)**2
       ENDDO

       j = Npoint/100

       IF(MOD(Niter,Nmil).EQ.0)
      &                    WRITE(8,*) Niter+Nitdon,deltax/DFLOAT(Npoint)
       Niter = Niter + 1

       IF(Niter .LT. Ntot) GOTO 786

       CLOSE(8)

  10   FORMAT(2x,i7,1x,10(f15.8,2x,i5,2x))

       STOP
       END
c-------------------------------------------------------------------------
c Random number generator
c-------------------------------------------------------------------------
SUBROUTINE rand(iseed,r)
       integer iseed
    double precision dseed,d2p31m,d2p31
       real r
    d2p31m = 2147483647.D0
    d2p31  = 2147483648.D0
    dseed = iseed
    dseed = dmod(16807.D0*dseed,d2p31m)
    r     = dseed/d2p31
```

```
    iseed = int(dseed)
    return
    end
c**********************************************************************

c**********************************************************************
c       SOURCE CODE FOR ILLUSTRATION OF DYNAMICS
c**********************************************************************

      IMPLICIT NONE
      integer*8 i,j,mm(30000000),Npoint,Np,Ntot,Niter,Nitdon,Nmil,wstep
      integer Icont,iseed
      double precision X(30000000),Y(30000000),deltax
      double precision slice
      real r

      OPEN(8,file='Parameters',form='formatted',status='old')
           READ(8,*) slice,Npoint,Ntot
           READ(8,*) iseed,r,Icont,wstep
      CLOSE(8)

      Nmil= wstep

      OPEN(7,file='IC',form='formatted',status='unknown')
      DO i = 1,Npoint
         CALL rand(iseed,r)
              X(i) = r
         CALL rand(iseed,r)
              Y(i) = r
         WRITE(7,*) i,X(i),Y(i)
         mm(i) = 0
```

```
      ENDDO
      CLOSE(7)

 785  CONTINUE

      OPEN(8,file='msd',form='formatted',status='unknown')
      Niter = 0

 786  CONTINUE

      deltax = 0.0D0

      DO Np = 1,Npoint                          -
         slice = 1.0D0/((DABS(DFLOAT(mm(Np)))+4)**0.5)
     IF(mm(Np) .GT. 0) THEN
           IF(X(Np) .LE. 1.0D0 - slice) mm(Np) = mm(Np) - 1
           IF(X(Np) .GT. 1.0D0 - slice) mm(Np) = mm(Np) + 1
        ELSEIF(mm(Np) .LT. 0) THEN
           IF(X(Np) .LE. slice) mm(Np) = mm(Np) - 1
           IF(X(Np) .GT. slice) mm(Np) = mm(Np) + 1
        ELSE
           IF(X(Np) .LE. 0.50D0) mm(Np) = mm(Np) - 1
           IF(X(Np) .GT. 0.50D0) mm(Np) = mm(Np) + 1
       ENDIF
         deltax = deltax + mm(Np)**2
      ENDDO

      j = Npoint/100

      IF(MOD(Niter,Nmil).EQ.0)
     &                    WRITE(8,*) Niter+Nitdon,deltax/DFLOAT(Npoint)
```

```
      Niter = Niter + 1

       IF(Niter .EQ. 1) THEN
          OPEN(7,file='Passo1',form='formatted',status='unknown')
          DO Np = 1,Npoint
          WRITE(7,*)Niter,X(Np)+mm(Np),Y(Np)
          ENDDO
          CLOSE(7)
       ENDIF

       IF(Niter .EQ. 2) THEN
          OPEN(7,file='Passo2',form='formatted',status='unknown')
          DO Np=1,Npoint
          WRITE(7,*)Niter,X(Np)+mm(Np), Y(Np)
          ENDDO
          CLOSE(7)
       ENDIF

       IF(Niter .EQ. 3) THEN
         OPEN(7,file='Passo3',form='formatted',status='unknown')
         DO Np = 1,Npoint
         WRITE(7,*) Niter,X(Np)+mm(Np),Y(Np)
         ENDDO
         CLOSE(7)
       ENDIF

       IF(Niter .EQ. 4) THEN
         OPEN(7,file='Passo4',form='formatted',status='unknown')
         DO Np = 1,Npoint
         WRITE(7,*) Niter,X(Np)+mm(Np),Y(Np)
         ENDDO
```

```
  CLOSE(7)
ENDIF

IF(Niter .EQ. 5) THEN
  OPEN(7,file='Passo5',form='formatted',status='unknown')
  DO Np = 1,Npoint
  WRITE(7,*) Niter,X(Np)+mm(Np),Y(Np)
  ENDDO
  CLOSE(7)
 ENDIF

 IF(Niter .EQ. 6) THEN
   OPEN(7,file='Passo6',form='formatted',status='unknown')
   DO Np = 1,Npoint
   WRITE(7,*) Niter,X(Np)+mm(Np),Y(Np)
   ENDDO
   CLOSE(7)
  ENDIF

IF(Niter .EQ. 7) THEN
  OPEN(7,file='Passo7',form='formatted',status='unknown')
  DO Np = 1,Npoint
      WRITE(7,*) Niter,X(Np)+mm(Np),Y(Np)
      ENDDO
      CLOSE(7)
 ENDIF

 IF(Niter .EQ. 8) THEN
    OPEN(7,file='Passo8',form='formatted',status='unknown')
    DO Np = 1,Npoint
      WRITE(7,*) Niter,X(Np)+mm(Np),Y(Np)
```

```
            ENDDO
            CLOSE(7)
         ENDIF

         IF(Niter .EQ. 9) THEN
            OPEN(7,file='Passo9',form='formatted',status='unknown')
            DO Np = 1,Npoint
            WRITE(7,*) Niter,X(Np)+mm(Np),Y(Np)
            ENDDO
            CLOSE(7)
         ENDIF

         IF(Niter .EQ. 10) THEN
           OPEN(7,file='Passo10',form='formatted',status='unknown')
           DO Np = 1,Npoint
             WRITE(7,*) Niter,X(Np)+mm(Np),Y(Np)
             ENDDO
             CLOSE(7)
         ENDIF

      IF(Niter .LT. Ntot) GOTO 786
      CLOSE(8)

  10  FORMAT(2x,i7,1x,10(f15.8,2x,i5,2x))

      STOP
      END
c-----------------------------------------------------------------------
c Random number generator
c-----------------------------------------------------------------------
SUBROUTINE rand(iseed,r)
```

```
      integer iseed
    double precision dseed,d2p31m,d2p31
      real r
    d2p31m = 2147483647.D0
    d2p31  = 2147483648.D0
    dseed = iseed
    dseed = dmod(16807.D0*dseed,d2p31m)
    r     = dseed/d2p31
    iseed = int(dseed)
    return
    end
c**********************************************************************
```

A.2 Slicer Map $S_{1/3}$

```
c**********************************************************************
c        NON-EXPANDING MULTI-BAKER MAP  alfa=1/3
c         SOURCE CODE FOR MSD CALCULATION
c**********************************************************************

      IMPLICIT NONE
      integer*8 i,j,mm(30000000),Npoint,Np,Ntot,Niter,Nitdon,Nmil
      integer Icont,iseed
      double precision X(30000000),Y(30000000),deltax
      double precision slice
      real r

      Nmil=10
      OPEN(8,file='Parameters',form='formatted',status='old')
           READ(8,*) slice,Npoint,Ntot
```

```
          READ(8,*) iseed,r,Icont
      CLOSE(8)

      OPEN(7,file='IC',form='formatted',status='unknown')
      DO i = 1,Npoint
         CALL rand(iseed,r)
              X(i) = r
         CALL rand(iseed,r)
              Y(i) = r
         WRITE(7,*) i,X(i),Y(i)
         mm(i) = 0
      ENDDO
      CLOSE(7)

      OPEN(8,file='msd',form='formatted',status='unknown')

      Niter = 0
 786  CONTINUE

      deltax = 0.0D0

      DO Np = 1,Npoint
       slice = 1.0D0/((DABS(DFLOAT(mm(Np)))+8)**0.34)
       IF(mm(Np) .GT. 0) THEN
           IF(X(Np) .LE. 1.0D0 - slice) mm(Np) = mm(Np) - 1
           IF(X(Np) .GT. 1.0D0 - slice) mm(Np) = mm(Np) + 1
        ELSEIF(mm(Np) .LT. 0) THEN
         IF(X(Np) .LE. slice) mm(Np) = mm(Np) - 1
          IF(X(Np) .GT. slice) mm(Np) = mm(Np) + 1
        ELSE
           IF(X(Np) .LE. 0.50D0) mm(Np) = mm(Np) - 1
```

```
            IF(X(Np) .GT. 0.50D0) mm(Np) = mm(Np) + 1
         ENDIF
           deltax = deltax + mm(Np)**2
        ENDDO

        j = Npoint/100

        IF(MOD(Niter,Nmil).EQ.0)
       &                    WRITE(8,*) Niter+Nitdon,deltax/DFLOAT(Npoint)
        Niter = Niter + 1

        IF(Niter .LT. Ntot) GOTO 786

        CLOSE(8)

  10    FORMAT(2x,i7,1x,10(f15.8,2x,i5,2x))

        STOP
        END
c-----------------------------------------------------------------------
c Random number generator
c-----------------------------------------------------------------------
SUBROUTINE rand(iseed,r)
        integer iseed
      double precision dseed,d2p31m,d2p31
        real r
      d2p31m = 2147483647.D0
      d2p31  = 2147483648.D0
      dseed = iseed
      dseed = dmod(16807.D0*dseed,d2p31m)
      r     = dseed/d2p31
```

```
    iseed = int(dseed)
    return
    end
c**********************************************************************
c
c
c**********************************************************************
c       NON-EXPANDING MULTI-BAKER    alfa=1/3
c       SOURCE CODE FOR ILLUSTRATION OF DYNAMICS
c**********************************************************************

      IMPLICIT NONE
      integer*8 i,j,mm(30000000),Npoint,Np,Ntot,Niter,Nitdon,Nmil,wstep
      integer Icont,iseed
      double precision X(30000000),Y(30000000),deltax
      double precision slice
      real r

      OPEN(8,file='Parameters',form='formatted',status='old')
           READ(8,*) slice,Npoint,Ntot
           READ(8,*) iseed,r,Icont,wstep
           CLOSE(8)
      Nmil= wstep

      Nitdon = 0

      OPEN(7,file='IC',form='formatted',status='unknown')
      DO i = 1,Npoint
         CALL rand(iseed,r)
              X(i) = r
         CALL rand(iseed,r)
```

```
            Y(i) = r
         WRITE(7,*) i,X(i),Y(i)
         mm(i) = 0
      ENDDO
      CLOSE(7)

      OPEN(8,file='msd',form='formatted',status='unknown')

      Niter = 0
 786  CONTINUE

      deltax = 0.0D0

      DO Np = 1,Npoint
        slice = 1.0D0/((DABS(DFLOAT(mm(Np)))+8)**0.34)
        IF(mm(Np) .GT. 0) THEN
           IF(X(Np) .LT. 1.0D0 - slice) mm(Np) = mm(Np) - 1
           IF(X(Np) .GT. 1.0D0 - slice) mm(Np) = mm(Np) + 1
        ELSEIF(mm(Np) .LT. 0) THEN
           IF(X(Np) .LT. slice) mm(Np) = mm(Np) - 1
           IF(X(Np) .GT. slice) mm(Np) = mm(Np) + 1
        ELSE
           IF(X(Np) .LT. 0.50D0) mm(Np) = mm(Np) - 1
           IF(X(Np) .GT. 0.50D0) mm(Np) = mm(Np) + 1
       ENDIF
         deltax = deltax + mm(Np)**2
      ENDDO

      j = Npoint/100

      IF(MOD(Niter,Nmil).EQ.0)
```

```
&                    WRITE(8,*) Niter+Nitdon,deltax/DFLOAT(Npoint)
 Niter = Niter + 1

 IF(Niter .EQ. 1) THEN
     OPEN(7,file='Passo1',form='formatted',status='unknown')
     DO Np = 1,Npoint
     WRITE(7,*)Niter,X(Np)+mm(Np),Y(Np)
     ENDDO
     CLOSE(7)
  ENDIF

   IF(Niter .EQ. 2) THEN
     OPEN(7,file='Passo2',form='formatted',status='unknown')
     DO Np=1,Npoint
     WRITE(7,*)Niter,X(Np)+mm(Np), Y(Np)
     ENDDO
     CLOSE(7)
   ENDIF

  IF(Niter .EQ. 3) THEN
    OPEN(7,file='Passo3',form='formatted',status='unknown')
    DO Np = 1,Npoint
    WRITE(7,*) Niter,X(Np)+mm(Np),Y(Np)
    ENDDO
    CLOSE(7)
   ENDIF

  IF(Niter .EQ. 4) THEN
    OPEN(7,file='Passo4',form='formatted',status='unknown')
    DO Np = 1,Npoint
    WRITE(7,*) Niter,X(Np)+mm(Np),Y(Np)
```

```
  ENDDO
  CLOSE(7)
ENDIF

IF(Niter .EQ. 5) THEN
  OPEN(7,file='Passo5',form='formatted',status='unknown')
  DO Np = 1,Npoint
  WRITE(7,*) Niter,X(Np)+mm(Np),Y(Np)
  ENDDO
  CLOSE(7)
 ENDIF

 IF(Niter .EQ. 6) THEN
   OPEN(7,file='Passo6',form='formatted',status='unknown')
   DO Np = 1,Npoint
   WRITE(7,*) Niter,X(Np)+mm(Np),Y(Np)
   ENDDO
   CLOSE(7)
  ENDIF

IF(Niter .EQ. 7) THEN
  OPEN(7,file='Passo7',form='formatted',status='unknown')
  DO Np = 1,Npoint
      WRITE(7,*) Niter,X(Np)+mm(Np),Y(Np)
      ENDDO
      CLOSE(7)
 ENDIF

 IF(Niter .EQ. 8) THEN
    OPEN(7,file='Passo8',form='formatted',status='unknown')
    DO Np = 1,Npoint
```

```
            WRITE(7,*) Niter,X(Np)+mm(Np),Y(Np)
            ENDDO
            CLOSE(7)
         ENDIF

         IF(Niter .EQ. 9) THEN
            OPEN(7,file='Passo9',form='formatted',status='unknown')
            DO Np = 1,Npoint
            WRITE(7,*) Niter,X(Np)+mm(Np),Y(Np)
            ENDDO
            CLOSE(7)
         ENDIF

         IF(Niter .EQ. 10) THEN
           OPEN(7,file='Passo10',form='formatted',status='unknown')
           DO Np = 1,Npoint
            WRITE(7,*) Niter,X(Np)+mm(Np),Y(Np)
            ENDDO
            CLOSE(7)
         ENDIF
      IF(Niter .LT. Ntot) GOTO 786

      CLOSE(8)

  10  FORMAT(2x,i7,1x,10(f15.8,2x,i5,2x))

      STOP
      END
c-----------------------------------------------------------------------
c Random number generator
c-----------------------------------------------------------------------
```

```
SUBROUTINE rand(iseed,r)
       integer iseed
     double precision dseed,d2p31m,d2p31
       real r
     d2p31m = 2147483647.D0
     d2p31  = 2147483648.D0
     dseed = iseed
     dseed = dmod(16807.D0*dseed,d2p31m)
     r     = dseed/d2p31
     iseed = int(dseed)
     return
     end
c**********************************************************************
```

A.3 Traslating Slicer Dynamics

```
c**********************************************************************
c            TRANSLATING SLICER
c**********************************************************************

      IMPLICIT NONE
      integer*8 i,j,mm(10000000),Npoint,Np,Ntot,Niter,Nitdon,Nmil
      integer Icont,iseed
      double precision X(10000000),Y(10000000),deltax,Xmin
      double precision a,b,alfa,slicepos,sliceneg,slicezero
      real r

      Nmil=10
      OPEN(8,file='Parameters',form='formatted',status='old')
```

```
          READ(8,*) Npoint,Ntot,a,b
          READ(8,*) iseed,r,Icont
      CLOSE(8)

       OPEN(7,file='IC',form='formatted',status='unknown')
       DO i = 1,Npoint
         CALL rand(iseed,r)
              X(i) = r
         CALL rand(iseed,r)
              Y(i) = r
         WRITE(7,*) i,X(i),Y(i)
         mm(i) = 0
       ENDDO
       CLOSE(7)

       OPEN(8,file='msd',form='formatted',status='unknown')

      Niter = 0
       slicepos = 0.5D0
       sliceneg = 0.5D0
       slicezero = 0.5D0

 786  CONTINUE

      deltax = 0.0D0

       alfa = 1.0D0/(a**b)

      DO Np = 1,Npoint
       IF (mm(Np) .GT. 0.0D0) THEN
          IF (X(Np) .LE. slicepos) THEN
```

```
                        mm(Np) = mm(Np) - 1
      ELSE
                        mm(Np) = mm(Np) + 1
      ENDIF
    ELSEIF (mm(Np) .LT. 0.0D0) THEN
      IF (X(Np) .LE. sliceneg) THEN
                        mm(Np) = mm(Np) - 1
      ELSE
                        mm(Np) = mm(Np) + 1
      ENDIF
    ELSE
      IF (X(Np) .LT. slicezero) THEN
                        mm(Np) = mm(Np) - 1
      ELSE
                        mm(Np) = mm(Np) + 1
      ENDIF
    ENDIF
      deltax = deltax + mm(Np)**2
   ENDDO

   IF(MOD(Niter,Nmil).EQ.0)
  &                   WRITE(8,*) Niter, deltax/DFLOAT(Npoint)

   IF (slicepos .LE. 1.0D0 - alfa) THEN
     slicepos = slicepos + alfa
   ELSE
     slicepos = slicepos + alfa - 0.5D0
   ENDIF

   IF (sliceneg .GE. alfa) THEN
     sliceneg = sliceneg - alfa
```

```
      ELSE
        sliceneg = sliceneg - alfa + 0.5D0
      ENDIF

      Niter = Niter + 1

      IF(Niter .LT. Ntot) GOTO 786
      CLOSE(8)

 785  CONTINUE
  10  FORMAT(2x,i7,1x,10(f15.8,2x,i5,2x))

      STOP
      END
c-----------------------------------------------------------------------
c Random number generator
c-----------------------------------------------------------------------
  SUBROUTINE rand(iseed,r)
        integer iseed
        double precision dseed,d2p31m,d2p31
        real r
        d2p31m = 2147483647.D0
        d2p31  = 2147483648.D0
        dseed = iseed
        dseed = dmod(16807.D0*dseed,d2p31m)
        r     = dseed/d2p31
        iseed = int(dseed)
       return
       end
c*******************************************************************
```

A.4 Double Translating Slicer Dynamics

```
c**********************************************************************
c        DOUBLE TRANSLATING SLICER
c**********************************************************************

      IMPLICIT NONE
      integer*8 i,j,mm(10000000),Npoint,Np,Ntot,Niter,Nitdon,Nmil
      integer Icont,iseed
      double precision X(10000000),Y(10000000),deltax,Xmin,h,k,beta
      double precision a,b,alfa,sp,sn,spc,snc,sv
      real r

      Nmil=1000000
      OPEN(8,file='Parameters',form='formatted',status='old')
           READ(8,*) Npoint,Ntot,a,b,h,k
           READ(8,*) iseed,r,Icont
      CLOSE(8)

       OPEN(7,file='IC',form='formatted',status='unknown')
       DO i = 1,Npoint
         CALL rand(iseed,r)
              X(i) = r
         CALL rand(iseed,r)
              Y(i) = r
         WRITE(7,*) i,X(i),Y(i)
         mm(i) = 0
       ENDDO
       CLOSE(7)

       OPEN(8,file='msd',form='formatted',status='unknown')
```

```
      Niter = 0
       sp = 0.5D0
       sn = 0.5D0
       spc = 0.7D0
       snc = 0.3D0
       sv = 1.0D0

 786  CONTINUE

      deltax = 0.0D0

       alfa = a**b
       beta = h**k

      DO Np = 1,Npoint
       IF(X(Np) .GE. 0.5D0) THEN
       IF ((X(Np) .GE. sp) .AND. (Y(Np) .LE. sv)) THEN
                                  mm(Np) = mm(Np) + 1
       ELSEIF ((X(Np) .GT. sp) .AND. (Y(Np) .GT. sv)) THEN
                                  mm(Np) = mm(Np)
       ELSEIF ((X(Np) .GT. spc) .AND. (X(Np) .LT. sp) .AND.
     &                                      (Y(Np) .LT. sv)) THEN
                                  mm(Np) = mm(Np) + 1
       ELSEIF ((X(Np) .GT. spc) .AND. (X(Np) .LT. sp) .AND.
     &                                      (Y(Np) .GT. sv)) THEN
                                  mm(Np) = mm(Np) + 1
       ELSEIF ((X(Np) .LT. spc) .AND. (Y(Np) .LT. sv)) THEN
                                  mm(Np) = mm(Np) - 1
       ELSEIF ((X(Np) .LT. spc) .AND. (Y(Np) .GT. sv)) THEN
                                  mm(Np) = mm(Np) - 1
```

```
      ENDIF
      ENDIF

      IF (X(Np) .LE. 0.5D0) THEN
      IF ((X(Np) .LE. sn) .AND. (Y(Np) .LE. sv)) THEN
                              mm(Np) = mm(Np) - 1
      ELSEIF  ((X(Np) .LT. sn) .AND. (Y(Np) .GT. sv)) THEN
                              mm(Np) = mm(Np)
      ELSEIF  ((X(Np) .GT. sn) .AND. (X(Np) .LT. snc) .AND.
     &                                        (Y(Np) .LT. sv)) THEN
                              mm(Np) = mm(Np) - 1
      ELSEIF  ((X(Np) .GT. sn) .AND. (X(Np) .LT. snc) .AND.
     &                                        (Y(Np) .GT. sv)) THEN
                              mm(Np) = mm(Np) - 1
      ELSEIF  ((X(Np) .GT. snc) .AND. (Y(Np) .LT. sv)) THEN
                              mm(Np) = mm(Np) + 1
      ELSEIF  ((X(Np) .GT. snc) .AND. (Y(Np) .GT. sv)) THEN
                              mm(Np) = mm(Np) + 1
      ENDIF
      ENDIF

        deltax = deltax + mm(Np)**2

      ENDDO

     IF(MOD(Niter,Nmil).EQ.0)
     &                   WRITE(8,*) Niter, deltax/DFLOAT(Npoint)

      IF (sp .LE. 1.0D0 - alfa) THEN
          sp = sp + alfa
      ELSE
```

```
          sp = sp + alfa - 0.5D0
       ENDIF

       IF (sn .GE. alfa) THEN
          sn = sn - alfa
       ELSE
          sn = sn - alfa + 0.5D0
       ENDIF

       IF (sv .GE. beta) THEN
          sv = sv - beta
       ELSE
          sv = sv - beta + 1.0D0
       ENDIF

       Niter = Niter + 1

      IF(Niter .LT. Ntot) GOTO 786

      CLOSE(8)

 785  CONTINUE
  10  FORMAT(2x,i7,1x,10(f15.8,2x,i5,2x))

      STOP
      END
c-----------------------------------------------------------------------
c Random number generator
c-----------------------------------------------------------------------
  SUBROUTINE rand(iseed,r)
        integer iseed
```

```
        double precision dseed,d2p31m,d2p31
        real r
        d2p31m = 2147483647.D0
        d2p31  = 2147483648.D0
        dseed = iseed
        dseed = dmod(16807.D0*dseed,d2p31m)
        r     = dseed/d2p31
        iseed = int(dseed)
       return
       end
c**********************************************************************
```

A.5 Fix Slicer and Translating Points

```
c**********************************************************************
c       NON-EXPANDING MULTI-BAKER MAP with POINT TRASLATION

      IMPLICIT NONE
      integer*8 i,j,mm(10000000),Npoint,Np,Ntot,Niter,Nitdon,Nmil
      integer Icont,iseed
      double precision X(10000000),Y(10000000),deltax
      double precision slice,alfa
      real r

      Nmil=10000
      OPEN(8,file='Parameters',form='formatted',status='old')
           READ(8,*) slice,Npoint,Ntot
           READ(8,*) iseed,r,Icont
      CLOSE(8)
```

```
      OPEN(7,file='IC',form='formatted',status='unknown')
      DO i = 1,Npoint
         CALL rand(iseed,r)
              X(i) = r
         CALL rand(iseed,r)
              Y(i) = r
         WRITE(7,*) i,X(i),Y(i)
         mm(i) = 0
      ENDDO
      CLOSE(7)

  785 CONTINUE
      OPEN(8,file='msd',form='formatted',status='unknown')

      Niter = 0
  786 CONTINUE

      deltax = 0.0D0

      alfa = 1.0D0/((7.0D0)**(1.0D0/7.0D0))

      DO Np = 1,Npoint
        IF (X(Np) .LT. 1.0D0 - alfa) THEN
                X(Np) = X(Np) + alfa
        ELSEIF (X(Np) .GT. 1.0D0 - alfa) THEN
                X(Np) = X(Np) + alfa - 1
        ENDIF
        IF(mm(Np) .GT. 0) THEN
           IF(X(Np) .LT. 1.0D0 - slice) mm(Np) = mm(Np) - 1
           IF(X(Np) .GT. 1.0D0 - slice) mm(Np) = mm(Np) + 1
        ELSEIF(mm(Np) .LT. 0) THEN
```

```
           IF(X(Np) .LT. slice) mm(Np) = mm(Np) - 1
           IF(X(Np) .GT. slice) mm(Np) = mm(Np) + 1
         ELSE
           IF(X(Np) .LT. 0.50D0) mm(Np) = mm(Np) - 1
           IF(X(Np) .GT. 0.50D0) mm(Np) = mm(Np) + 1
        ENDIF
        deltax = deltax + mm(Np)**2
        ENDDO

       IF(MOD(Niter,Nmil).EQ.0)
      &                    WRITE(8,*) Niter+Nitdon,deltax/DFLOAT(Npoint)
        Niter = Niter + 1

       IF(Niter .LT. Ntot) GOTO 786
       CLOSE(8)

  10   FORMAT(2x,i7,1x,10(f15.8,2x,i5,2x))

       STOP
       END
c-----------------------------------------------------------------------
c Random number generator
c-----------------------------------------------------------------------
  SUBROUTINE rand(iseed,r)
        integer iseed
        double precision dseed,d2p31m,d2p31
        real r
        d2p31m = 2147483647.D0
        d2p31  = 2147483648.D0
        dseed = iseed
        dseed = dmod(16807.D0*dseed,d2p31m)
```

```
        r     = dseed/d2p31
        iseed = int(dseed)
        return
        end
c*********************************************************************
```

Bibliography

[1] K. Huang, *Statistical Mechanics*, Wiley and Sons, USA, 1987

[2] H.T. Hammel, W.M. Schlegel, Cell. Biochem. Biophys. **42** (2005) 277

[3] E.E. Sakallioghu, B. Ayas, U. Sakallioghu, U. Yavuz, G. Acikgoz and E. Firatli, J. Periodontal. **28** (2007) 757

[4] Y.C. Su, L.W. Lin, J. Micro-Electromech. System **13** (2004) 75

[5] R.K. Verma, S. Arora, S. Garg, Crit. Rev. Theor. Drug **21** (2004) 477

[6] J.H. van't Hoff, *The function of osmotic pressure in the analogy between solutions and gases* traslated by W. Ramsey, Philosophical Magazine **26,59** (1888) 81

[7] H.N. Morse, J.C.W. Frazer, F.M. Rogers, J. Am. Chem. **38** (1907) 75

[8] M.P. Tombs, A.R. Peackocke, *The Osmotic Pressure of Biological Macromolecules*, CharendoN Press, Oxford, 1974

[9] H. Coll, *Determination of Molecular Weight*, Wiley, New York, 1989

[10] R. Chang, *Physical Chemistry with Application to Biological Systems*, Macmillan, New York, 1981

[11] J.E.J. Trevor, Phys. Chem. **10** (1906) 392

[12] A.W.Porter, Proc. Roy. Soc. Lond. A **6** (1907) 519

[13] G.N.Lewis, J. Am. Chem. Soc. **30** (1908) 668

[14] W. Washburn, J. Am. Chem. Soc. **32** (1910) 653

[15] V.T.Granik, B.R. Smith; S.C. Lee, M. Ferrari, Biomed. Microdev. **4:4** (2002) 309

[16] A Grattoni, M. Merlo, M. Ferrari, J. Phys. Chem. B **111** (2007) 11770

[17] M. Pizzi, A. Botrugno, P.M. Calderale, Memoria Accademia delle Sciene di Torino: Classe di Scienze Fisiche, **32** (2008) 47

[18] C.Cosentino, F.Amato, R. Walczak, A. Boiarski, M. Ferrari, J. Phys. Chem. B **109** (2005) 7358

[19] G. Peskir, Stoch. Models **19** (2003) 383

[20] T. Chou, Journal of Chemical Physics **110** (1999) 1

[21] M. Bathe, G.C. Rutledge, A.J. Grodzinsky, B. Tidor, Biophysical Journal **89** (2005) 2357

[22] A. Igarashi, L. Rondoni, A. Botrugno, M. Pizzi, Commun. Theor. Phys. **56** (2011) 352

[23] O.G. Jepps, L. Rondoni, J. Phys. A **39** (2006) 1311

[24] O.G. Jepps, C. Bianca, L. Rondoni, Chaos, **18** (2008) 013127

[25] U. Marini Bettolo Marconi, A. Puglisi, L. Rondoni, A. Vulpiani, Phys. Rep. **461** (2008) 111

[26] O.G. Jepps, L. Rondoni, Journal of Physics A **43** (2010) P05015-1

[27] O.G. Jepps, S.K. Bathia, D.J. Searles, Phys. Rev. Lett. **91** (2003) 126102

[28] S.K. Bathia, D. Nicholson, Chem. Eng. Sci. **66** (2011) 284

[29] P. Gaspard, *Chaos, Scattering and Statistical Mechanics* Cambridege University Press, Cambridge, 1998

[30] R. Dorfmann *An Introduction to Chaos in Nonequilibrium Statistical Mechanics* Cambridege University Press, Cambridge, 1999

[31] J. Vollmer, Phys. Rep. **372** (2002) 131

[32] S.R. de Groot, P. Mazur, *Nonequilibrium Thermodynamics,I*, Courier Dover, New York, 1984

[33] S. Chapman, T.G.Cowling, *The Mathematical Theory of Non-Uniform Gases*, Cambridge University Press, Cambridge, 1970

[34] A. Einstein, Annalen Der Physik **17** (1905) 549

[35] N. Wax, *Selected Papers on Noise and Stochastic Process* Dover, New York, 1954

[36] R. Metzler, J. Klafter, Phys. Rep. **339** (2000) 1

[37] R. Klages, G. Radons, I.M. Sokolov *Anomalous Transport* Wiley-VHC, Berlin, 2008

[38] J. Guckenheimer, P. Holmes, *Nonlinear Oscillations, Dynamical Systems and Bifurcations of Vector Field*, Springer-Verlag, New York, 1983

[39] G. Benettin, Introduzione ai Sistemi Dinamici, Note del Corso Scuola Galileiana 2011-2012 http://www.math.unipd.it/∼benettin/Galileiana/dispense.pdf

[40] S. Tasaki, P. Gaspard, J. Stat. Phys. **81** (1995) 935

[41] R. Klages, From Deterministic Chaos to Anomalous Diffusion, Reviews of Nonlinear Dynamics and Complexity, Vol.3, H.G. Schuster (Ed.), Wiley-VCH, Weinheim, 2010

[42] R. Klages *Microscopic Chaos, Fractals and Trasport in Non-equilibrium Statistical Mechanics* World Scientific, Singapore, 2007

[43] Y. Pomeau, P. Manneville, Comm. Math. Phys. **74** (1980) 189

[44] H.G. Schuster, *Deterministic Chaos*, Wiley-VCH, Wenheim, 1989

[45] E. Ott, *Chaos in Dynamical Systems*, Cambridge University Press, Cambridge, 1993

[46] L.A. Bunimovich, Dynamical Systems of Hyperbolic Type with Singularities in Encycclopedia of Mathematical Sciences Vol.2, Sinai (Ed.) (1989) 151

[47] N. Chernov, J. Stat. Phys. **88** (1997) 1

[48] Y.G. Sinai, Russ. Math. Surv. **25** (1970) 137

[49] E. Gutkin, J. Stat. Phys. **83** (1996) 7

[50] E. Gutkin, Physica D **19** (1986) 311

[51] P. Civitanović, R. Artuso, R. Mainieri, G. Tanner, G. Vattay *Chaos: Classical and Quantum*, chaosbook.org, Niels Bohr Institute, Copenaghen, 2009

[52] E. Gutkin, Regular Chaotic Dyn. **8** (2003) 1

[53] D. Alonso, A. Ruiz, I. de Vega, Physica D **187** (2004) 184

[54] D.P. Sanders, H. Larralde, Phys. Rev. E **73** (2006) 026205

[55] R. Artuso, G. Casati, I. Guarnieri, Phys. Rev. E **55** (1997) 6384

[56] G. Galerpin, T. Kruger, S. Troubetzkoy, Comm. Math. Phys. **169** (1995) 463

[57] C.P. Dettmann, E.G.D. Cohen, H. van Beijeren, Nature **401** (1999) 875

[58] S.Lepri, L. Rondoni, G. Benettin, J. Stat. Phys. **99** (2000) 857

[59] R. Burioni, L. caniparoli, A. Vezzani, Phys. Rev. E **81** (2010) R060101

[60] W. Feller, *An Introduction to Probability Theory and Its Applications, Vol.2*, Wiley, USA, 1971

[61] S.P.Lalley, Lévy processes, Stable processes and Subordinators, Lecture Notes, http://galton.uchicago.edu/∼lalley/courses/385/LevyProcesses.pdf

[62] A.A. Dubkov, B.Spagnolo, V.V. Uchaikin, Int. J. Bifurcation Chaos Appl. Sci. Eng. **18** (2006) 2649

[63] A.V. Checkin, R. Metzler, J. Klafter, V. Yu. Gonchar *Introduction to the Theory of Lévy flights* in Anomalous transport:Foundations and Applications (R. Klages, G. Radons, I.M. Sokolov Ed.) Wiley-VCH, Weinheim, 2008

[64] J. Klafter, A. Blumen, G. Zumofen, M.F. Shlesinger, Physica A, **168** (1990) 637

[65] J. Klafter, A. Blumen, M.F. Shlesinger, Phys. Rev. A **35** (1987) 3081

[66] J.W. Hans, K.W. Keher, Phys. Rep. **150** (1987) 263

[67] E.W. Montroll, G.H. Weiss, J. Math. Phys. **6** (1965) 167

[68] G.H. Weiss, R.J. Rubin, Adv. Chem. Phys. **52** (1983) 363

[69] P.G. Doyle, J.L. Snell *Random Walks and Electric Networks* The Mathematical Association of America, Washington D.C., 1999

[70] C.W.J. Beenakker, C.W. Groth, A.R. Akhmerov, Phys. Rev. B **79** (2009) 024204